ASSEMBLY-BASED VULNERABILITY OF BUILDINGS AND ITS USES IN SEISMIC PERFORMANCE EVALUATION AND RISK-MANAGEMENT DECISION-MAKING

by

Keith Alan Porter

and

Anne S. Kiremidjian

Report No. 139

February 2001

Porter, K.A., and A.S. Kiremidjian, 2001, *Assembly-Based Vulnerability of Buildings and its Uses in Seismic Performance Evaluation and Risk-Management Decision-Making, Report 139,* John A. Blume Earthquake Engineering Research Center, Stanford, CA

ERRATA

Section 2.3 erroneously states that Kustu, Miller, and Brokken [1982] expand on Scholl's [1981] methodology for developing theoretical motion-damage relationships. The methodology was conceived and developed by Kustu as confirmed by Kustu [2001] and Brokken [2001]. The approach accounts for variability in component damageability and distinguishes between the cost to construct a new component in a new building and the cost to repair a damaged component in an existing building. Additional detail on this work is provided by Scholl, Kustu, Perry, *et al.* [1982]. (References absent from the present report are shown below.)

Brokken, S.T., 2001, personal communication

Kustu, O., 2001, personal communication

Scholl, R.E., O. Kustu, C. Perry, and J.M. Zanetti, 1982, ***Seismic Damage Assessment for High-Rise Buildings, JAB-8020, Final Technical Report to U.S. Geological Survey,*** URS/John A. Blume & Associates, Engineers, San Francisco

ASSEMBLY-BASED VULNERABILITY OF BUILDINGS AND ITS USES IN SEISMIC PERFORMANCE EVALUATION AND RISK-MANAGEMENT DECISION-MAKING

A REPORT SUBMITTED TO THE DEPARTMENT OF CIVIL AND ENVIRONMENTAL ENGINEERING
AND THE COMMITTEE ON GRADUATE STUDIES
OF STANFORD UNIVERSITY
IN PARTIAL FULFILLMENT OF THE REQUIREMENTS
FOR THE DEGREE OF DOCTOR OF PHILOSOPHY

Keith Alan Porter

August 2000

ABSTRACT

A methodology is presented to evaluate the seismic vulnerability of buildings on a building-specific basis. The methodology, entitled assembly-based vulnerability, estimates repair cost, repair duration, and loss-of-use cost as functions of spectral acceleration. It treats the building as a unique collection of standard assemblies with probabilistic fragility, repair costs, and repair durations. The procedure applies Monte Carlo methods to simulate ground motion, structural response, assembly damage, repair costs, and repair duration. The methodology is illustrated using a realistic example office building.

The report also presents a decision-analysis approach to making seismic risk-management decisions for individual buildings, using the assembly-based vulnerability methodology. The decision analysis accounts for the decision-maker's business practices and risk attitude, and produces a recommendation of the best alternative on an expected-utility basis. A detailed procedure for eliciting the decision-maker's risk attitude is presented. The methodology is illustrated using a realistic example decision situation. It is found that risk attitude can make a material difference in the selection of the optimal risk-management alternative, thus calling into question techniques that assume risk neutrality and rely on cost-effectiveness as the key measure of desirability.

Various techniques are presented for developing empirical and theoretical assembly fragilities; these techniques are illustrated through the creation of fragility functions for a wide variety of structural, nonstructural, and content assemblies. The fragility functions can be reused in subsequent analyses. Fragilities are defined within the framework of a standardized, detailed, and highly adaptable assembly taxonomy that can facilitate unambiguous communication of assembly types, fragilities, and costs.

ACKNOWLEDGMENTS

Financial support for this report was provided by the Haresh Shah Family Foundation, the Kajima Corporation, and the ARCS Foundation. A number of individuals contributed their time to several aspects of the research: Satwant Rihal and Phil Weir contributed engineering expertise on key topics; Professor Jim Beck, Drs. Masoud Zadeh and Mahmoud Khater, Ron Hamburger, Sam Swan, and Bill Holmes all provided valuable time and feedback. .

Chapter Page

Appendices

Page

Page

CHAPTER 1
INTRODUCTION

1.1. BACKGROUND

This study addresses the creation of seismic vulnerability functions on a building-specific basis, accounting for the unique structural, architectural, mechanical, electrical, and plumbing aspects of the building. In addition, the study develops a risk-management decision procedure that uses the building-specific vulnerability function and accounts for the risk attitude, planning period, and other financial practices of the decision maker.

Currently, no consistent and systematic methodology exists to evaluate single-building seismic vulnerability, accounting for uncertainties in ground motion, structural response, damage, and loss. Existing methods either lack probabilistic basis, fail to account for a building's unique setting and design, or rely heavily on expert judgment. Using such methodologies, high-cost economic decisions regarding seismic risk mitigation must be made on a highly subjective basis, with significantly less information available than for other business decisions with similar stakes. The building-specific seismic vulnerability functions to be developed here are intended to overcome this shortcoming.

Current procedures commonly used for seismic risk management select the optimal risk-management alternative using cost-benefit analysis. While such procedures are proper for use in situations without uncertainty, or where stakes are small, they are inappropriate for situations with uncertain outcome and severe consequences. The assumption of risk neutrality implicit in cost-benefit analysis can result in the rejection of desirable strategies such as the purchase of insurance, whose benefit-to-cost ratio is

typically less than 1.0. The present study employs expected-utility decision-making to account for risk attitude.

1.2. OBJECTIVE

The overall objective of this report is to develop a consistent, systematic methodology for producing a probabilistic model of building-specific seismic vulnerability, and show how it can be used to inform risk-management decision-making using a decision-analysis approach. The study includes the following tasks:

- Review existing methodologies to estimate earthquake damage and loss to buildings and to select appropriate risk-mitigation measures.

- Establish a framework for making seismic risk-management decisions, accounting for common structural and nonstructural seismic retrofit measures, seismic setting, building-specific seismic vulnerability with and without retrofit, decision-maker risk attitude, and all relevant uncertainties.

- Establish an assembly category system to identify individual assemblies within buildings, accounting for construction details and conditions of installation that affect seismic vulnerability.

- Create enough assembly fragility and cost functions to represent typical structural, architectural, mechanical, electrical, and plumbing components of a realistic building.

- Establish a procedure for combining structural analysis, assembly fragility, repair cost and duration, and repair scheduling, to create a seismic vulnerability function for the whole building. The procedure is referred to here as assembly-based vulnerability (ABV).

- Illustrate the risk-management methodology using a case study of a seismic retrofit decision situation for a particular building.

1.3. SCOPE

While a general approach will be presented, the individual assemblies examined will be limited to those appearing in the case-study building: a hypothetical 3-story pre-Northridge welded-steel moment-frame office building in Los Angeles, subject to earthquake damage.

Life-safety issues will be addressed only in summary form. The focus of the present study is on the damage caused to the vast majority of structures affected by earthquakes, that is, damage that results in economic loss but not casualties or damage that reaches the level of partial collapse.

1.4. ORGANIZATION OF REPORT

Chapter 2 reviews current practice in earthquake risk evaluation and risk management. Assembly fragilities and cost functions are developed in Chapter 3. The ABV algorithm is detailed in Chapter 4. Chapter 5 develops procedures for making risk-management decisions using ABV. Conclusions and recommendations for future work are presented in Chapter 6. References are presented in Chapter 7. Appendix A presents a preliminary assembly taxonomy. Appendix B details the development of fragility, repair cost and repair duration distributions for a variety of structural and nonstructural assemblies and contents. Appendix C provides details of a methodology to elicit a decision-maker's risk attitude. Finally, Appendix D contains a list of terms and abbreviations used in the report.

CHAPTER 2
LITERATURE REVIEW

2.1. INTRODUCTION: DAMAGE AND LOSS ESTIMATES IN RISK MANAGEMENT

Various parties hold a financial stake in the uncertain future performance of a building in earthquakes. Owners, lenders, insurers, and occupants of buildings in seismic regions are each exposed to economic risk. Standard practice among lenders and insurers compels them actively to manage that risk. Prior to underwriting a commercial mortgage, for example, banks typically demand an earthquake risk study be performed on the building. If the estimated loss in a large earthquake scenario exceeds a predefined fraction, the lender requires earthquake insurance before underwriting the mortgage. One investor in San Francisco commercial real estate reports that a common threshold of scenario loss is 20% [Flynn, 1998].

Similarly, insurers purchase reinsurance to transfer a portion of their own risk to others; their decisions about reinsurance needs are typically informed by annual evaluations of probable maximum loss (*PML*) – a commonly used term, albeit ambiguously defined [Steinbrugge, 1982; Rubin, 1991]. ASTM [1999] presents generic procedures and qualifications for earthquake loss estimation "to reflect a commercially prudent and reasonable inquiry." The standard does not contain algorithms for performing loss estimates, but rather recommends the use of "commercially available computer assessment tools." No restrictions are stated on the nature or demonstrated validity of those tools.

Most software and other loss-estimation algorithms for estimating earthquake damage to buildings use seismic *vulnerability functions* that relate loss to seismic shaking intensity. Economic loss in an earthquake can result from several sources. Losses dealt with here are building repair cost, content repair or replacement cost, and costs

associated with the loss of building usability. All are strongly dependent on physical damage to the building in question. Economic losses ignored for the present study include damage caused by fire following earthquake, business interruption associated with loss of offsite services, and business losses associated with supply chain interruption. These losses are less readily associated with physical damage to the building in question.

One can categorize methodologies to create seismic vulnerability functions in two groups: techniques based on structure type – a broad category into which a particular building falls – and techniques based on a detailed structure analysis of the unique building. Both categories are discussed here. Analytical structural evaluation procedures employed in prescriptive building codes are ignored here, as they are intended to verify conformance with minimum design standards, rather than to estimate economic loss.

2.2. CATEGORY-BASED APPROACHES TO BUILDING VULNERABILITY

Several studies have developed relationships between ground motion and building damage. Scholl [1981] discusses an approach to derive empirical motion-damage relationships for highrise buildings, using a database gathered for the project. The database contains 4100 records containing information on buildings exposed to 81 earthquakes that occurred in 26 urban centers in 12 countries between 1906 and 1979, with magnitudes from 4.5 to 8.3. The database contains 118 fields reflecting building location, size, configuration, structural systems, motion, and damage descriptions. Data were gathered from a literature review. An extract shows the database to be sparsely populated.

ATC [1985] summarizes available empirical, theoretical, and judgment-based vulnerability data on a wide variety of structure types and other engineered facilities.

The authors find that the available data on earthquake damage to some facility types are inadequate or nonexistent. Other types have adequate data to estimate damage for moderate-sized earthquakes, but not large events. The authors therefore develop seismic vulnerability functions using expert opinion gathered from 157 earthquake engineering academics and practitioners using a Delphi Process [Gordon and Helmer, 1964] modified to account for expert self-rating [Dalkey, Brown, and Cochrane, 1970].

In the ATC [1985] process, experts estimate damage factor (repair cost as a fraction of replacement cost) to 40 categories of California buildings (as well as 38 categories of industrial, lifeline, and other assets) as a function of modified Mercalli Intensity (MMI). Damage factor probability distributions are then evaluated for each MMI level. Damage probability matrices are then created by discretizing the damage probability distributions. Seven damage state intervals are used, which are associated with semantic damage states, from 1-None to 7-Destroyed. Several types of loss are evaluated: building repair cost, content repair cost, loss of use duration, minor injuries, major injuries, and fatalities. The ATC [1985] approach is intended for macroscopic (i.e., societal) loss estimation, and does not account for a building's unique detailed design. Its vulnerability functions are therefore most useful in the present study for comparison with independently developed single-building vulnerability functions.

The HAZUS Standard Methodology [NIBS, 1995] uses a similar category-based approach to seismic vulnerability. Like ATC-13 [ATC, 1985], HAZUS is intended for use in macroscopic loss estimation and is therefore inappropriate for single-building loss estimation. Its vulnerability functions are based on estimated fragility of three building elements: structural components, drift-sensitive nonstructural components, and acceleration-sensitive nonstructural components. Structural response under a particular earthquake is determined using the capacity spectrum method [Mahaney, Paret, Kehoe et al., 1993], which estimates peak response by the intersection of the earthquake response spectrum and a building capacity curve that is characteristic of the model

building category of interest. Overall building damage is calculated based on the sum of estimated damage to structure, nonstructural drift-sensitive components, and nonstructural acceleration-sensitive components. The damage state of each of these categories is treated as a random variable whose distribution is determined based on a set of four fragility curves. Each curve indicates the probability of the model building category exceeding a descriptive damage state, conditioned on spectral displacement. The fragility curves are defined in linguistic terms (slight, moderate, extensive, and complete) and are taken to be lognormal. Each linguistic damage state is equated with a damage ratio (repair/replacement cost): 5% for slight, 15% for moderate, 50% for extensive, and 100% for complete. The fragility-curve parameters (median and logarithmic standard deviation) are based on cyclic laboratory testing of building components and other empirical data, with results adjusted using judgment.

2.3. STRUCTURAL ANALYSIS APPROACHES TO BUILDING VULNERABILITY

Several researchers have attempted to estimate seismic vulnerability of individual buildings with techniques that do not rely on characteristic damage to categories of buildings. In addition to his work on category-based motion-damage relationships discussed above, Scholl [1981] set out to develop theoretical motion-damage relationships based on detailed structural analysis of highrise buildings, followed by an assessment of damage to a variety of components based on structural response. One uses spectral methods to estimate structural response on a floor-by-floor basis, and applies these structural response parameters to appropriate component vulnerability functions. The term *component* refers to a category of building elements; the list of components considered by the author is shown in Table 2-1. The damage ratio for each component is evaluated for each floor and multiplied by the value of each component. Damage to the whole building is obtained by adding the damage to its modules or pieces. Figure 2-1 summarizes the component-based approach.

Kustu, Miller, and Brokken [1982] and Kustu [1986] expand on many aspects of the Scholl [1981] methodology, most notably providing mean damage functions based on laboratory tests of several structural and architectural components. The resulting approach is deterministic, and does not account for variability in ground motion, structural response, component damageability, or unit repair costs. It does not distinguish between the cost to construct a new component in a new building and the cost to repair a damaged component in an existing building. The aggregated component categories make it impossible to distinguish between similar building elements with vastly different seismic vulnerability, for example between a fragile suspended ceiling system and a rugged one. The present study extends the component-based approach to overcome these and other deficiencies.

Table 2-1. Building components considered by Scholl [1981].

Damage component	Motion parameter
Structural	
Steel frame	Maximum interstory drift
Concrete frame	Maximum interstory drift
Masonry shear wall	Maximum interstory drift
Braced frames	Maximum interstory drift
Foundations	
Nonstructural	
Drywall partitions	Maximum interstory drift
Brick infill walls	Maximum interstory drift
Concrete block infill walls	Maximum interstory drift
Glazing	Maximum interstory drift
Cladding	Max. floor acceleration or velocity
Other (ceilings, mechanical, and electrical equipment)	Max. floor acceleration or velocity
Contents	Acceleration

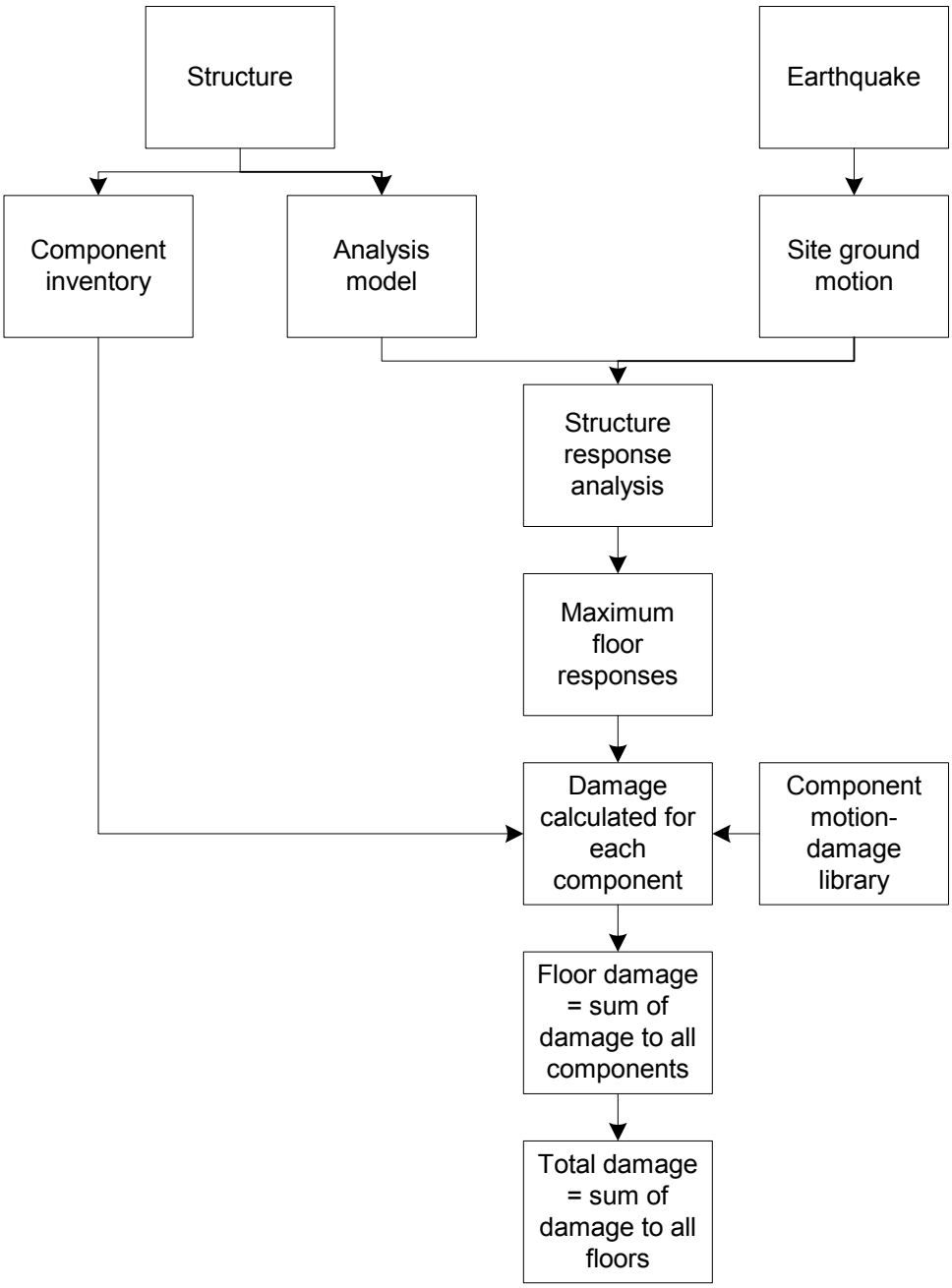

Figure 2-1. Component-based damage prediction [after Scholl, 1981]

In contrast to the deterministic approach offered by previous researchers, Singhal and Kiremidjian [1997] propose a probabilistic, building-specific model of damage to reinforced concrete moment frame buildings. Ground motion is simulated using autoregressive moving-average (ARMA) techniques [e.g., Box, Jenkins, and Reinsel, 1994]. For each of many ground motion simulations, damage to moment-frame elements is estimated in terms of the local Park-Ang damage index [Park, Ang, and Wen, 1984], a unitless value reflecting peak deformation demand and hysteretic energy absorption on a joint-by-joint basis. The approach is not intended to characterize loss to other building components. Repair cost is taken as the global Park-Ang index [Park, Ang, and Wen, 1984] – a weighted average of the local indices – times total building value. The approach demonstrates the means to include randomness in ground motion, material properties, and overall modeling uncertainty, and offers a component damage model for reinforced concrete elements.

2.4. ASSEMBLY DAMAGEABILITY

2.4.1. Form of the fragility function

For many types of assemblies, component damageability may be defined in terms of fragility, defined as the probability that some limit state is exceeded, conditioned on an input level of demand. A graph of this relationship is referred to as a *fragility function*. In the present study, fragility functions depict the probability that a building assembly reaches or exceeds some (damage) limit state conditioned on structural response. A characteristic fragility function is desired for each assembly type and limit state. What mathematical idealization may be used to model these relationships?

Kennedy and Ravindra [1984] presented a model for estimating the probability that a structure or equipment component in a nuclear power plant would fail to operate

conditioned on peak ground acceleration. The model considers a binary failure condition (failed or not failed). The authors present a 3-parameter compound lognormal fragility model, given by Equation 2-1. If mean failure frequency is needed, the two-parameter model given by Equation 2-2 can be used to account for combined aleatory and epistemic uncertainty with a single parameter β (Equation 2-3), simplifying the analysis. A rigorous equipment risk assessment procedure proposed recently by Johnson, Sheppard, Quilici, et al. [1999] uses the two-parameter lognormal model to describe probability of operational failure. Equation 2-2 is therefore considered here, with the exceptions that X is expressed in terms of any appropriate structural response parameter such as diaphragm acceleration or peak transient drift, and that other limit states besides operational failure are considered.

$$f' = \Phi\left(\frac{\ln(x/x_m) + \beta_U \Phi^{-1}(Q)}{\beta_R} \right) \tag{2-1}$$

$$f' = \Phi\left(\frac{\ln(x/x_m)}{\beta} \right) \tag{2-2}$$

where

$$\beta = \sqrt{\beta_U^2 + \beta_R^2} \tag{2-3}$$

f' is the frequency of failure at any nonexceedance probability level Q.

$\Phi(\ )$ is the standard normal cumulative distribution; $\Phi^{-1}(\ )$ is its inverse

x is the peak ground acceleration level

x_m is the median ground acceleration capacity

β_U reflects epistemic uncertainty (imperfect knowledge)

β_R reflects aleatory uncertainty inherent in the damage process

Q = P[$F < f' \mid a$] is the probability that the conditional frequency of failure, F, is less than f', conditioned on x.

2.4.2. Development of empirical fragility functions

Given the assembly fragility model, the question is how to determine the assembly capacity function $F_X(x)$ for a particular assembly and limit state. Three approaches to determining $F_X(x)$ are available: empirical, theoretical, and judgment-based. The empirical method involves estimating the parameters through regression analysis of earthquake experience or laboratory data. Swan and Kassawara [1998] describe such a methodology using an empirical dataset, where the limit state considered is operational failure, and capacity is assumed to be lognormally distributed and measured in terms of peak ground acceleration. In this approach, failure data are binned by peak ground acceleration. One plots fraction of failed components in each bin versus bin-average PGA. Regression analysis is performed on these data to determine median capacity and logarithmic standard deviation of capacity. (In the present study, this approach is generalized to various forms of the fragility function besides lognormal, as well as considering other limit states and capacity parameters.)

2.4.3. Theoretical fragility functions based on reliability methods

In some cases, empirical data are unavailable or inadequate to describe assembly capacity. Systems reliability methods may be used to develop theoretical fragility functions in cases where the assembly may be modeled as a structural system comprised of components with known or estimated capacity distributions. Freudenthal, Garrelts, and Shinozuka [1966] formulate reliability as the probability that demand S exceeds resistance capacity R. The difference ($S - R$) represents the *performance function*. For continuous R and S, failure probability is then evaluated as shown in Equation 2-4. In

the present study, Monte Carlo techniques are used to evaluate the integral. The demand parameter S is controlled and the parameters that contribute to capacity R are allowed to vary according to known or assumed probability distributions.

$$P_f = P[R - S < 0] = \int_0^\infty [1 - F_S(y)] f_R(y) dy \tag{2-4}$$

2.4.4. Judgment-based fragility modeling

No judgment-based fragility functions are used in the present study, but the issue is considered briefly for completeness. For assemblies where empirical data are inadequate and reliability methods cannot be applied, a judgment-based fragility model may be employed. This may involve an individual or group of experts making an informed guess of median capacity x_m and uncertainty β. Such an approach may be appropriate for assemblies with relatively small effect on overall earthquake losses, either because the assembly represents a small fraction of the overall value of the facility, or because the assembly is judged to be relatively rugged.

Bier [1999] points out that expert opinion in risk analyses is often perceived by decision-makers to weaken the credibility of probabilistic risk analyses. The author personally observed this during 1996 and 1997 hearings by the State of Florida's Commission on Hurricane Loss Projection Methodologies. When expert opinion must nevertheless be used, its quality can be maximized through careful means of eliciting judgment. Tversky and Kahneman [1974] discuss some of the potential problems – biases of judgment – that arise when eliciting judgments of probability. Spetzler and Von Holstein [1972] detail a methodology to interview experts to encode probability beliefs, with due attention to minimizing the effect of such biases.

2.5. ASSEMBLY DEFINITIONS

2.5.1. Assembly taxonomy

Before reviewing literature on particular assembly fragility functions, formal assembly categorization systems are discussed. Scholl [1981] and Kustu, Miller, and Brokken [1982] and Kustu [1986] deal with a building as a collection of highly aggregated components, as shown in Table 2-1. Under such a highly aggregated taxonomy, it is problematic to define limit states in unambiguous, physical terms such as collapse or fracture.

Highly aggregated taxonomies are avoided here also because they are incapable of reflecting building-specific design features to which damage is strongly sensitive, such as bracing or anchorage of equipment and presence or absence of fragile finishes. It is desirable therefore to define assemblies in greater detail, to facilitate creation of meaningful fragility functions and choices between similar components.

More-detailed systems of classifying building components exist. The taxonomic systems most commonly used in the United States construction industry are those documented by the RS Means Corp., publishers of popular construction cost-estimation manuals. RS Means Corp. publishes cost manuals under two basic systems. One taxonomy [RS Means Corp., 1997a] is extended from the CSI MasterFormat classification system [Construction Specifications Institute, 1995], which describes building parts to a very detailed level, e.g., individual panels of gypsum wallboard. This system is appropriate to the creation of final construction cost estimates, but is too detailed to be practical for present purposes.

RS Means' second system – more useful here – describes buildings as a collection of higher-level assemblies. For example, whole gypsum-board partitions, assembled and in place, is one assembly. The taxonomy of the RS Means Corp. [1997b] assembly

numbering system is an extension of the UniFormat system [ASTM, 1996]. Each assembly is identified by three sets of numbers: division, class, and line. Division is the same as the UniFormat division, and indicates the order of construction in new structures, with tasks in lower division numbers being constructed first. Class and line indicate detailed descriptions of an assembly type. Table 2-2 provides a sample of the assembly numbering system. Note that this taxonomy provides inadequate detail to indicate installation conditions with regard to seismic resistance, for example, whether a piece of electrical equipment has been bolted to the floor slab. For present purposes, the system is modestly extended with the addition of an assembly code to account for condition.

Table 2-2. Sample assembly numbering system, RS Means Corp. [1997b].

Building assembly			
Division	**Class**	**Line**	**Description**
1. Foundations			
	1.1	120	0000 Spread footing
	1.1	140	0000 Strip footing
	1.1	210	0000 Walls cast in place
	1.1	292	0000 Foundation dampproofing
	1.9	100	0000 Excavation & backfill

2.5.2. Units of assemblies

A related issue is how to discretize assemblies within an assembly type. Should suspended ceilings be counted by square foot, by room, by floor, or by the entire building? No universal rule presents itself to answers all specific cases. Generally, it appears reasonable to define a unit of an assembly to coincide with a common

understanding of an assembly, with a discrete physical damage phenomenon, or with a common unit of repair. The appropriate unit will therefore vary from assembly type to assembly type. Some assemblies are easily quantified in this way: packaged electrical and mechanical equipment such as a single fan or transformer are readily discretized.

Furthermore, since assembly fragilities are used here, an assembly must be defined so that a single measure of input hazard can be applied. Thus, an assembly type that is distributed throughout several floors of a building must be discretized at most by floor, or by floor and direction, so that floor-level structural response parameters such as transient interstory drift and diaphragm acceleration can be applied unambiguously and without averaging.

2.6. FRAGILITY STUDIES OF PARTICULAR COMPONENTS

To model an entire building, it is necessary to create fragility functions for a variety of structural, architectural, mechanical, electrical, and plumbing assemblies. Given general techniques of developing assembly fragility, what component fragility functions or data exist to model particular assemblies?

2.6.1. Welded steel moment-frame connections

The 1994 Northridge Earthquake demonstrated the damageability of a common pre-qualified beam-to-column welded steel moment-frame connection. In this type of connection, the beam is first supported in shear using a single-plate shear connector that has been welded to the column and field-bolted to the beam web. The moment connection is then made by field-welding the beam flanges to the column using complete-penetration groove welds. It was primarily these latter welds that exhibited unexpected failures. After the earthquake, SAC Steel Project investigators exposed and examined for damage approximately 2,300 connections in 31 frames of 6 buildings

affected by the earthquake [Engelhardt, Kim, Sabol, et al., 1995; Hart, Huang, Lobo, et al., 1995; Kariotis and Eiamani, 1995; Krawinkler, Al Ali, Thiel, et al., 1995; Naeim, DiJulio, Benuska, et al., 1995; and Uang, Yu, Sadre, et al., 1995]. The investigators also perform structural analyses of the buildings, and provide estimates of peak structural response experienced by the connections during the earthquake. Data from these analyses are used here to relate failure probability to structural response.

2.6.2. Gypsum wallboard partition on metal studs with drywall screws

Rihal [1982] presents results of a number of experimental investigations of drift-fragility of 8′-0 x 8′-0 building partitions. This study included in-plane racking tests of 12 specimens, of which 11 were constructed of 5/8″ gypsum wallboard connected with drywall screws to 3-5/8″ metal studs (9 tests) or to 2-5/8″ metal studs (2 tests). Pseudostatic cyclic loading is applied. Interstory drifts associated with four performance levels were recorded, of which the two of interest are *noticeable damage* and *significant damage*. Rihal [2000] believes the former limit state may be equated with the onset of damage requiring tape, mud, and paint. The latter limit state may be associated with the onset of damage requiring demolition and replacement.

2.6.3. Gypsum wallboard partition on wood studs with drywall nails

Oliva [1990] performed a series of laboratory tests to examine the behavior of wood-framed gypsum panels. Tested specimens were 8′-0 x 8′-0 wall segments with ½-in. gypsum wallboard on one side only, framed on 2x4 wood studs spaced 24″ OC, and nailed with 4d drywall nails. The author tested specimens using three in-plane racking regimens: monotonic, pseudostatic cyclic, and dynamic cyclic. He identified two limit states that are of interest here: visible damage and severe damage, which correspond well with those identified by Rihal [1982]. The study reports the interstory drift values

associated with each limit state, although in inadequate detail to determine uncertainty in capacity.

2.6.4. Suspended ceilings

A suspended ceiling is a manufactured modular structure of extruded metal or plastic linear T-shaped elements connected into a rectangular grid at centers between 9 to 48-inch, hung from the diaphragm above by wires at 24-inch to 48-inch centers. The grid of main runners connected by cross tees supports light panels of acoustical tile, acoustical board, gypsum board, linear metal panels, or rectangular metal pans. The grid is typically attached to the perimeter wall at two adjacent edges for purposes of facilitating installation.

ANCO Engineers, Inc., [1983] performed full-scale shake-table tests on a light acoustical tile ceiling system. A variety of lateral restraint systems were tested, and the ceiling was subjected to a variety of shaking regimens. The report discusses ceiling performance under each test, providing peak diaphragm acceleration, peak ceiling acceleration, and horizontal peak response spectrum ordinate of actual table motion. Two tests produced incipient ceiling failure; the ceiling was tested to collapse in one test.

Rihal and Granneman [1984] present results of 12 full-scale dynamic tests of suspended ceilings under a variety of installation conditions. All tests are of a ceiling system 12 ft. x 16 ft. in plan, with 2 ft. x 4 ft. exposed grid elements and lay-in acoustical tiles. The authors find that the behavior of ceilings is influenced by input acceleration and frequency. They find that ceiling perimeter details significantly influence damage, and note that the presence of hangers near the ends of grid elements mitigates drop-out of ceiling tiles at the perimeter.

Griffin and Tong [1992] report observations of ceiling performance in more than 100 electric power and industrial facilities affected by the Loma Prieta and Whittier

earthquakes. The authors present three major conclusions. First, ceiling damage was widespread, with more than half of these facilities experiencing some damage to suspended ceilings. Second, there is no obvious threshold of peak ground acceleration causing ceiling damage, with some damage occurring at PGA values below 0.10g, and some facilities experiencing no ceiling damage despite PGA in excess of 0.50g. Finally, all observed ceiling damage is attributable to tensile failure of grid connections, compression failure of grid elements, falling of above-ceiling components, and interaction of the ceiling with overhead utilities. The authors also note that perimeter connection of the grid to the wall acts as the de facto seismic restraint of the ceiling; diagonal bracing do not become active.

Eidinger and Goettel [1998] present median capacity and uncertainty values for suspended ceilings. They do not report the source of these figures or the methodology used to develop them. Their results are therefore also useful primarily for comparison purposes.

The observations of ANCO Engineers Inc. [1983], Rihal and Granneman [1984], and Griffin and Tong [1992], and Eidinger and Goettel [1998] can be used to inform and test the development of a theoretical fragility model, but are not comprehensive enough to develop a probabilistic fragility model.

2.6.5. Glazing

Laboratory tests on curtain-wall glazing subject to racking as in earthquake are presented in Pantelides and Behr [1994], Behr, Belarbi, and Culp [1995], and Behr and Worrell [1998]. Behr and Worrell [1998] present results of displacement-controlled cyclic load tests of several dozen samples of 5-ft by 6-ft architectural glass assemblies. (An assembly comprises lites in aluminum extruded frames with standard mounting of lite in frame). The assemblies are a standard manufactured glazing system called Horizon

Wall, by the Cupples Company. The study reports mean and standard deviation of in-plane interstory drift index associated with cracking and glass fallout, for 14 different combinations of framing system, glass type, and sealant.

Nakata, Itoh, Baba, et al. [1984] report results of dynamic tests of a full-scale seven-story reinforced concrete building that included a variety of nonstructural elements, including aluminum-framed windows. Glazing included sliding windows; fixed windows sealed with hardened putty and with elastic sealant; windows with wired-glass panes; and windows with polyester adhesive film attached to the glass. The authors report transient drifts associated with glass cracking.

2.6.6. Buried pipeline

Most buildings have buried water pipe providing fresh water and buried sewer pipe carrying away wastewater. These service lines run from the street to the building, and are occasionally fractured by permanent ground displacement resulting from liquefaction, lateral spreading, or landslide. Such pipeline failure affects building operability in general, and potentially fire safety. Cases of damage in the Loma Prieta earthquake are described in Porter, Scawthorn, Honegger, et al. [1992]. This study presents fragility experience in Loma Prieta for several classes of buried pipeline, using damage data to express mean number of pipe breaks per 1,000 feet of pipe as a function of permanent ground displacement. Using these relationships for mean occurrence rate of a Poisson distribution, one may model the distribution of pipe capacity per segment.

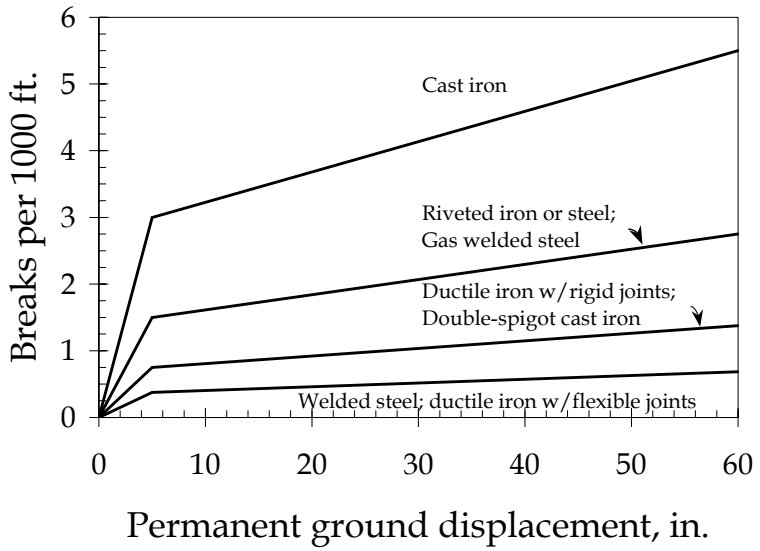

Figure 2-2. Break rate of buried pipeline in failed ground [Porter et al., 1992]

2.6.7. Desktop computers

Jin and Astaneh [1998] present results of 34 shake-table tests of IBM PS-2 desktop microcomputers resting on typical office desks, of which 21 were conducted on computers attached to the desk, the other 13 relying solely on friction. Even when subjected to levels of shaking exceeding 6g, desktop computers continue to operate unless they fall to the floor. In the tests of unattached computers, friction did seem to inhibit movement of unrestrained computers [Astaneh, 2000], but displacement records indicate that once friction was overcome, computers tended to translate slowly and constantly from their initial position, rather than moving in rare sudden jerks. During four of these tests, one or both monitors fell from the desk. In three tests, system units fell from the table. In the remaining tests of computers connected to the desk, the authors found that the mechanical connectors adequately prevented movement of the equipment at all tested accelerations, and no damage occurred. The report provides

details on the acceleration imposed on the desk in each test, thereby providing a limited basis on which to model desktop computer fragility.

2.6.8. Household contents

Saeki, Tsubokawa, and Midorikawa [2000] present data on household property loss resulting from the 1995 Kobe earthquake. The data come from 965 questionnaire respondents living in the Hyogo and Osaka prefectures. The questionnaires asked about a variety of durable possessions such as furniture and non-durables such as clothing. The authors created vulnerability functions for six classes of durables and four of non-durable possessions. Each vulnerability function relates fraction of items of the class damaged to shaking intensity, measured in Japan Meteorological Agency (JMA) intensity. The authors assume property vulnerability functions in the form of a cumulative normal distribution (Equation 2-5). They use regression analysis to determine distribution parameters for each class of property. The parameters are shown in Table 2-3.

$$P = \Phi\left(\frac{\ln(I) - \mu}{\sigma}\right) \tag{2-5}$$

where

P = Damage ratio ((damaged items)/(total items))

I = JMA intensity

μ = mean intensity at which items experience damage

σ = standard deviation of intensity at which items experience damage

Table 2-3. Parameters of household property vulnerability functions.

Property type	μ	σ
Large freestanding storage furniture subject to overturning, e.g., chests, shelves, cupboards	6.27	0.88
Large freestanding household electrical appliances subject to overturning, e.g., refrigerators and washing machines	6.69	0.73
Small countertop household electrical appliances subject to falling, e.g., microwave ovens	6.42	0.80
Household entertainment equipment subject to falling or overturning, e.g., audiovisual equipment, personal computers, musical instruments	6.95	1.16
Floor-standing furniture subject to crushing, e.g., dining tables, chairs	6.78	0.76
Heaters and air conditioning equipment subject to crushing or overturning	7.26	0.92
Indoor accessories, e.g., curtains, health and medical equipment, sporting goods, bags, shoes, carpets	7.15	1.13
Tableware	5.05	0.36
Small home entertainment items subject to falling, e.g., clocks, cameras, lights, records, CDs, toys	6.64	1.21
Clothing and bedclothes subject to damage or contamination by broken glass or other foreign matter	7.00	0.98

2.6.9. Other sources of fragility data

Kao, Soong, and Vender [1999] present an electronic database of historic damage to nonstructural components in various earthquakes since the 1964 Anchorage earthquake. Data are gathered from available literature, so their content and quality vary. The database represents an instructive attempt to impose order on heterogeneous material. The data are used in the present study to develop a set of fragility functions for elevators. The database provides details on 235 instances of seismic damage involving elevators at various facilities examined after earthquakes. In 70 records,

enough detail is provided to identify failure modes and determine a frequency of occurrence within the facility. Of these records, 30 are provided with horizontal peak ground acceleration as a measure of shaking intensity.

Swan and Kassawara [1998] present functionality fragility for a number of industrial equipment components (Table 2-4). All use peak ground acceleration as the input parameter: PGA for components at ground level, 2*PGA for components at roof level, implying that it is actually the peak diaphragm acceleration (PDA) that is the input, and that PGA is used as a proxy for PDA. These fragilities functions relate probability of operational failure as a function of acceleration. The components dealt with are all fairly rugged. The cost to restore them to operation primarily involves shifting them back to their original position and anchoring them to their slab or plinth, as opposed to replacing the component. Fragility parameters are regressed from empirical data gathered through detailed investigations of some 25 earthquakes.

Table 2-4. Miscellaneous MEP component fragilities.

Component	x_m	β
Unanchored cabinet	0.52	0.62
Motor control center	0.79	0.52
Transformer	1.23	0.62
Low voltage switchgear	1.12	0.64
Med voltage switchgear	1.60	0.80
Distribution panel	1.75	0.68
Diesel generator	0.87	0.51
Inverter	1.20	0.57
Fan	2.69	0.93

2.6.10. Fragility of complex systems

Some losses may occur as a result of the failure of complex systems. Porter, Johnson, Zadeh et al. [1993] illustrate functional relationships among equipment components using fault-tree diagrams for various equipment systems in several commercial and industrial facilities. In addition, the report presents performance data adequate to develop fragility functions with respect to operational failure and physical damage for four types of equipment systems: uninterruptible power supply (UPS), engine generators, air conditioning, and power distribution.

2.7. REPAIR COSTS AND LOSS OF USE DURATION

Peurifoy [1975] details the practice of estimating construction costs for new engineered structures. In summary, one itemizes a construction project as individual tasks to be accomplished. Each task is associated with a quantity of labor, material, and equipment required, based on an examination of construction documents. Unit costs for each item are attached, and the total direct cost is summed. Unit costs are commonly published in cost manuals such as RS Means Corp. [1997b]. Contractor overhead and profit figures are added to the total to produce the cost to the owner.

Construction duration is estimated using Gantt scheduling, in which the order and precedence relationship among individual tasks is charted on a time line, with their duration, labor involvement, start and stop dates, and slack time. Duration of individual tasks is calculated by assuming a crew size for each task, and estimating labor productivity, that is, the quantity of work that can be accomplished on that task per hour or day. Productivity for common construction tasks is published in cost manuals such as RS Means Corp. [1997b].

Wetherill [1989] discusses the application of standard cost estimation techniques to repair of existing buildings. The process is essentially the same as for new

construction, except that one accounts for additional tasks that would not be required for new construction. For example, labor, material, and equipment costs may be associated with heat and dust protection, demolition of damaged assemblies, and demolition and replacement of assemblies that may be undamaged but must be removed to access the damaged assemblies.

2.8. SEISMIC RISK MANAGEMENT MEASURES

Assembly-based vulnerability is intended to facilitate decisions regarding seismic retrofit and other risk-management measures. What resources discuss typical seismic retrofit measures?

URS/John A Blume & Associates, Engineers [1989] describes schematic measures for the seismic retrofit of various structural systems, through the addition of shear walls, through steel-frame connection strengthening, and so on. In addition, the study describes seismic strengthening schemes for various equipment and building contents. The study does not provide cost or labor estimates for these measures.

FIMS, Inc. [1987] provides detailed risk mitigation measures for building service equipment, data processing equipment, and other nonstructural components of data processing facilities. The authors describe common damage modes and schematic strengthening schemes, although construction costs are not discussed. The study is particularly useful in its detailed graphics illustrating, for example, elevator construction and modes of earthquake damage.

FEMA-74 [FEMA, 1994] and FEMA-157 [FEMA, 1989] discuss typical measures to increase seismic resistance. The former provides typical unit costs; the latter shows statistical distributions for common retrofit measures.

Anderson and Duan [1998] present analytical and experimental studies on four repair and upgrade details, finding that the best results are obtained by the use of cover plates to both flanges. SAC-95-02 [SAC Steel Project, 1995b] proposes various seismic retrofit alternatives for welded steel moment frame connections that vary depending on the nature of the damage. ATC 29-1 [ATC, 1998] presents several studies dealing with retrofit for nonstructural components.

Johnson, Sheppard, Quilici, et al. [1999] present detailed guidelines for the seismic risk evaluation and retrofit of critical equipment systems. Checklists are used to quantify equipment components and characterize their installation condition with respect to seismic resistance. The checklists provide a risk score for each component, using a basic score adjusted with modifiers to account for installation condition. The component risk score reflects the component's failure probability under the design level earthquake. Logic trees that are closely analogous to standard fault trees are constructed to describe how system operation depends on individual components. Component risk scores are then combined using a simplified approximation to fault tree analysis, producing an estimate of the probability of system failure under the design level earthquake. By repeating the process under what-if conditions, the analyst may examine the reduction of system failure probability that would result from improving the installation conditions of individual components, or by the addition of redundant components.

2.9. SEISMIC RISK-MANAGEMENT DECISION-MAKING

What frameworks exist for evaluating risk-management alternatives? Scholl and Kustu [1984] describe an earthquake-resistant design optimization technique based on minimum total cost. Total cost is taken as the sum of expected post-earthquake loss and pre-earthquake risk mitigation cost. It is assumed that expected loss and mitigation cost can each be expressed as a unique continuous function of earthquake resistance

(capacity). Expected loss monotonically decreases with capacity; mitigation cost increases with capacity. An optimal design may therefore exist where the sum of mitigation cost and expected loss is minimized (Figure 2-3).

A related approach for seismic risk management is illustrated by Kleindorfer and Kunreuther [1999] and by Kunreuther [2000]. A scalar measure of risk is evaluated as the product of discounted loss and probability. Using this scalar measure, risk-mitigation alternatives are evaluated in terms of reduction in risk versus up-front cost. If the former exceeds the latter, the mitigation measure is considered cost-effective and should be undertaken. This is the cost-effectiveness approach to risk management decision-making.

Both the least-cost and cost-effectiveness approaches can be categorized as expected-value decision-making. They assume risk neutrality, that the decision-maker be indifferent between two alternatives whose uncertain outcomes possess the same expected value of cost. Bier, Haimes, Lambert, et al. [1999] summarize the pitfalls of expected-value decision-making for rare events with severe consequences: "Essentially, expected value decision-making treats low-probability, high-consequence (i.e., extreme) events the same as more routine high-probability, low-consequence events, despite the fact that they are unlikely to be viewed in the same way by most decision-makers." In circumstances where the stakes are high and uncertainties significant, decision-makers are not risk neutral. For example, while insurance is seldom justified by the least-cost or cost-effectiveness approach, it can be nonetheless desirable and consistent with sound financial practice. Likewise, many earthquake risk-management measures are not cost effective, but are fully justified when non-neutral risk attitude is accounted for. One alternative powerful alternative to expected-value decision-making is expected-utility decision-making, which offers a framework that can account for non-neutral risk attitude. Decision analysis is such an approach.

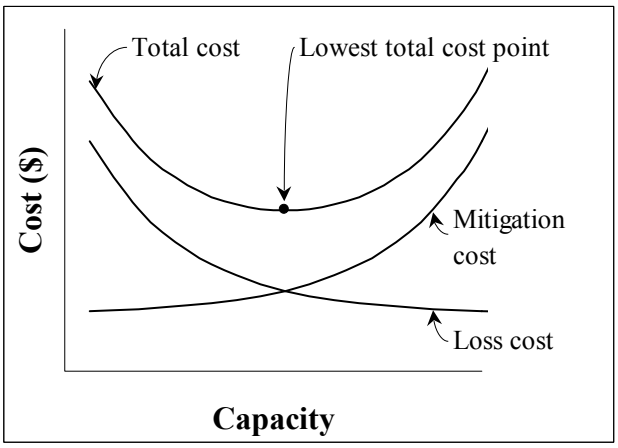

Figure 2-3. Earthquake-resistant design optimization (Scholl and Kustu, 1984).

Von Neumann and Morgenstern [1944] created the foundation for decision analysis by describing a set of rules for the mathematical treatment of decisions under uncertainty. They account for the decision-maker's risk attitude using a *utility function*, a mathematical relationship between the decision-maker's wealth state and an abstract quantity called *utility*. (Jeffrey [1965] referred to the same concept as *desirability*.) The relationship between the decision-maker's utility and his or her wealth state x is referred to as a *utility function* $u(x)$. Given five conditions outlined by Howard [1970, 1992], decision theory dictates that the most preferable alternative – the one the decision-maker *should* take if he or she is to act consistently with his or her utility function – is the one that maximizes the expected value of utility. That is, if there are several alternatives, each with a vector of possible outcomes $\underline{x} = \{x_1, x_2, \ldots x_N\}$ and associated outcome probabilities $\underline{p} = \{p_1, p_2, \ldots p_N\}$, then the preferred decision is the one with the greatest value of $E[u(x)]$, as shown in Equation 2-6. Note that N, $\underline{x}$, and $\underline{p}$ are allowed to vary between alternatives. A decision-analysis (expected-utility) approach to risk management, accounting for risk attitude, is presented in this study.

$$E[u(x)] = \sum_{i=1}^{N} p_i u(x_i) \tag{2-6}$$

What forms of utility functions are preferable? Howard [1970] shows that if the decision-maker can accept the additional condition of the delta property, then the utility curve becomes independent of wealth state. (The delta property states that if the outcomes of a particular deal are all increased by an amount Δ, the decision-maker values the new deal at the same price as the old deal plus Δ. This is a desirable feature of a decision analysis because it allows the analyst to ignore all the other unrelated financial activity in which the decision-maker is engaged that might affect his or her wealth state.) Only two mathematical forms of the utility function meet this condition: linear, which embodies risk neutrality and is therefore inappropriate in the current application, and exponential (Equation 2-7). In Equation 2-7, a is an arbitrary constant, b is an arbitrary negative constant, x represents wealth gain, and ρ is a positive constant referred to as *risk tolerance*, which reflects the decision-maker's risk attitude. A larger value of ρ corresponds to greater risk tolerance, and a closer approximation to risk neutrality. The present study applies the exponential curve to risk attitude.

$$u(x) = a + be^{-x/\rho} \tag{2-7}$$

Howard [1997] sketches a methodology for determining a decision-maker's risk attitude under the assumption of an exponential utility curve. Spetzler [1968] describes in greater detail a methodology for creating a utility function based on a series of 40 questions in which the decision-maker is asked to judge whether he or she should accept or reject a hypothetical financial deal. Each deal relates to an initial investment of $\$x_0$, yielding two possible financial outcomes, a positive outcome $\$x_1$ with probability p, and a negative outcome $\$x_2$ with probability $1 - p$. In addition, to make the question as intuitive as possible, each deal is described in terms of equivalent uniform annual cashflow and of rate of return. In each deal, the interviewer finds the probability p such

that the decision-maker (DM) is just indifferent between accepting the deal and rejecting it. After the interview, the expected utility of each deal is calculated as in Equation 2-6. Since the DM is indifferent between accepting and rejecting the final deal, it is inferred that $u(x_0) = u_{deal}$. The non-arbitrary parameters of the assumed utility function are found by regression analysis. This approach is used in the present study.

Howard [1966] summarizes the application of decision analysis for normative decision-making. First, the decision is defined, alternatives identified, values are assigned to outcomes, state variables are selected and the relationships between them established. Next, probability distributions are attached to state variables, and the decision-maker's utility curve is encoded. In the analysis, state variables are allowed to vary according to their assigned distribution, and expected value of utility calculated for each alternative. The alternative that produces the greatest expected value of utility is the preferred one.

CHAPTER 3
ASSEMBLY FRAGILITY FUNCTIONS, REPAIR COST AND REPAIR DURATION DISTRIBUTIONS

3.1. GENERAL TECHNIQUES

3.1.1. Assembly fragility functions

Each damageable assembly type is supplied with at least one fragility function. A fragility function is defined as the probability of exceeding a limit state conditioned on input structural response. The fragility function is equivalent to a cumulative distribution on assembly capacity. Each point on the cumulative distribution indicates the probability that the capacity of an assembly is less than or equal to x is $F_X(x)$. Equivalently, each point $(x, F_X(x))$ indicates that, of all assemblies subjected to a level of structural response x, the fraction $F_X(x)$ is expected to exceed the limit state in question, or finally, if a particular assembly is subjected to a structural response of level x, the probability of exceeding the limit state is $F_X(x)$.

Creation of fragility functions is potentially the most time-consuming aspect of an ABV analysis, if preexisting functions are unavailable. This chapter presents the development of ten fragility functions that are generally applicable to other ABV analyses of buildings with similar assemblies. Three methods are available for developing such functions: empirical, theoretical, and judgment-based. Empirically derived fragility functions can be developed either using earthquake experience or from laboratory data.

3.1.2. Creating empirical fragility functions

In the case of earthquake experience, the damage state of a set of J similar assemblies must be known, along with knowledge of the likely peak response to which each assembly was exposed. The response at which each assembly actually entered a damage state need not be known. The data set must be unbiased with respect to damage, that is, it must not be selected solely from damaged assemblies. Let

$$\underline{x} = \{x_1, x_2, \ldots x_J\} \tag{3-1}$$

$$\underline{d} = \{d_1, d_2, \ldots d_J\} : d_i \in \{0, 1\}, i \in \{1, 2, \ldots J\} \tag{3-2}$$

where d_i represents the damage state of assembly i, a value of 1 indicating that the assembly has exceeded the limit state in question, a value of 0 indicating otherwise. The term x_i refers to the peak response to which assembly i was exposed. The response parameter is selected to be appropriate for the assembly in question, such as peak transient drift, peak diaphragm acceleration, peak load, and so on.

When this type of (x, d) data is available, a fragility function is developed using the technique described by Swan and Kassawara [1998]. Failure frequency is calculated by dividing the number of failed components by the total number of observed components in K discrete response ranges. Median response in each range is used with calculated failure frequency in the regression analysis. The result of the regression analysis is a cumulative distribution of capacity. Let

$$\underline{r} = \{(x^*_0, x^*_1], (x^*_1, x^*_2], \ldots (x^*_{K-1}, x^*_K]\} \tag{3-3}$$

$$\underline{r}_m = \{r_{m1}, r_{m2}, \ldots r_{mM}\} : r_{mi} = (x^*_{i-1} + x^*_i)/2, i \in \{1, 2, \ldots K\} \tag{3-4}$$

$$\underline{n} = \{n_1, n_2, \ldots n_K\} \tag{3-5}$$

$$\underline{N} = \{N_1, N_2, \ldots N_K\} : \Sigma N_i = J \tag{3-6}$$

$$\underline{f} = \{f_1, f_2, \ldots f_K\} : f_i = n_i/N_i, i \in \{1, 2, \ldots K\} \tag{3-7}$$

where $r_i = (x^*_{i-1}, x^*_i]$ indicates the range of responses $x^*_{i-1} < x \leq x^*_i$, and r_{mi} indicates the median response of range r_i. Ranges can be selected at equal intervals, or dictated by equal N_i. The vector $\underline{n}$ indicates the number of assemblies in the dataset that failed by response range r_i (Equation 3-8) and $\underline{N}$ indicates the total number of assemblies in the dataset by response range r_i. The vector $\underline{f}$ then indicates failure frequency of assemblies within each response range.

A distribution is fit to the (r_m, f) data. If the distribution $F_X(x)$ has a set of parameters Ψ, the fitting is performed by minimizing the objective function $g(\Psi)$, shown in Equation 3-9. Note that the (r_{mi}, f_i) data points are independent, so it is acceptable to fit a curve to the cumulative distribution.

$$n_i = \Sigma d_j : x_j \in r_i,\ i \in \{1, 2, \ldots K\}, j \in \{1, 2, \ldots J\} \tag{3-8}$$

$$g(\Psi) = \sum_{i=1}^{K} \left(F_X(r_{mi}) - f_i\right)^2 \tag{3-9}$$

Swan and Kassawara [1998] use a lognormal distribution for capacity $F_X(x)$, measure response x solely in terms of peak ground acceleration, and d solely in terms of operational failure. The methodology is readily generalized to allow x to measure other response parameters, d to indicate limit states other than operational failure, and using distributions other than the lognormal. Several distributions can be tried. In general, for the same number of distribution parameters in $F_X(x)$, a lower value of the objective function $g(\Psi^*)$ indicates a better fit, where Ψ^* indicates the optimum value of distribution parameters for a particular distribution.

An alternative technique that uses earthquake experience data but avoids binning is to consider each assembly observation as a discrete data point (x, d), where x is a continuous variable and d is a binary variable, as shown in Equations 3-1 and 3-2. In this case, for a distribution $F_X(x)$ with parameters $\underline{\phi}$, the fitting is performed by minimizing the objective function $g(\underline{\phi})$ shown in Equation 3-10. Note that once again the (x, d) data are independent, so it is acceptable to fit a curve to the cumulative distribution.

$$g(\underline{\phi}) = \sum_{i=1}^{K} \left(F_X(x_i) - d_i\right)^2 \tag{3-10}$$

Thus, a binary regression analysis can be performed of performance data on a component-by-component basis. In theory, this approach reduces modeling uncertainty by preserving x-data that is otherwise lost to binning. In practice, the two methods

produce nearly identical results in cases where a large sample set allows for small bin sizes. The disadvantage of the binary regression is that it is difficult to assess the distribution visually, unlike the binning approach. Of course, the binary approach can be used to create the capacity distribution, which can then be checked visually using the binning approach.

A third empirical method to create fragility functions requires laboratory data of the assemblies in question, including knowledge of the structural response $\underline{x}_d = \{x_{d1}, x_{d2}, \ldots x_{dJ}\}$ at which each tested assembly $i \in \{1, 2, \ldots J\}$ exceeded the limit state in question. (Such data are typically unavailable from earthquake experience.) In this case, $\underline{x}_d$ represents the statistics of the assembly capacity, which can be used directly, or a distribution can be fit to the data.

A fourth empirical method involves creating a single fragility function for a mixture of N existing fragilities. This method is used when an assembly under consideration may be any one of several types whose fragilities are known. In the present methodology, known fragilities are represented by a probability distribution. Calculating the moments of a mixture (besides the mean) of such mixtures is not straightforward, since a mixture of random variables is not the same as a linear function of them. A simulation technique is used to determine an appropriate distribution. The simulation is straightforward. Let

N = the number of existing fragility functions

P = the membership cumulative probability distribution, i.e., that the new assembly under consideration belongs to each of the existing types

p = membership probability mass function, i.e., $p(i)$ is the probability that the new assembly belongs to existing type $i \in \{1, 2, \ldots N\}$

First, one of the N types, whose index is denoted by i, is selected at random using Equation 3-11. The capacity of the type is then simulated using the inverse method as

shown in Equation 3-12. Equations 3-11 and 3-12 are iterated many times to create a large sample set of capacity statistics, which can then be used directly or a distribution can be fit to the data. In Equations 3-11 and 3-12, u_1 and u_2 are independent samples of a uniform (0,1) random variate.

$$i = P^{-1}(u_1) \tag{3-11}$$

$$x = F_{Xi}^{-1}(u_2) \tag{3-12}$$

If no prior information is available on the membership function P, a discrete uniform distribution can be used instead, and i is selected using Equation 3-13. If the member capacities are normally distributed, the inverse method takes the form of Equation 3-14.

$$i = \lceil N u_1 \rceil \tag{3-13}$$

$$x = \sigma_i \Phi^{-1}(u_2) + \mu_i \tag{3-14}$$

3.1.3. Creating theoretical fragility functions

In cases where empirical data on the performance of the system are lacking, it may be possible to create a theoretical fragility function using reliability methods. In such a method, one or more performance functions, as shown in Equation 3-15, are created to describe the assembly. In the equation, $\underline{X} = \{X_1, X_2, \ldots X_r, \ldots X_N\}$ represents a vector of random variables relevant to capacity and demand. Their distributions and correlation must be known or estimated. In the present analysis, $\underline{X}$ contains one structural response parameter X_r that will be used as the fragility parameter.

The performance function $g(\underline{X})$ represents the difference (capacity – demand). The limit state is the boundary between a positive and negative performance function, i.e., the set of $\underline{X}$ such that capacity equals demand, $g(\underline{X}) = 0$. The limit state is exceeded when $g(\underline{X}) < 0$, i.e., when demand exceeds capacity.

The performance function can have a variety of forms; the appropriate form must be determined considering the particular conditions of the assembly and of the limit state under consideration. Equation 3-16 gives the theoretical fragility, denoted by $F_{X^*}(x)$. As shown in the equation, the fragility is equivalent to the probability of exceeding the limit state given the seismic response parameter, denoted by X_r. In Equation 3-16, the capacity is denoted by X^* to distinguish it from the vector of performance parameters $\underline{X}$.

$$g(\underline{X}): \underline{X} = \{X_1, X_2, \ldots X_r \ldots X_N\} \tag{3-15}$$

$$F_{X^*}(x) = P[g(\underline{X}) < 0 \mid X_r = x] \tag{3-16}$$

A variety of methods are available to evaluate Equation 3-16. Melcher [1999] summarizes a number of analytical and simulation approaches to assessing failure probability. In the present study, a simulation approach is employed. The performance function is created considering the conditions that would lead in theory to the failure of the assembly, for example, through bucking, tensile fracture, and so on. The vector $\underline{X}$ includes the element X_r that is hypothesized to represent the structural response parameter most strongly related to assembly failure.

First, $g(\underline{X})$ is formulated considering the materials and geometry of the assembly design under consideration. The vector X is then simulated a large number of times, controlling X_r. The failure probability $P[g(\underline{X}) < 0 \mid X_r = x]$ is then estimated by m/M, where m represents the number of trials in which $g(\underline{X}) < 0$, and M is the total number of trials. The statistics of the capacity distribution $F_{X^*}(x)$ can then be used directly as the assembly fragility, or a distribution can be fit to them. Recall that the cumulative distribution of capacity is equivalent to the probability that the assembly will fail when subjected to structural response x.

3.1.4. Assembly repair-cost distributions

For each fragility function, a probability distribution on repair cost and repair duration is prepared. Fragility functions are defined in terms of physical damage. In most cases, a common construction task is required for repair. For example, to repair a broken window requires the purchase and delivery of a replacement pane, and installation by a professional glazier. Mean labor, material, and equipment demands of most repairs are taken from published construction cost manuals, e.g., RS Means Corp. [1997b]. Dispersion on these parameters is typically unavailable and must be assumed. Cost manuals typically reflect new construction, rather than repair of existing buildings. Demolition costs must be added to account for removal of damaged material. Cost manuals also show adjustment factors to account for local construction costs. For a building in Los Angeles, for example, union labor is assumed and the local construction cost factor of 1.15 is applied.

In some cases, more than one alternative to repair is available. In such cases, one repair method must be selected, and appropriate costs modeled. The resulting vulnerability function represents the cost of repairs using the selected technique. Other techniques can be considered by creating separate vulnerability functions for each.

The general techniques described here for developing empirical and theoretical capacity, repair-cost and repair-duration distributions are now applied to a variety of assembly types. These distributions are used in Chapter 4 to illustrate assembly-based vulnerability for an example building.

3.2. DEVELOPMENT OF VARIOUS ASSEMBLY FRAGILITY FUNCTIONS

The methods described in Section 3.1 are used to create a variety of assembly fragility functions. Details of this work are provided in Appendix B, including the data and analytical techniques used to create the fragility functions, repair cost distributions, and repair duration distributions. The work is summarized in the following sections. It

includes fragility functions for a variety of structural and nonstructural assemblies and building contents.

Note that the fragility functions and cost and repair duration distributions that are detailed in Appendix B and summarized here are not intended to be definitive or all-inclusive. Rather, they represent illustrations of how the methods presented in Section 3.1 can be applied to a variety of assemblies. These examples can serve as the basis for further development of an expanding library of capacity and cost distributions.

3.2.1. Pre-Northridge WSMF connections

Earthquake experience is used to develop an empirical fragility function for the type of pre-Northridge welded steel moment frame (WSMF) connections that exhibited such surprisingly brittle behavior in the 1994 Northridge earthquake. A large database of connection capacity is available from the SAC Steel Project, which examined a number of buildings affected by the Northridge earthquake. SAC investigators examined approximately 2,300 connections in these buildings; they determined the location and nature of damage, and performed dynamic structural analyses to estimate the loads to which the connections were subjected [Engelhardt, Kim, Sabol, et al., 1995; Hart, Huang, Lobo, et al., 1995; Kariotis and Eiamani, 1995; Krauwinkler, Alali, Thiel, et al., 1995; Naeim, DiJulio, Benuska, et al., 1995; and Uang, Yu, Sadre, et al., 1995].

Two capacity parameters are available for examination: the ratio of the peak beam-end bending moment to the beam yield moment, which is referred to as the demand-capacity ratio (*DCR*); and the estimated inelastic beam-end hinge rotation (*IBHR*). When the fraction of connections damaged is plotted against *DCR*, a significant trend exists. No such trend appears to exist between connection damage and *IBHR*. Figure 3-1 shows data and curves fit to the data for two limit states. For the first limit state, failure is represented as the occurrence of any of the damage modes identified by the SAC Steel Project. For the second limit state, failure is defined as any SAC Steel

Project damage mode except incipient flange cracks and incipient weld fractures in the beam-flange-to-column weld (denoted C1 and W1, respectively).

The cost and duration to repair WSMF connections is difficult to estimate, as little published information is available. However, a construction cost estimate made for a WSMF building damaged by the Northridge earthquake was provided to the investigator, on the condition of anonymity. It shows in detail the estimator's cost estimate on a connection-by-connection basis. As a result, a probability distribution can be fit to the data, as shown in Figure 3-2. Based on the cost estimate, a probability distribution is inferred to the repair duration: a lognormal distribution with median x_m = 65 hours and logarithmic standard deviation $\beta = 0.80$. A project manager of the Parsons Corporation who dealt with the seismic retrofit of two WSMF buildings on the campus of the California State University at Northridge corroborates both the range of repair cost and repair duration [Owens, 2000].

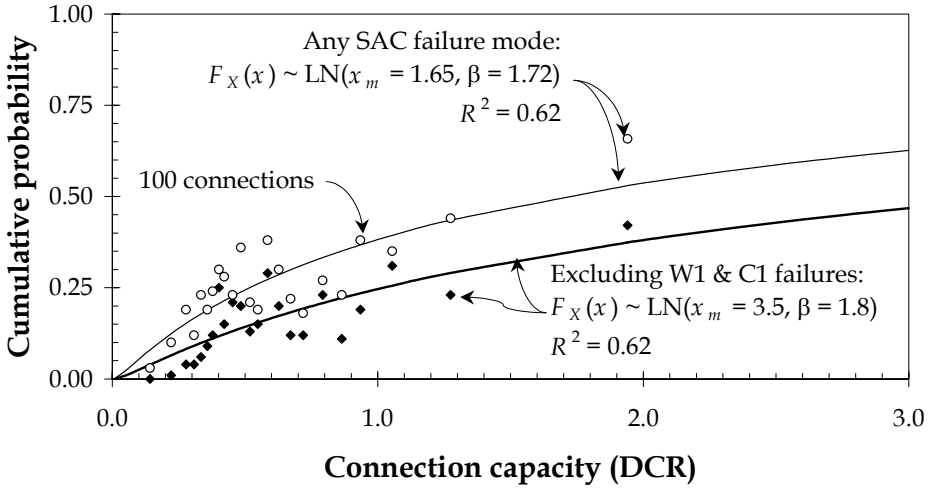

Figure 3-1. Pre-Northridge WSMF connection capacity in terms of *DCR*.

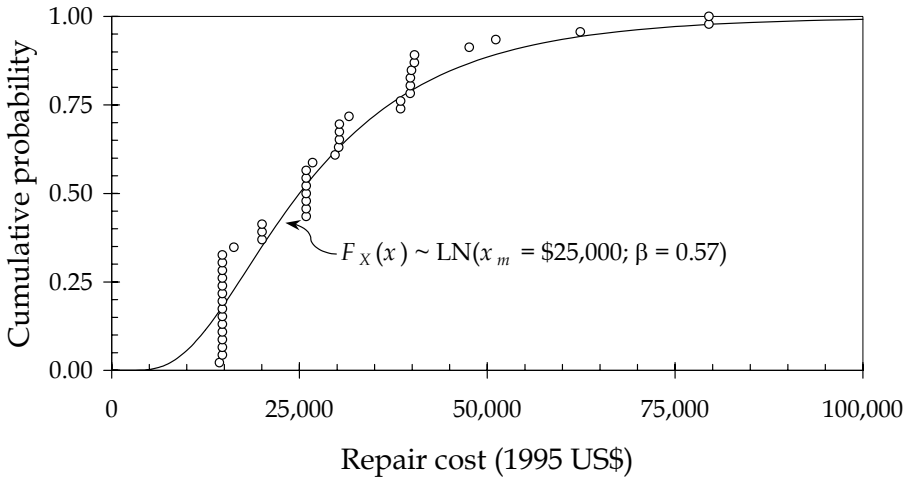

Figure 3-2. Per-connection repair cost.

3.2.2. Wallboard partitions

Rihal's [1982] experimental investigations of 8'-0 x 8'-0 building partitions are used to create fragility functions for 5/8" wallboard partitions on 3-5/8" metal stud with screw fasteners. Two limit states are identified: onset of noticeable damage (limit state 1) and onset of failure and significant damage (limit state 2). The loading condition is purely in-plane racking, and no vertical loads are applied, so the fragility results are primarily useful for nonstructural partitions of this type of construction. The resulting lognormal capacity distributions are shown in Figure 3-3.

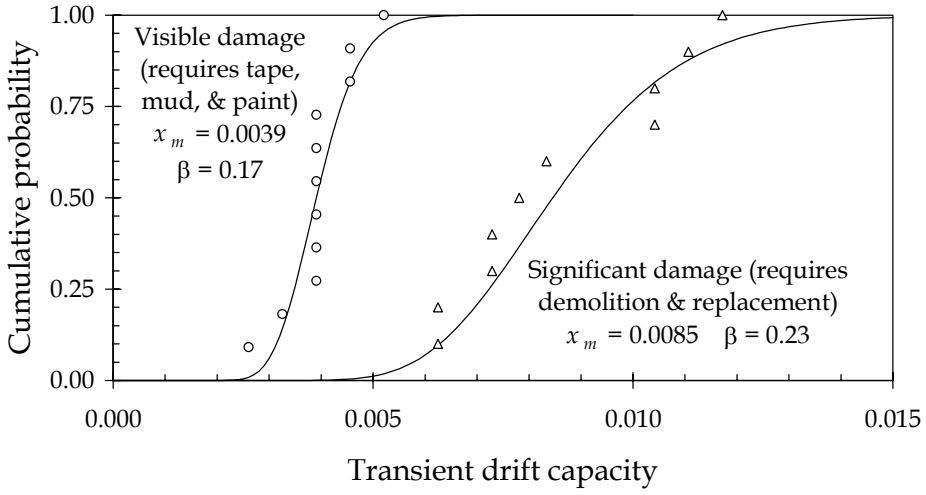

Figure 3-3. Fragility of 5/8" wallboard partitions on 3-5/8" metal-stud framing.

Repairs for limit state 1 are taken to be tape, mud, and paint, while limit state 2 is repaired by demolishing the existing wall and installing a new wall. RS Means Corp. [1997a and 1997b] is used as a basis for estimating mean repair cost and duration. A lognormal distribution is assumed, and a logarithmic standard deviation is estimated based on judgment.

3.2.3. Glazing

Behr and Worrell's [1998] laboratory test data for in-plane racking capacity of Horizon Wall glazing systems are used to create cracking and glass fallout fragility functions for 14 combinations of glazing, framing system, and sealant. The cracking and fallout fragilities for a uniform mixture of these types is shown in Figure 3-4.

This glazing system may be more rugged than other systems, such as those tested by Nakata, Itoh, Baba, et al. [1984], who reported window cracking at transient drift ratios of 0.008 to 0.014. Therefore, the fragility functions shown in Figure 3-4 are appropriate only for in-plane racking of glazing systems similar to those tested by Behr and Worrell [1998]: 5-ft by 6-ft lites with framing systems, glazing type, and sealant similar to the Horizon Wall system.

RS Means Corp. [1997a and 1997b] is used to estimate labor and material costs for installation of new glazing. Labor costs are corroborated by the U.S. Bureau of Labor Statistics [Pilot, 1998] and Dillon [1999], which also provides a measure of uncertainty on cost.

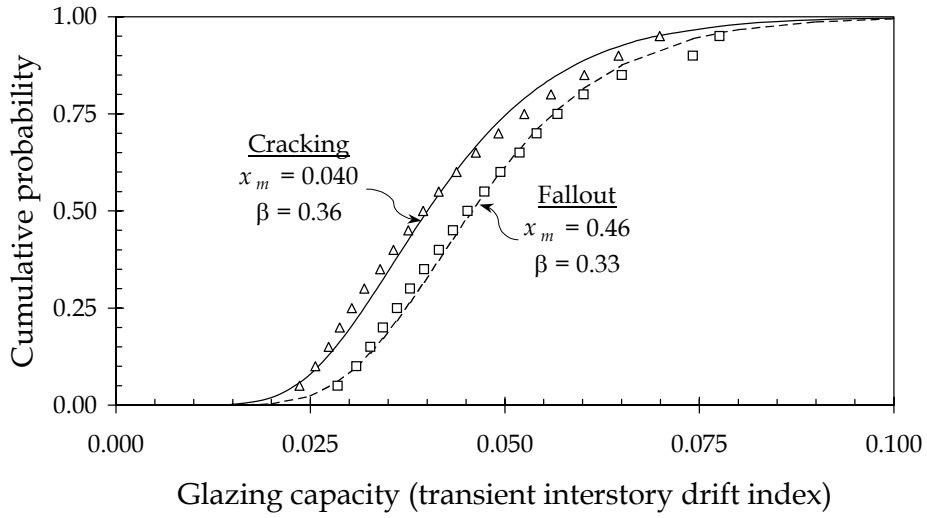

Figure 3-4. Glass fragility functions.

3.2.4. Suspended acoustical ceilings

As noted in Chapter 2, inadequate empirical data are available to create an empirical fragility function for suspended ceilings. However, member material properties and assembly geometry are readily modeled, so the theoretical approach described in Section 3.1.3 is therefore used.

It is found that ceiling collapse fragility is strongly related to ceiling dimensions. A relationship between ceiling dimensions and median capacity is shown in Figure 3-5. The logarithmic standard deviation of capacity is found to be approximately constant, at 0.80. This lognormal fragility function is intended only for use with lightweight suspended ceilings in 4-ft-by-2-ft aluminum tee-bar grid system.

Some empirical data are available to compare the theoretical fragility function with laboratory experience. Both ANCO Engineers, Inc. [1983] and Eidinger and Goettel [1998] tend to confirm the theoretical fragility. Costs and durations are estimated using RS Means Corp. [1997a and 1997b].

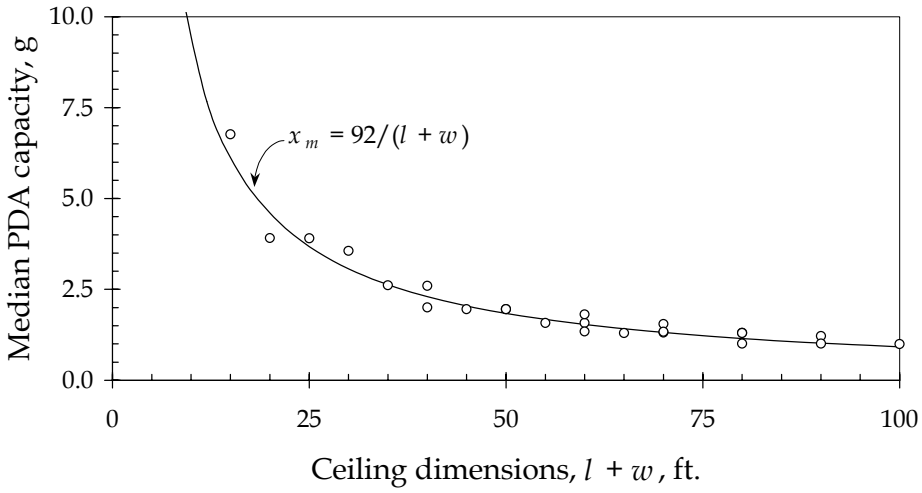

Figure 3-5. Simplified median ceiling capacity.

3.2.5. Automatic sprinklers

It is problematic to develop fragility functions for automatic sprinklers, as little published data exist and the dynamic and material properties of the system are not readily modeled. Some damage data are available from reports compiled by the Sprinkler Fitters U.A. Local 483 [1989]. Data for five buildings affected by the 1989 Loma Prieta earthquake are shown in Figure 3-6, along with a fragility function fit to the data. It is expected that research currently under consideration by the PEER Project will be able to provide an improved fragility function for automatic sprinklers.

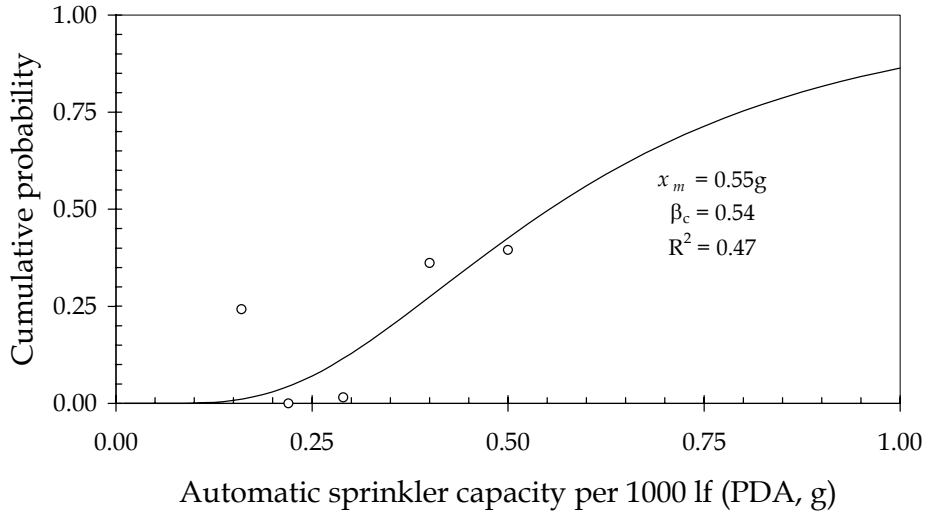

Figure 3-6. Automatic sprinkler pipe capacity.

3.2.6. Desktop computers

Jin and Astaneh's [1998] test data are used to create fragility functions for desktop computers. Two limit states are defined: limit state 1 comprises CRT monitor falloff alone. Limit state 2 comprises CRT monitor and system-unit falloff. The test data are analyzed using the binary regression technique described in Section 3.1.2. The data and fitted capacity distributions are shown in Figure 3-7. Costs are estimated based on a brief survey of computer advertisements.

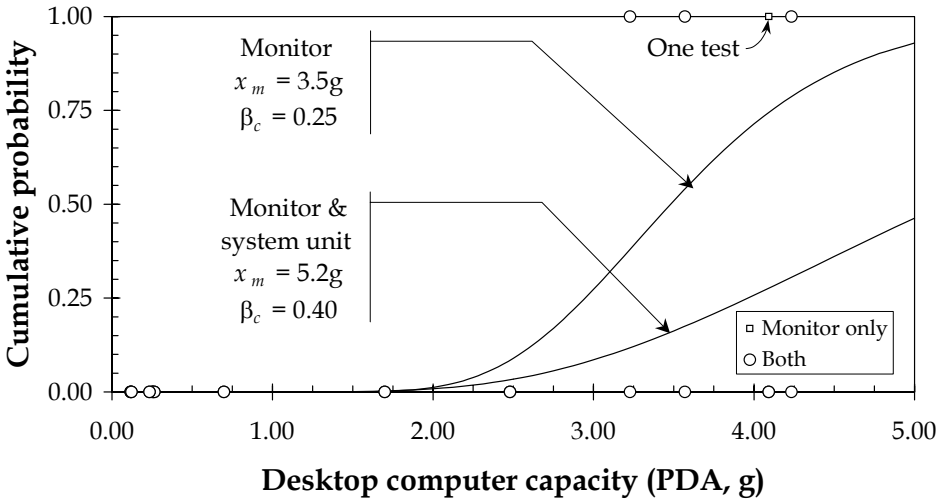

Figure 3-7. Unattached desktop computer capacity.

CHAPTER 4
METHODOLOGY FOR CREATING BUILDING-SPECIFIC SEISMIC VULNERABILITY FUNCTIONS

4.1. FORMULATION OF ABV FRAMEWORK

4.1.1. Description of seismic vulnerability function

The goal of the method is a probabilistic seismic vulnerability function for a whole building. The vulnerability function is defined in terms of the total cost resulting from damage and loss of use of the building, as functions of the ground motion. The costs are considered to be random; thus, a probability distribution or appropriate statistics are required to represent the costs. Letting C = total cost and S_a = spectral acceleration, the vulnerability function is therefore represented by $P[C \le c \mid S_a = s]$, or equivalently by the conditional probability density function $f_{C|Sa}(c|s)$, as shown in Figure 4-1. The left-hand figure shows curves corresponding to the median cost C, as well as the 16th and 84th percentiles, and illustrates the probability density of cost at a given value of s. The right-hand figure shows a normalized version of the vulnerability function, with total cost C normalized by a convenient value, denoted by V, such as building replacement cost. (The normalized variable, denoted by Y, is referred to as the total damage factor, and differs from damage factors used by other references in that it represents total cost divided by building replacement cost, as opposed to building repair cost divided by replacement cost.)

In the present formulation, the total cost is comprised of repair cost, denoted by C_R, and loss of use cost, denoted by C_U, as shown in Equation 4-1. The terms C_R and C_U are random variables with μ_{CR}, μ_{CU}, σ_{CR}, and σ_{CU}, respectively, their mean values and standard deviations.

$$C = C_R + C_U \tag{4-1}$$

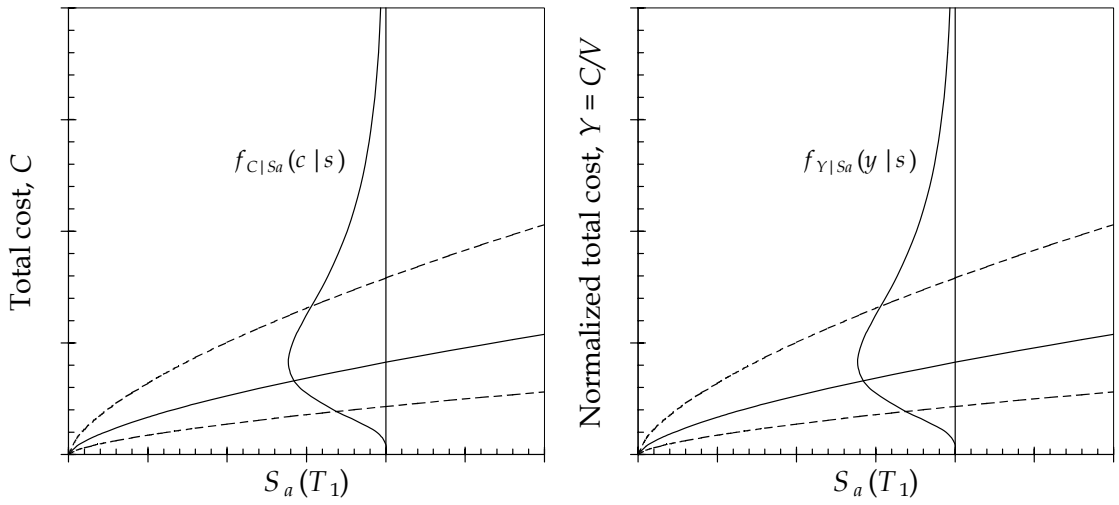

Figure 4-1. Seismic vulnerability functions.

4.1.2. Derivation of repair cost

In general, the repair cost for the building is the sum of the repair costs of individual assemblies, as shown in Equation 4-2, where C_{Ri} is the repair cost for assembly *i: i = 1, 2, … N_A*, and N_A is the number of assemblies. The repair cost for an individual assembly can vary greatly, depending on the nature of the damage, on local construction practices, and on local material and labor costs. Material and labor costs typically vary geographically, and can be strongly affected by macroeconomic conditions.

$$C_R = \sum_{i=1}^{N_A} C_{Ri} \tag{4-2}$$

The relationship between cost and the nature of the damage is considered first. A partition, for example, can experience modest damage that can be repaired by the application of mud, tape, sanding, and painting. Alternatively, the damage to the partition can be so severe as to require its demolition and replacement, which is far costlier and more time-consuming.

In the present approach, therefore, repair costs are defined by assembly type and damage state, both of which are discretized. The cost to repair one unit of assembly type

j from damage state d to the undamaged state is denoted by $C_{j,d}$, which reflects the total direct cost to the building owner, including labor, material, equipment, contractor overhead and profit. Unit repair costs are assumed to be random variables with mean and standard deviation $\mu_{Cj,d}$ and $\sigma_{Cj,d}$, respectively. Repair cost can then be restated as shown in Equation 4-3, where $N_{j,d}$ = number of assemblies of type j in damage state d.

$$C_R = \sum_j \sum_d C_{j,d} N_{j,d} \tag{4-3}$$

The unit costs, $C_{j,d}$, are readily estimated using standard construction cost estimation techniques. Mean values for common tasks are typically available in standard construction cost manuals, which also include multiplicative cost factors to account for local material and labor costs. Equation 4-4 provides $C_{j,d}$ for a particular location. In the equation, I is a factor to account for transient macroeconomic factors at the time of the repair, L is a factor to account for local costs relative to a large-scale average cost $C^*_{j,d}$.

$$C_{j,d} = ILC^*_{j,d} \tag{4-4}$$

The factor I can account for ordinary macroeconomic fluctuations, as well as post-catastrophe increases in the cost of material and labor, often referred to as *demand surge*. A value of I = 1 represents average conditions without significant demand surge. In a post-disaster environment, I could be somewhat higher, perhaps significantly so. Detailed investigation of demand surge and other macroeconomic fluctuations in repair cost is beyond the scope of the present study.

The number of damaged assemblies, $N_{j,d}$, is calculated based on the seismic fragility of individual components, and the structural response to which each component is exposed. To develop fragilities, one or more damage states, in addition to the undamaged state, may be defined for each assembly type. Limit states define the boundaries of damage states. Thus, an assembly with N limit states can be in one of N+1 mutually exclusive damage states $D \in \{0, 1, \ldots N\}$, where D = 0 refers to the undamaged

state. $N = 0$ implies that the assembly is assumed to be rugged, not damageable in an earthquake.

Each limit state is associated with a capacity distribution $F_{X_d}(x)$. The capacity distribution represents the probability that the capacity of the assembly to resist the associated limit state is less than or equal to x. The form of $F_{X_d}(x)$ can be any cumulative distribution for $x \geq 0$, as negative capacity is undefined.

The probability of the assembly reaching or exceeding limit state d given that it is subjected to structural response z is therefore equal to the probability that its capacity $X_d < z$ as defined by Equation 4-5.

$$\mathrm{P}[D \geq d | z] = \mathrm{P}[X_d < z] = F_{X_d}(z) \tag{4-5}$$

where

$D \in \{0, 1, \ldots N\}$, represents damage state, and $D = 0$ refers to the undamaged state; and

N = number of limit states defined for the assembly.

Each assembly is either undamaged ($D = 0$) or in one of several damage states $1 \leq D \leq N$. Damage states are assumed to be *progressive*, that is, $D_i < D_{i+1}$ for all i. An assembly passes through damage state d to reach damage state $d+1$. Hence, for $N > 1$, multiple capacity variables $X_1, X_2, \ldots X_N$, are considered and

$$F_{X_j}(x) \leq F_{X_i}(x) \qquad \text{for } x > 0,\ 1 \leq i < j \leq N \tag{4-6}$$

Equations 4-5 and 4-6 imply that

$$P[D = d \mid z] = P[D \geq d \mid z] - P[D \geq d + 1 \mid z] \tag{4-7}$$

Hence, a conditional probability mass function on damage state D can be created (Equation 4-8). Its summation represents the cumulative distribution of damage state conditioned on structural response, z (Equation 4-9). The random variable $N_{j,d}$ of

Equation 4-3 is determined by evaluating Equation 4-7 for each assembly of type j in the building.

$$p_{D|Z}(d \mid z) = \begin{cases} 1 - F_{X1}(z) & d = 0 \\ F_{Xd}(z) - F_{Xd+1}(z) & 1 \le d \le N-1 \\ F_{Xd}(z) & d = N \end{cases} \quad (4\text{-}8)$$

$$P[D \le d | Z = z] = P_{D|Z}(d|z) = \sum_{\delta=0}^{d} p_{D|Z}(\delta \mid z) \qquad d \le N \quad (4\text{-}9)$$

Some assemblies can be modeled as a continuous system whose damage is calculated in terms of damages per unit of assembly, that is, per unit length, area, volume, etc. Damage rate, denoted by λ, is modeled as a function of structural response. For example, pipeline damage can be quantified in terms of breaks per unit length of pipe, with break rate for a particular type of pipe and installation condition calculated as a function of structural response. The number of damage instances N_j is a random with Poisson distribution, as shown in Equation 4-10, in which $v = \lambda(z)L$, where L denotes the quantity of the distributed system, such as length of pipe, and z denotes the structural response to which the system is subjected.

$$p_{Nj|Z}(n \mid z) = \frac{v^n \exp(-v)}{n!} \qquad n \in \{0, 1, \ldots\} \quad (4\text{-}10)$$

Thus, either for discrete or continuous assemblies, damage probability is described as a function of structural response, denoted by z. The structural response is in turn a function of ground motion and structural design, and is determined using standard structural analysis techniques, such as dynamic time-history analysis of the idealized structure subjected to a particular ground motion record.

Ground motion is measured in the present methodology by spectral acceleration evaluated at the first elastic period of the building, $S_a(T_1)$. Randomness in ground motion for a given value of S_a is modeled either by the selection of a variety of appropriate real ground motion recordings or by simulation methods.

4.1.3. Derivation of loss-of-use cost

Compared with repair costs, C_R, the cost due to loss of use, C_U, is considerably more difficult to estimate. It depends on the order in which areas of the building are repaired, the repair duration for each area, and the financial consequences of loss of use of each area. The order in which areas must be repaired can depend on tenant needs, lease conditions, the owner's financial considerations, and other issues idiosyncratic to a particular building. The cost associated with loss of use can therefore be quite complex.

In cases where tenant requirements and lease conditions significantly constrain repairs, a generic approach to estimating loss-of-use cost may be impossible to formulate, although repair-task durations can inform the specific scheduling problem. In cases where such tenant and lease constraints can be ignored, a generic approach to loss-of-use cost can be formulated, after making several assumptions to simplify the problem:

- Buildings can often be divided into logical units, referred to here as operational units, in which repair tasks can be performed in series. For example, an office building can be divided into operational units coinciding with individual floors or rental suites. Different operational units can be repaired in parallel or series.

- Repairs within an operational unit are performed in an order that follows the numbering of UniFormat divisions, following standard procedure for new construction.

- In an operational area, one trade operates at a time. When that trade completes its work, the next trade is free to begin, once it completes its work elsewhere on site. If the next trade is not currently on site, a change-of-trade delay occurs. The duration of this delay varies depending on the size and complexity of the work and on labor and subcontractor availability, which may in turn depend on local economic factors. Bounding cases can be assumed: the slow-repair case has long change-of-trade

delays of days or weeks; the fast-repair bounding case has short change-of-trade delays of one or two days.

- Repairs to different operational units may begin simultaneously, if sufficient contractor labor is available. Alternatively, a contractor may concentrate on one operational unit until work for its trade is completed, then move on to the next operational unit where repairs appropriate for the contractor's trade await. These situations can be included in the bounding cases: the first, fast repair; the second, slow.

Given these assumptions, the loss-of-use cost, denoted by C_U, is related to loss-of-use duration for the operational units through a deterministic function f, as shown in Equation 4-11. In Equation 4-11, R_m represents the random time to repair restore operational unit m, and N_m refers to the number of operational units in the building. A simple case is the function shown in Equation 4-12, in which loss-of-use cost is linearly related to loss-of-use duration, as shown in Equation 4-12. The term U_m represents the known rate of loss-of-use cost, for example, the daily cost associated with an inoperative area.

$$C_U = f(R_1, R_2, \ldots R_{Nm}) \tag{4-11}$$

$$C_U = \sum_{m=1}^{N_m} R_m U_m \tag{4-12}$$

Peculiarities of individual lease arrangements are not reflected in the simple linear relationship of Equation 4-12, for example, costs associated with breaking a lease if the building is unavailable for an extended period of time, relocation costs, or costs reflecting higher lease at the temporary location of the tenant. For a specific building these costs are understood relatively well and can be easily included in a model of Equation 4-11.

The random variables R_m depend on the damage state of each assembly, the sequence of repairs, and on the availability and productivity of work crews. Some

repairs can be performed in parallel, while others are necessarily done sequentially. The sequence of repairs in any small area typically follows a logical pattern dictated by construction practice, with structural elements being repaired first and architectural finishes last. Work crews in separate areas can perform this sequence in parallel, simultaneously repairing different portions of the building.

Let R_m^* represent the time to repair operational unit m, measured in calendar days from the date on which repair work is begun anywhere in the facility. Then R_m, the time to repair operational unit m in calendar days from the earthquake, is found considering R_m^*, plus the time between the earthquake and the date on which work is begun. R_m is bounded below by repair duration for building-service equipment and repair duration for common access areas. Equation 4-13 estimates the time required to repair damage in operational unit m.

$$R_m^* = \sum_j \sum_d R_{j,d,m} + n_m R_T + R_{T0,m} \tag{4-13}$$

where

$R_{j,d,m}$ = time to restore all instance of assembly type j located in operational unit m from damage state d to an undamaged state, measured in calendar days.

R_T = change-of-trade delay, in calendar days. Can be assumed based on bounding cases.

$R_{T0,m}$ = initial delay before first task in operational unit m. Can be assumed based on bounding cases.

n_m = number of trade changes involved in the repair of operational unit m, based on the damage to assemblies in the operational unit.

The time to restore all instances of a given assembly type, damage state, and operational unit depends on the number of such assemblies, the unit repair time for each one, and the availability of work crews, as shown in Equation 4-14.

$$R_{j,d,m} = \frac{N_{j,d,m} U_{j,d}}{w_1 w_2 E_j} \tag{4-14}$$

where

$U_{j,d}$ = unit repair time, that is, the time for a work crew to restore a single instance of assembly type j from damage state d to an undamaged state. Unit repair time is taken as a random variable with mean and standard deviation $\mu_{Uj,d}$ and $\sigma_{Uj,d}$, respectively.

$N_{j,d,m}$ = number of assemblies of type j located in operational unit m that are in damage state d, a random variable dependent on assembly fragilities and on the structural response.

w_1 = number of working hours per workday.

w_2 = fraction of calendar days that are workdays.

E_j = number of crews available for restoring assembly type j. The type of work and construction practice typically determines the crew size, and E_j is based on bounding cases.

Note that $N_{j,d}$ of Equation 4-3 is related simply to $N_{j,d,m}$ of Equation 4-14 by Equation 4-15.

$$N_{j,d} = \sum_m N_{j,d,m} \tag{4-15}$$

4.2. IMPLEMENTATION OF ABV

4.2.1. Simulation approach used

Section 4.1 presents the theoretical framework for a probabilistic, assembly-based vulnerability function. Because of the large number of random variables involved, a simulation approach is used to implement the framework. A large number of simulations of cost C are performed for each $S_a \in \{s_1, s_2, \ldots s_{max}\}$. The set of (s, c) pairs represents statistics that can be used to form the vulnerability function shown in Figure 4-1. The simulation methodology involves six steps, illustrated in Figure 4-2.

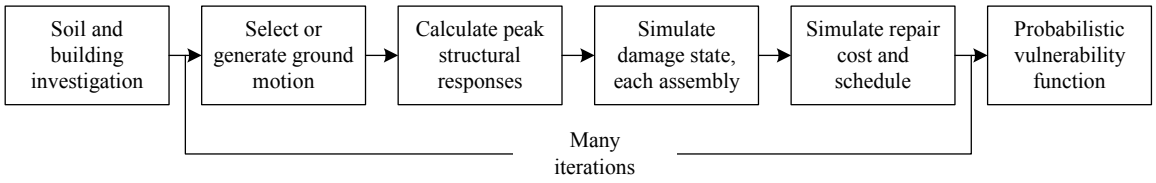

Figure 4-2. ABV methodology.

4.2.2. Soil and building investigation

The first step involves preparation for the analysis: an examination of the building in question to characterize its soil conditions and its structural and nonstructural design at the detailed level of individual assemblies. An idealized structural model is created for the building in question, and the building is divided into operational units. These are identified based on any convenient system appropriate to the use of the facility. Commercial real estate, for example, is readily disaggregated into rental suites, utility areas, and common access areas. Unit loss-of-use costs are tabulated for each operational area. An inventory is created of building assemblies, with quantities of each assembly type determined for each operational area. Assemblies are defined at a highly detailed level, similar to the RS Means Corp. [1997b] assembly numbering system. A provisional assembly taxonomy developed for ABV modeling is presented in detail in Appendix A.

Each damageable assembly in the building is provided with one or more fragility functions, as discussed in Chapter 3 and shown in Equation 4-5. Repair cost and repair duration distributions for each assembly type j and damage state d ($C_{j,d}$ and $U_{j,d}$ of Equations 4-3 and 4-14, respectively) are also prepared. The creation of these functions is one of the most time-consuming aspects of the approach. However, assemblies are defined in a standard taxonomy, so if capacity, cost, and duration distributions have already been developed for the assemblies present in the building, then these can be used directly rather than generating new distributions. The methodology is cumulative in this respect, in that a library of distributions can be developed over time and used in subsequent analyses. Existing cost functions must be adjusted to account for local construction costs and inflation.

4.2.3. Simulation of ground motion

The next step is to prepare a ground-motion time history of appropriate spectral acceleration S_a. The number of simulations required to produce a vulnerability function is prohibitively large to rely solely on historic ground motion time history recordings; hence an autoregressive moving-average (ARMA) model is used to generate sufficient artificial time histories. Recordings used as input to ARMA simulations are selected to match the site soil conditions and local faulting characteristics.

Simulated recordings are then scaled in amplitude to produce the desired value of S_a. The ARMA model is used for the present study because it has been successfully used in the past and because it generates ground motion time histories that have non-stationary amplitude and frequency content [Singhal and Kiremidjian, 1997]. In particular, a nonstationary ARMA(2,1) model is used, defined by the difference equation shown in Equation 4-16. [Conte, Pister, and Mahin, 1992; Polhemus and Cakmak, 1981].

$$a_k - \phi_{1,k\text{-}1} a_{k\text{-}1} - \phi_{2,k\text{-}2} a_{k\text{-}2} = e_k - \theta_{1,k\text{-}1} e_{k\text{-}1} \tag{4-16}$$

where

a_k = ground acceleration at time $k\Delta t$

k = 0, 1, 2, … ($T_d/\Delta t$ – 1), a discrete time-step index

T_d = duration of strong motion, sec.

Δt = sampling time interval, typically 0.02 sec

$\phi_{1,k}$, $\phi_{2,k}$ = autoregressive parameters at time $k\Delta t$

$e_k = e(k\Delta t)$ a Gaussian white-noise process with zero mean and variance $\sigma^2_{e,k}$

$\theta_{1,k}$ = moving-average parameter at time $k\Delta t$

To set up a simulated ground-motion time history, the values $\phi_{1,k}$, $\phi_{2,k}$, $\theta_{1,k}$ and $\sigma^2_{e,k}$ are regressed from a recorded ground-motion time history. These parameters provide the simulated ground motion with nonstationarity in amplitude and frequency content similar to that of the original records. In principle, a similar procedure is followed for the Y- and Z- directions. In the present analysis, a 2-dimensional structural model is used and vertical motion is ignored, hence only one ground motion time history is required for each simulation. Once the setup is completed, a simulated ground-motion time history is created in three steps:

1. Let u_k be a sample $k \in \{0, 1, \ldots T_d/\Delta t - 1\}$ from a stream of Uniform(0,1) variates.

2. Let $e_k = \sigma_{e,k}\Phi^{-1}(u_k)$

3. Apply Equation 4-16 successively for k = 0, 1, … N-1, to generate a time history, initializing with $a_{-2} = a_{-1} = 0$

4.2.4. Calculation of peak structural responses

The simulated ground motion is input to a dynamic structural analysis, to simulate the peak structural response applied to each assembly. Standard analysis techniques are used. The precise nature of the analysis (for example, linear or nonlinear

dynamic) depends on the structural response parameters that must be captured, which in turn depend on assemblies present in the building and the response parameters that are input to their fragility functions. Typically, the structural analysis must capture peak transient interstory drift ratio (*TD*) and peak diaphragm acceleration (*PDA*) at each floor and in each direction. In addition, member displacements or forces must be tabulated for structural elements. Some elements may require calculation of absorbed hysteretic energy.

4.2.5. Simulation of assembly damage states

The peak structural response imposed on each assembly, denoted by z, is then applied to assembly fragility functions to determine the probability distribution of assembly damage state, $P_{D|Z}(d|z)$, according to Equations 4-8 and 4-9. The inverse method is used to simulate damage state (Equation 4-17), in which u is a sample from a stream of uniform(0,1) random numbers. Once the damage state of every assembly is simulated, the number of damaged assemblies, $N_{j,d,m}$ and $N_{j,d}$ of Equations 4-14 and 4-3, is determined by counting.

$$d = P_{D|Z}^{-1}(u \mid z) \tag{4-17}$$

For distributed systems, the damage rate $v(z)$ is evaluated using the relationship appropriate to the assembly. The number of damage instances $N_{j,d,m}$ for such a system is then simulated by the inverse method, as shown in Equation 4-18, in which $P_{Nj|Z}(n|z)$ is the cumulative distribution whose probability mass function is shown in Equation 4-10.

$$N_{j,d,m} = P_{Nj|Z}^{-1}(u \mid z) \tag{4-18}$$

4.2.6. Simulation of repair cost and loss-of-use cost

The unit repair cost and unit repair duration, $C_{j,d}$ and $U_{j,d}$ of Equations 4-3 and 4-14, are then simulated using the inverse method, as shown in Equations 4-19 and 4-20, in which u_1 and u_2 are samples of independent streams of uniform(0,1) random numbers.

$$C_{j,d} = F_{Cj,d}^{-1}(u_1) \tag{4-19}$$

$$U_{j,d} = F_{Uj,d}^{-1}(u_2) \tag{4-20}$$

The total repair cost is then calculated using Equation 4-3. The repair duration is calculated according to Equations 4-13 and 4-14. For loss-of-use cost linearly related to repair duration, C_U is determined using Equation 4-12. The total cost is calculated according to Equation 4-1.

4.2.7. Creation of the vulnerability function

The process is repeated many times for each $S_a \in \{\Delta s, 2\Delta s, \ldots N_s\Delta s\}$, accumulating numerous (c, s) pairs for each value of S_a. The increment of spectral acceleration Δs is selected based on convenience, while the maximum value $s_{max} = N_s\Delta s$ is determined considering modeling accuracy. A non-degrading structural model, for example, cannot reflect behavior near collapse; hence the vulnerability function is limited to spectral accelerations at or below the building-code design level.

The accumulated cost data are analyzed as follows. Let $C(s)$ represent total cost conditioned on spectral acceleration, denoted s, expressed as the product of total building value, a mean normalized vulnerability function, and an error term, as shown in Equation 4-21. In the equation, V represents building replacement cost, Y represents normalized total cost (defined here as total cost divided by V), and y represents the mean value of Y. The variable Ψ is an error term with unit mean and standard deviation $\sigma_{\Psi|Sa}$. In the equation, C, Y, y and possibly Ψ are dependent on spectral acceleration, but notation of their relationship to S_a is omitted for clarity.

$$C = VY = Vy\Psi \tag{4-21}$$

In Equation 4-21, V represents the cost to construct a substantially similar facility, that is, of the same quality, size, and functionality, designed to meet the current code for new construction. This can be problematic, as in the case of historic buildings that use archaic materials such as unreinforced masonry. Such buildings cannot be replaced by

an identical structure. Furthermore, even for newer construction, "substantially similar" is a qualitative description open to interpretation, hence V could be seen as a random variable. For present purposes it is assumed that a deterministic value of V can be calculated.

Note that in Equation 4-21, V and y are treated as deterministic values, while C, Y and Ψ are random variables, with C and Y distributed similarly to Ψ, as shown in Equation 4-22. As noted in Section 4.1, the ultimate objective of the ABV methodology is to determine the distribution $F_{C|Sa}(c|s)$ of Equation 4-22. Equation 4-23 gives the mean value of C. Equation 4-24 gives its standard deviation, and Equation 4-25 gives its coefficient of variation.

$$F_{C|Sa}(c|s) = F_{Y|Sa}\left(\frac{c}{V}|s\right) = F_{\Psi|Sa}\left(\frac{c}{Vy}|s\right) \tag{4-22}$$

$$\mu_{C|Sa=s} = Vy\mu_{\Psi|Sa} = Vy \tag{4-23}$$

$$\sigma_{C|Sa=s} = Vy\sigma_{\Psi|Sa} \tag{4-24}$$

$$\delta_{C|Sa=s} = \delta_{\Psi|Sa} \tag{4-25}$$

To derive the mean normalized vulnerability function y, the cost data $\{(c, s)\}$ are transformed to $\{(c/V, s)\}$ pairs. A curve is fit to these data to represent the function $y = y(s)$. Any convenient functional form for $y(s)$ may be used.

To evaluate Ψ, the cost data are transformed to $\{(\psi, s)\} = \left\{\left(\frac{c}{Vy(s)}, s\right)\right\}$ pairs. Because cost has been normalized by V and y, a regression line relating Ψ and S should be approximately constant at 1.0, and thus the correlation coefficient $\rho_{\psi,s}$ should be approximately zero. The variance of the $\{(\psi, s)\}$ data need not be independent of s; a regression line can be fit to the $\sigma_{\Psi|Sa} = \delta_{\Psi|Sa}$ data. If the variance of Ψ is conditionally independent of s, the marginal distribution of Ψ, denoted $F_\Psi(\psi)$, is used to evaluate the vulnerability function, as shown in Equation 4-26.

$$F_{C|Sa}(c \mid s) = F_{\Psi}\left(\frac{c}{Vy}\right) \tag{4-26}$$

4.3. ABV APPLIED TO AN EXAMPLE BUILDING

4.3.1. Description of example building

The methodology is illustrated using a hypothetical three-story Los Angeles office building. The lateral force resisting system was designed by the SAC Steel Project to meet pre-Northridge standards in Los Angeles. The floor plan, gravity framing, and nonstructural design and occupancy features were created solely for the present purpose of illustrating the ABV methodology.

The building has three bays in each direction. Outer bays are 40 ft. wide; the inner bay is 30 ft. wide. There are 10-ft. chamfers on all four corners, leaving the three bays each 30 ft. wide at the perimeter walls. The building houses commercial office space. Monthly rental income is $2.50 per square foot net, i.e., calculated based on tenant square footage exclusive of common spaces, as shown in Table 4-1. The ground floor is shared by office space (Suite 100), a lobby, and building service equipment. The upper stories are devoted to office space, with Suite 200 occupying the whole of Floor 2, and Suite 300 occupying Floor 3. The total building area is approximately 36,000 sf; its replacement cost at $135/sf is approximately $4.9 million.

The structural system comprises four welded steel moment frames at the building perimeter to carry lateral loads, and an interior steel gravity frame. Diaphragms are lightweight concrete topping on metal deck. The architectural cladding is lightweight glazed aluminum panels with gypsum board on the interior side. Interior partitions are constructed of gypsum board over 3-5/8 in. metal studs with wallboard screws. Ceilings are constructed of a suspended aluminum T-bar system with lightweight lay-in tiles, fluorescent lighting fixtures, and perimeter attachment. Two gearless traction elevators provide vertical transport. Soil is firm.

Figure 4-3 shows the framing plan for the typical floor. Figure 4-4 shows one typical perimeter moment frame. The contribution of interior gravity frames to structural response is accounted for by an additional column, column line E in Figure 4-4, tied to the frame by a rigid link. Beams are A36 steel; columns are A572 Grade 50. Several assumptions are made in the structural model:

- Damping ratio $\beta = 0.05$;
- Mean values are used for yield strength instead of nominal values;
- No splice or doubler plates are used;
- Columns are fixed at the base;
- Dimensions are centerline (panel zones ignored); and
- Beams are modeled as elastic elements with springs at each end.

Schematic floor plans are shown in Figure 4-5. The assembly inventory for the example building under as-is conditions is shown in Table 4-2, which includes only assemblies whose fragility is considered in the analysis. Quantities of other assemblies are omitted for clarity. Note that the fraction of initial construction cost represented by each assembly type is not used in the present analysis, as only repair cost is relevant to the objective of the methodology.

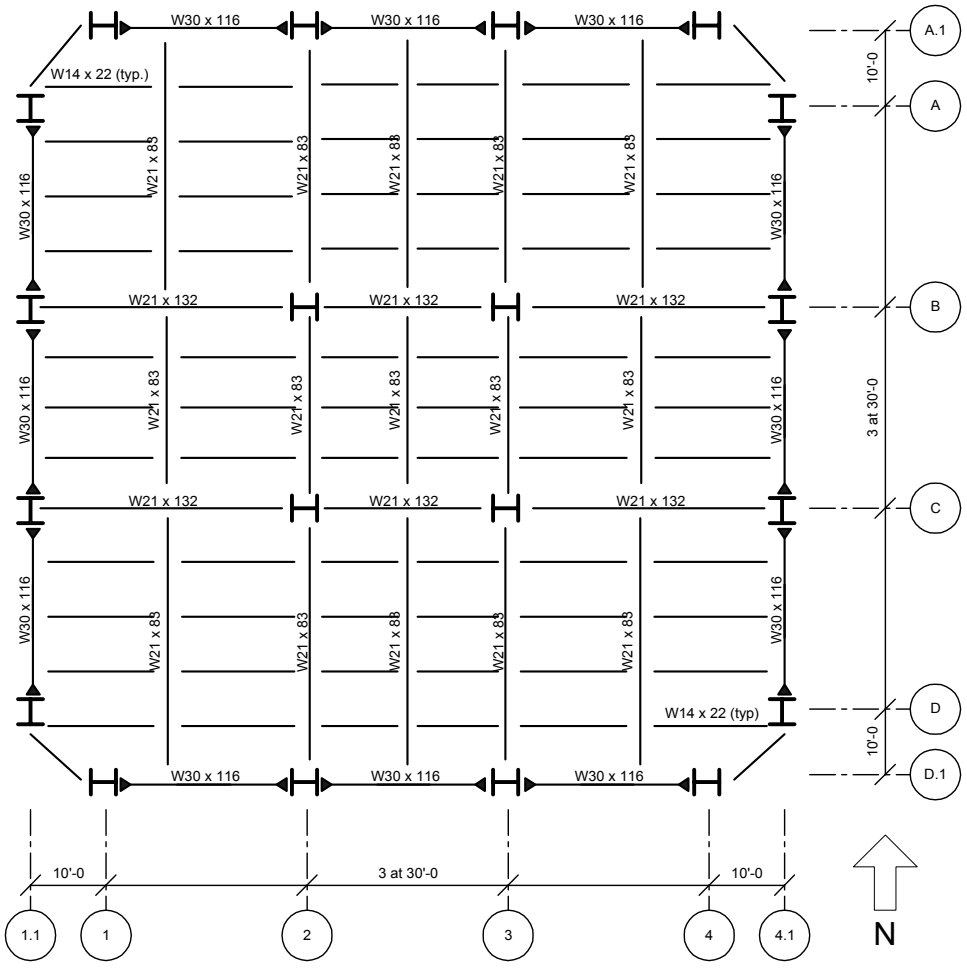

Figure 4-3. Typical floor framing plan.

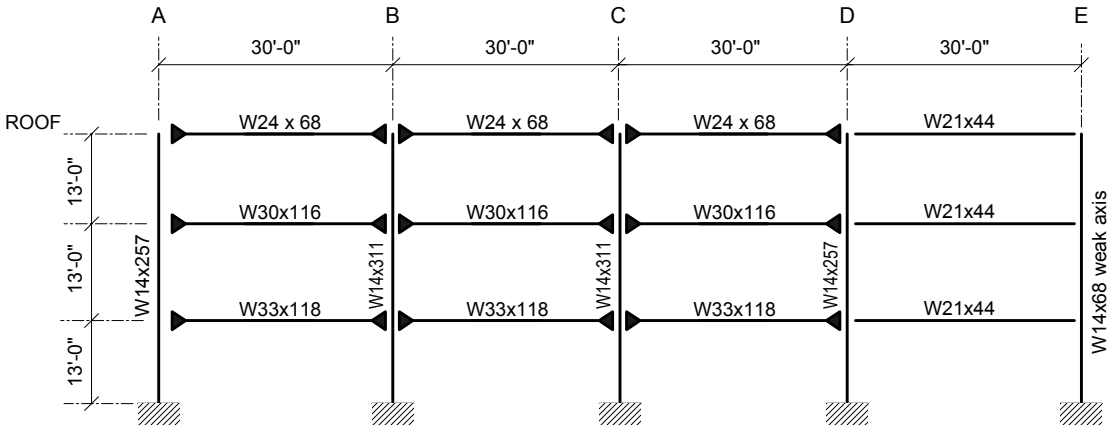

Figure 4-4. Example building structural model.

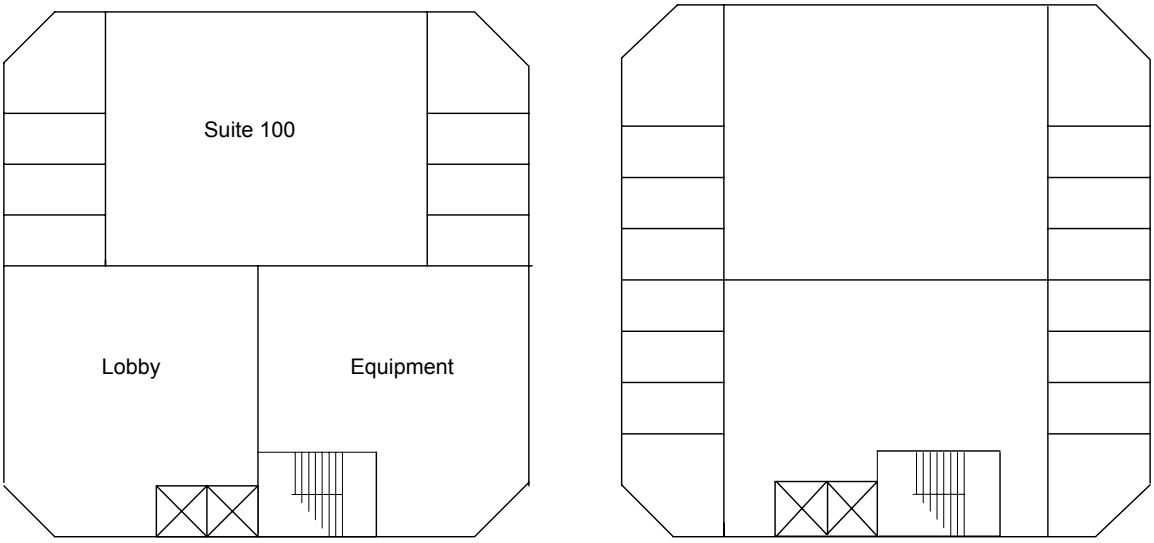

Figure 4-5. Example building schematic floor plan, 1st (left), 2nd and 3rd (right).

Table 4-1. Monthly rent for example building.

Rental unit	Area (sf)	Monthly rent
Suite 100	5,950	$14,875
Suite 200	11,900	$29,750
Suite 300	11,900	$29,750

Table 4-2. Assembly inventory considered for example 3-story office building

Assembly	Description	Unit	Lobby	Eqpmt	Ste 100	Ste 200	Ste 300	Roof
3.1.130.0002	WSMF connections pre-Northridge	ea	6	6	12	24	24	0
4.7.100.0001	Exterior glazing 5x6 panes Al frame	pane	16	0	40	72	72	0
6.1.500.0001	Drywall partition 5/8", 2 side, mtl stud,	8 lf	10	18	30	84	84	0
6.7.100.5802	Acoustical ceiling x_s in [11, 20] ft.	ea	0	0	6	12	12	0
6.7.100.5803	Acoustical ceiling x_s in [21, 30] ft.	ea	0	0	2	4	4	0
6.7.100.5806	Acoustical ceiling x_s in [51, 60] ft.	ea	1	0	0	0	0	0
6.7.100.5807	Acoustical ceiling x_s in [61, 70] ft.	ea	0	0	1	2	2	0
8.1.170.0001	Gas water heater - commercial unanchored	ea	0	1	0	0	0	0
8.2.110.0001	Wet-pipe sprinkler system unbraced	12 lf	21	21	43	83	83	0
8.4.120.0001	Chilled water cooling tower unanchored	ea	0	0	0	0	0	1
9.1.410.1001	Switchgear -- low voltage unanchored	ea	0	1	0	0	0	0
9.1.410.2001	Switchgear -- medium voltage unanchored	ea	0	1	0	0	0	0
9.2.700.0001	Motor installation unanchored	ea	0	1	0	0	0	0
9.4.310.0000	Generator unanchored	ea	0	1	0	0	0	0

4.3.2. Assembly capacity, repair cost, and repair duration

Assembly capacity, cost and repair-duration distributions are taken from Appendix B. All assembly fragilities are modeled using a lognormal capacity distribution (Equation 4-27). Units of capacity employed here are beam-end demand-capacity ratio (*DCR*), peak transient drift ratio (*TD*), and peak diaphragm acceleration (*PDA*).

$$F_X(x) = \Phi\left(\frac{\ln(x/x_m)}{\beta}\right) \tag{4-27}$$

Local construction costs (the factor L of Equation 4-4) are accounted for, and the temporal macroeconomic factor (I of Equation 4-4) is ignored, that is, set to unity. All costs and durations are assumed to be lognormally distributed.

4.3.3. Ground motions

The generation of time histories and structural analysis is performed by LeGrue and Kiremidjian [Beck, Kiremidjian, Wilkie et al., 1999]. They use as input a set of 36 earthquake ground motions created by Somerville, Graves, and Saikia [1995] for the SAC Steel Project. Table 4-3 lists the records used. For each recording, two ARMA simulations are performed according to Equation 4-16, resulting in 72 simulated records. Original and simulated recordings are then each scaled to spectral acceleration values of {0.1, 0.2, … 1.5g}, resulting in a total of 1620 records. Each record is used to create one simulation of structural response, damage, repair cost, and repair duration.

Table 4-3. Input ground motions.

SAC Name	Record	Magnitude
LA01 & LA02	Imperial Valley, 1940, El Centro	6.9
LA07 & LA08	Landers, 1992, Barstow	7.3
LA09 & LA10	Landers, 1992, Yermo	7.3
LA11 & LA12	Loma Prieta, 1989, Gilroy	7.0
LA13 & LA14	Northridge, 1994, Newhall	6.7
LA17 & LA18	Northridge, 1994, Sylmar	6.7
LA19 & LA20	North Palm Springs, 1986	6.0
LA21 & LA22	Kobe, 1995	6.9
LA27 & LA28	Northridge, 1994	6.7
LA29 & LA30	Tabas, 1974	7.4
LA45 & LA46	Kern, 1952	7.7
LA47 & LA48	Landers, 1992	7.3
LA49 & LA50	Morgan Hill, 1984	6.2
LA51 & LA52	Parkfield, 1966, Cholame 5W	6.1
LA53 & LA54	Parkfield, 1966, Cholame 8W	6.1
LA55 & LA56	North Palm Springs, 1986	6.0
LA57 & LA58	San Fernando, 1971	6.5
LA59 & LA60	Whittier, 1987	6.0

4.3.4. Structural analysis

A structural analysis of the building shown in Figure 4-3, Figure 4-4, and Figure 4-5 is performed for each ground motion record, and the resulting peak structural responses are recorded. An elastic structural analysis indicates a fundamental period of vibration of approximately 0.25 sec.

A non-degrading structural model is used, so the analysis is limited to values of $S_a \leq 1.5$g, an approximate upper bound of validity. At higher values, local and global collapse is increasingly likely and would not be reflected by the structural analysis. The emphasis of the present analysis is therefore on lower levels of damage. Furthermore, a deterministic structural model is used. In theory, the idealized structure can be generated anew for each simulation, to account for random material properties and dimensions. In the present example, these uncertainties are ignored, and a single

structural model is used for each simulation. The simulated time history is applied as input to a dynamic structural analysis of the idealized structure, and peak responses recorded.

Let $\underline{Z}$ represent the vector of peak structural responses for a single simulation. The vector $\underline{Z}$ includes *PDA* for each floor, *TD* for each floor and direction, and *DCR* for each connection. Because *DCR* is required for WSMF connections, the analysis is repeated using assumed linear elastic response, that is, with material and geometric nonlinearities removed from the model. Peak *DCR* is then recorded for each WSMF connection, and included in $\underline{Z}$. If 3-dimensional structural analyses are performed, each parameter of structural response is recorded for each direction. In the present approximation, *y*-direction peak values are assumed to be 30% of *x*-response. Structural response $\underline{Z}$ could include other parameters relevant to assemblies not examined here, for example residual interstory drift ratios (*RD)* could be calculated to determine whether exit doors are operable. The permanent ground displacement *GD* could be calculated and used as input to fragility of strip footings, buried pipeline, or slabs on grade.

The mean values of structural response are illustrated in Figure 4-6, Figure 4-7, and Figure 4-8. Transient drift (Figure 4-6) is shown for the north-south direction. The east-west TD was assumed to be 0.3 times the north-south direction. Peak diaphragm acceleration (Figure 4-7) is shown for the vector-maximum direction, again assuming east-west motion to be 0.3 times the north-south direction. Beam-end DCR (Figure 4-8) is shown for the north-south direction, with east-west DCRs assumed to be 0.3 times the north-south direction. Since the DCR is measured using a linear elastic analysis, the linear nature of Figure 4-8 is expected.

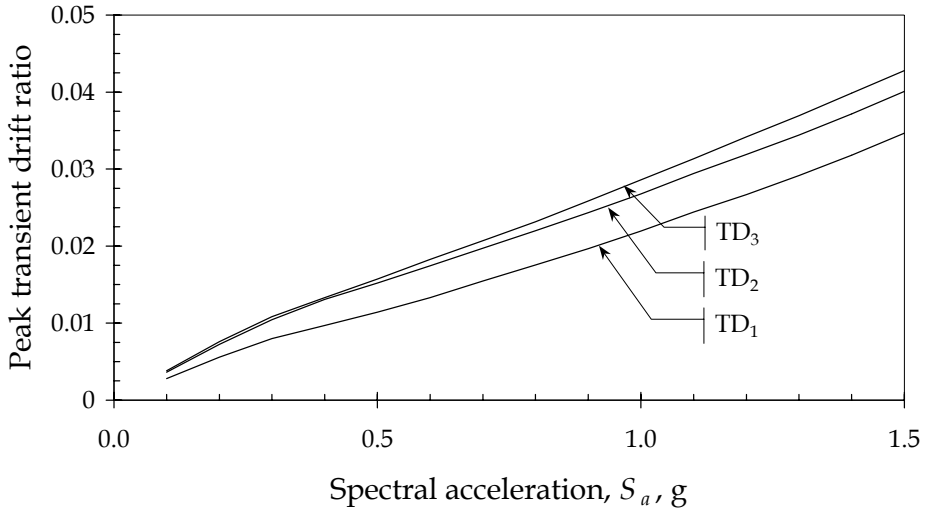

Figure 4-6. Mean transient drift (north-south direction).

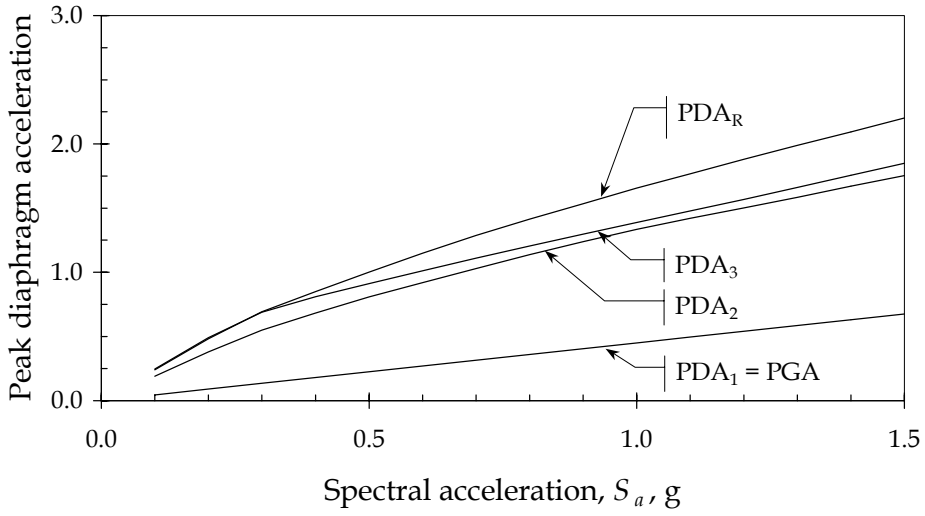

Figure 4-7. Mean peak diaphragm acceleration (maximum direction).

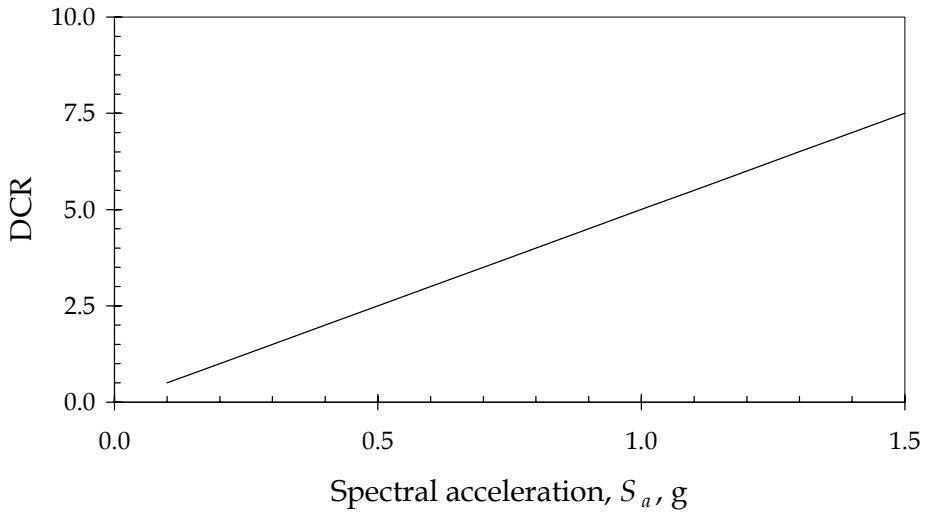

Figure 4-8. Mean beam-end demand-capacity ratio (north-south direction).

4.3.5. Damage and repair simulation

For each assembly, the probability mass function on damage state, denoted by $p_{D|Z}(d|z)$, is calculated using Equation 4-8. The assembly capacity distributions (denoted by $F_{Xd}(x)$) that are used in Equation 4-8 were specified using the procedures described in Chapter 3, and in this analysis have the distribution parameters listed in Appendix B. The cumulative probability distribution on assembly damage state, denoted by $P_{D|Z}(d|z)$, is calculated using Equation 4-9. The damage state of each assembly, denoted by d, is simulated using Equation 4-17. The number of damaged assemblies by operational unit, denoted by $N_{j,d,m}$, is calculated by counting simulated damages. The number of damaged assemblies, denoted by $N_{j,d}$, is calculated using Equation 4-15, by summing damaged assemblies per operational unit. The unit repair cost, denoted by $C_{j,d}$, is simulated using Equation 4-19, using the parameters listed in Appendix B. The repair cost, denoted by C_R, is calculated using Equation 4-3.

The time to restore each damaged assembly of type j from damage state d, denoted by $U_{j,d}$, is simulated using Equation 4-20. The probability distribution of restoration time, denoted by $F_{Uj,d}(u)$, is specified using the procedures described in

Chapter 3, using the parameters noted in Appendix B. The repair time per assembly and damage state, denoted by $R_{j,d,m}$, is calculated using Equation 4-14. The number of trade changes in operational unit m, denoted by n_m, is calculated by counting based on simulated damages.

The change of trade delay, denoted by R_T, is specified in Table 4-4, as are working hours per workday (denoted by w_1), ratio of working days to calendar days (denoted by w_2), and maximum number of crews available per repair task (denoted by E_j). The loss-of-use duration for operational unit m, denoted by R_m, is calculated using the scheduling assumptions of repair order, and considering the repair duration for each operational unit, denoted by R^*_m, which is calculated using Equation 4-13. The loss-of-use cost, denoted by C_U, is calculated using Equation 4-12. The monthly loss-of-use cost for operational unit m, denoted by U_m, is specified in Table 4-1. Finally, the total cost, denoted by C, is calculated using Equation 4-1.

Table 4-4. Bounding cases for repair scheduling of example building.

Parameter	Slow case	Fast case
Change-of-trade delay, R_T	14 days	2 days
Working hours per workday, w_1	8	16
Workdays/calendar day, w_2	5/7	7/7
Maximum crews E_j	1	3

4.3.6. Multiple simulations and the creation of a vulnerability function

Thus is completed a single simulation of ground motion, structural response, damage, repair, and total cost C. Numerous simulations are performed at each intensity increment S_a to model the distribution of C conditioned on S_a. The number of simulations required depends on the degree of accuracy required and on the observed sample variance of C. Regression analysis is performed on the simulation data to fit a curve to the relationship of C versus $S_a(T_1)$, the desired vulnerability function.

Figure 4-9 shows $\{(Y, S_a)\}$ data and a regression line y fit to total cost as a fraction of building replacement cost (that is, $Y = C/V$) for the slow-repair case. Figure 4-10 shows similar information for the fast-repair case. There are 108 data points for each S_a value in each plot. Figure 4-11 shows two regression lines for $y(s)$: one for the slow-repair case, one for fast. In addition, a third regression line shows repair cost as a fraction of building replacement cost, that is C_R/V, excluding loss-of-use cost C_U. Note that the curves for y have exponential form, but could have taken a variety of other functional forms. An exponential curve merely fit the data better than several other forms examined.

The figure shows that repair duration and repair rate significantly affect total cost. Furthermore, the figure shows that even with very detailed building-design information available, uncertainty on total cost is substantial, with the regression lines accounting for only one-third of the total variance.

Figure 4-12 shows the mean contribution to repair cost for several sets of assembly types by spectral acceleration. The figure shows that the contributions are relatively constant across the domain of S_a examined. Repair costs are dominated by WSMF connections, which represent on average 83% of the total. Collapse of suspended ceilings is the next-largest contributor, 11% of the total on average. Mechanical, electrical, and plumbing components (MEP) together comprise 4%, with the balance of 2% coming from partitions and glazing. One implication is that the uncertainty on pre-Northridge WSMF connection capacity, repair cost, and repair duration is responsible for the bulk of the uncertainty on the total cost. Thus, the failure of the mean vulnerability function to account for more of the total uncertainty is attributable in large part to pre-Northridge WSMF connections.

The error term Ψ is calculated using Equation 4-28, which is simply Equation 4-21 solved for Ψ. The mean value of Ψ, denoted by μ_Ψ, is 1.0 for both slow-repair and fast-repair cases, and its standard deviation, denoted by σ_Ψ, is approximately 0.57. The moments of the error term Ψ appear to be relatively independent of S_a, as shown in

Figure 4-13 and Figure 4-14. A lognormal distribution fits the data well, as shown in Figure 4-15, and passes a Kolmogorov-Smirnov goodness-of-fit test at the 5% significance level.

$$\Psi = C/Vy \tag{4-28}$$

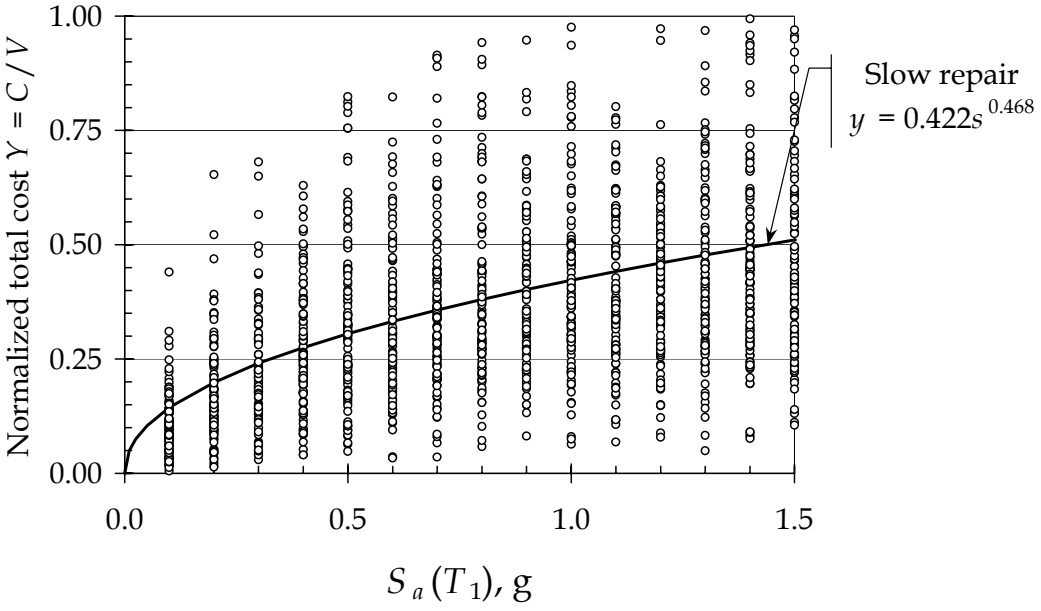

Figure 4-9. Total cost as a fraction of replacement cost, slow-repair case.

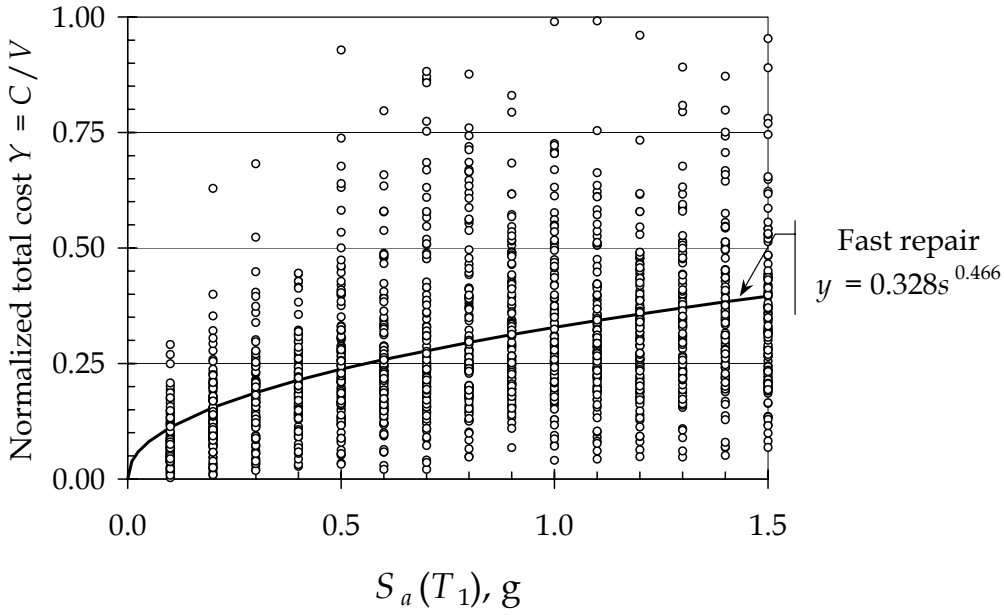

Figure 4-10. Total cost as a fraction of replacement cost, fast-repair case.

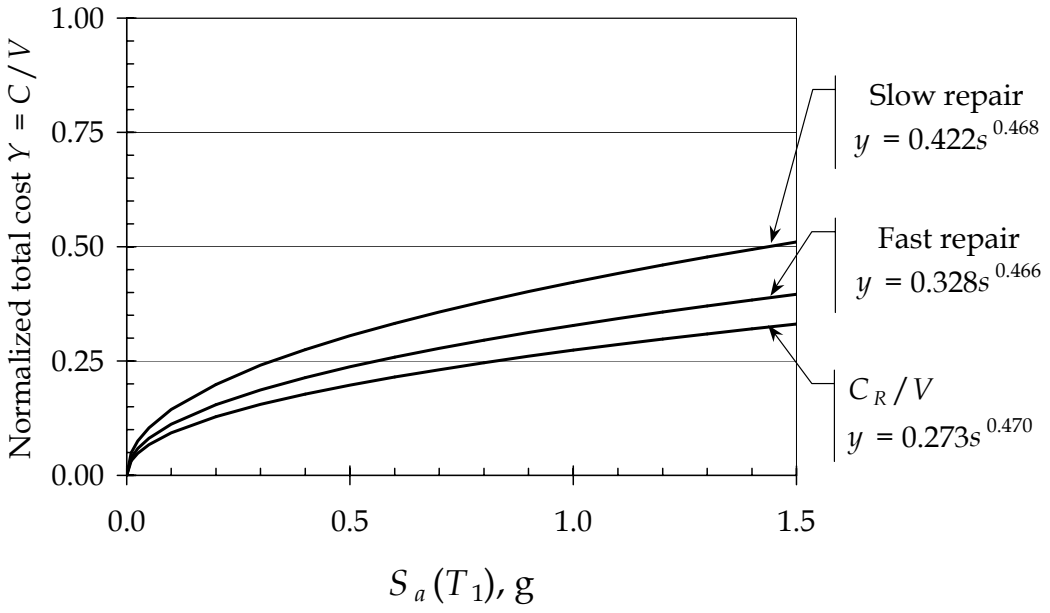

Figure 4-11. Sample building mean vulnerability functions.

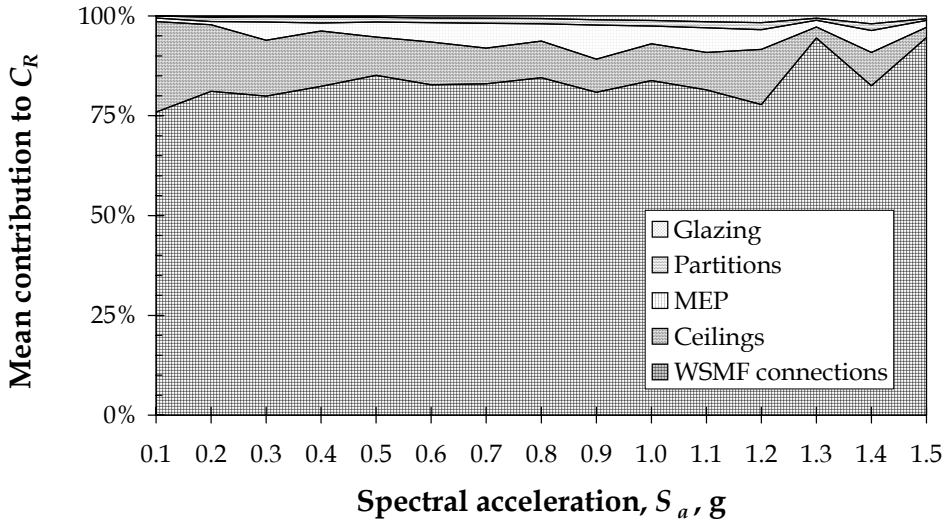

Figure 4-12. Dominance of WSMF connections in repair cost.

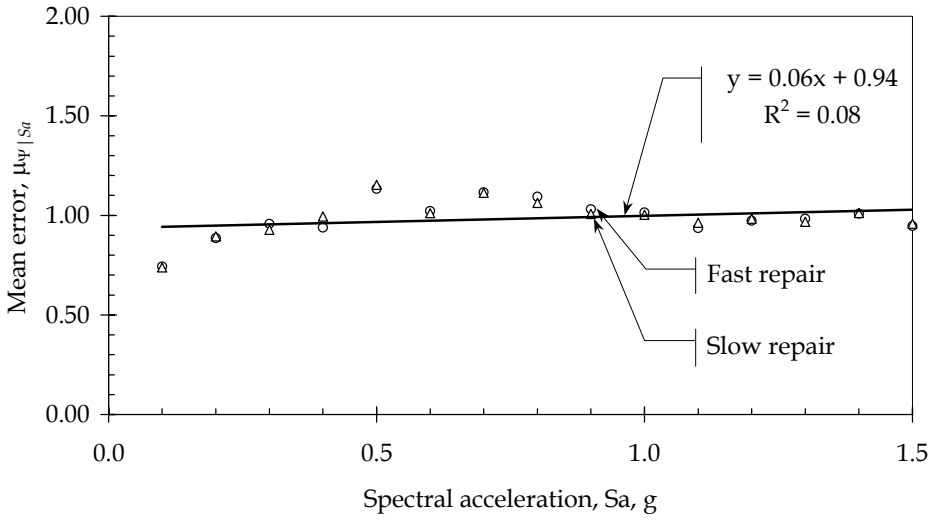

Figure 4-13. Relatively constant mean error.

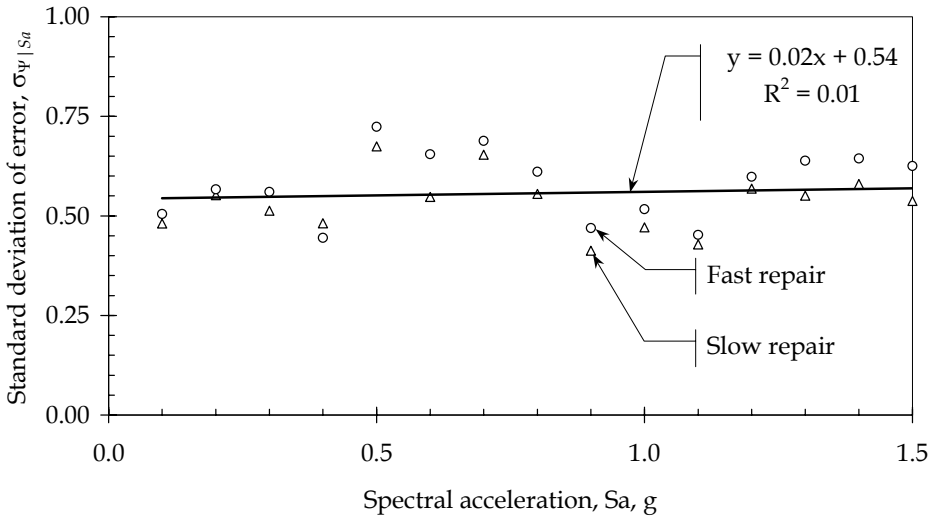

Figure 4-14. Relatively constant standard deviation of error.

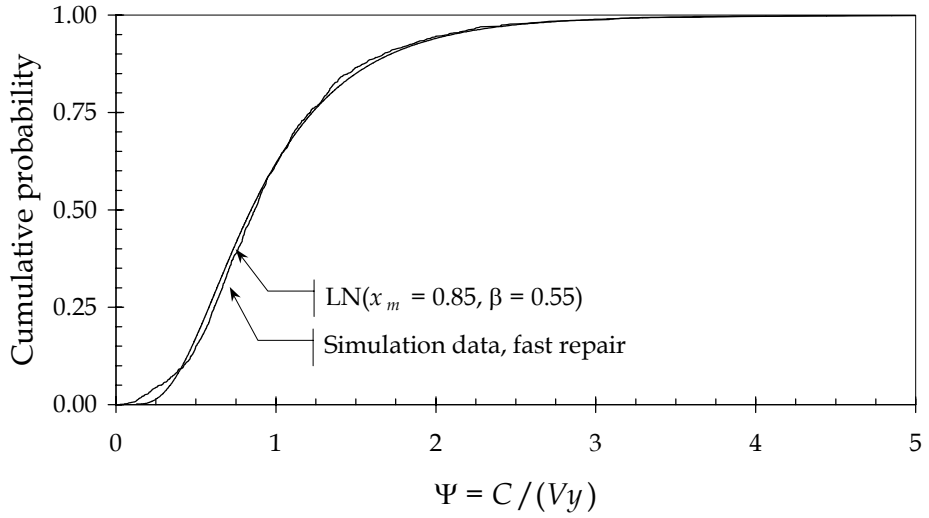

Figure 4-15. Lognormal distribution compared with error data.

4.4. DETERMINISTIC SENSITIVITY STUDY

A deterministic sensitivity study is performed to examine the effect on total cost from variation in the parameters of the ABV analysis. The analysis is somewhat simplified for the deterministic analysis. Number of damaged assemblies, denoted by N_j, is calculated using Equation 4-29, and is evaluated only for damage state d = 1. In Equation 4-29, B_j refers to the number of assemblies of type j in the entire building, and $I()$ is the step function, defined in Equation 4-30. Equation 4-29 can be compared with Equations 4-8 and 4-19, which are used for the probabilistic analysis. Repair cost, denoted by C_R, is calculated using Equation 4-31.

$$N_j = B_j I(z_j - x_j) \tag{4-29}$$

$$I(s) = \begin{cases} 0 & s < 0 \\ 1 & s \geq 0 \end{cases} \tag{4-30}$$

$$C_R = \sum_j C_j N_j \tag{4-31}$$

For purposes of the sensitivity study, a simplified loss-of-use duration for the entire building, denoted by R, is calculated using Equation 4-32. In the equation, repair-rate parameters w_1, w_2, and E_j are as shown in Table 4-4. The daily loss-of-use cost, denoted by U_U, is calculated for the entire building, based on total rented square footage and the monthly rent of \$2.50/sf. Loss-of-use cost is then calculated using Equation 4-33, and total cost, denoted by C, is calculated using Equation 4-34, which is identical to Equation 4-1.

$$R = \tfrac{1}{2}\left(\sum_j \frac{N_j U_j}{w_1 w_2 E_j} + n_m R_T \right) \tag{4-32}$$

$$C_U = R U_U \tag{4-33}$$

$$C = C_R + C_U \tag{4-34}$$

To perform the sensitivity analysis, a baseline total cost C is established using median values of spectral acceleration, structural response, assembly capacities, assembly repair costs, and assembly repair durations, using Equations 4-29 through 4-34. The calculation is repeated using median values for all parameters except one: for each parameter, the minimum value is used and total cost is calculated, and then the maximum value is used and C calculated. The procedure is repeated for all the parameters studied, and the effect on C of varying each parameter between minimum and maximum values is recorded.

For present purposes, minimum, median, and maximum values of S_a are set to 0.1, 0.5, and 1.5g. These values can be selected based on judgment of a low, medium, and high value of spectral acceleration that the site might experience. Table 4-5 shows minimum, average, and maximum values of structural response parameters *DCR*, *TD*, and *PDA*. These values are based on the median value of S_a, from the structural analyses performed as described above. Note that Table 4-5 shows average structural response parameters rather than median, as the average is more readily calculated from the structural response data.

Table 4-6 shows minimum, median, and maximum values of assembly capacity X, while Table 4-7 shows similar values of unit repair cost U_j, and Table 4-8 shows values of repair duration R_j. Minimum and maximum values in Table 4-6, Table 4-7, and Table 4-8 are set to 10th and 90th percentiles of the distributions summarized in Chapter 3 and detailed in Appendix B.

The effect of varying each parameter is measured by the absolute value of the swing in total cost C, that is, the difference between total cost calculated using the minimum and maximum value of the parameter. Spectral acceleration and the other parameters from Table 4-5, Table 4-6, Table 4-7, and Table 4-8 are then sorted in order of decreasing swing. Swing can then be plotted for each varying parameter using a graph called a tornado diagram [Howard, 1988]. The ten parameters with the greatest swing are shown in Figure 4-16. Horizontal bars in Figure 4-16 show the range of C resulting from varying each parameter between its minimum and maximum value. The vertical axis intersects C at the baseline total cost of $59,000.

The figure shows that total cost is dominated by spectral acceleration, DCR, and the capacity of pre-Northridge WSMF connections. Repair rate, nonstructural components, and the structural responses that affect nonstructural components have only secondary effect on total cost in this case. Based on these observations, it appears that efforts to reduce total cost for the example building should focus first on reducing costs associated with pre-Northridge WSMF connections. Possible means include: not requiring repair of connection failures of type W1; repair using mechanical connections that do not require preheat and post-heat; or installation of a new, stiff lateral-force resisting system to reduce demand on the existing moment frame.

Figure 4-16 shows that total cost appears to be relatively insensitive to repair rate, although Figure 4-11 shows repair rate to be a significant factor. The contradiction is explained by considering that with *DCR* and the capacity of pre-Northridge WSMF connections both set to their median values, no connection damage occurs. Hence, when all parameters except repair rate are set to their median values, repair rate is only

relevant to the repair of a few assemblies, and not to the dominant damage, that of WSMF connections.

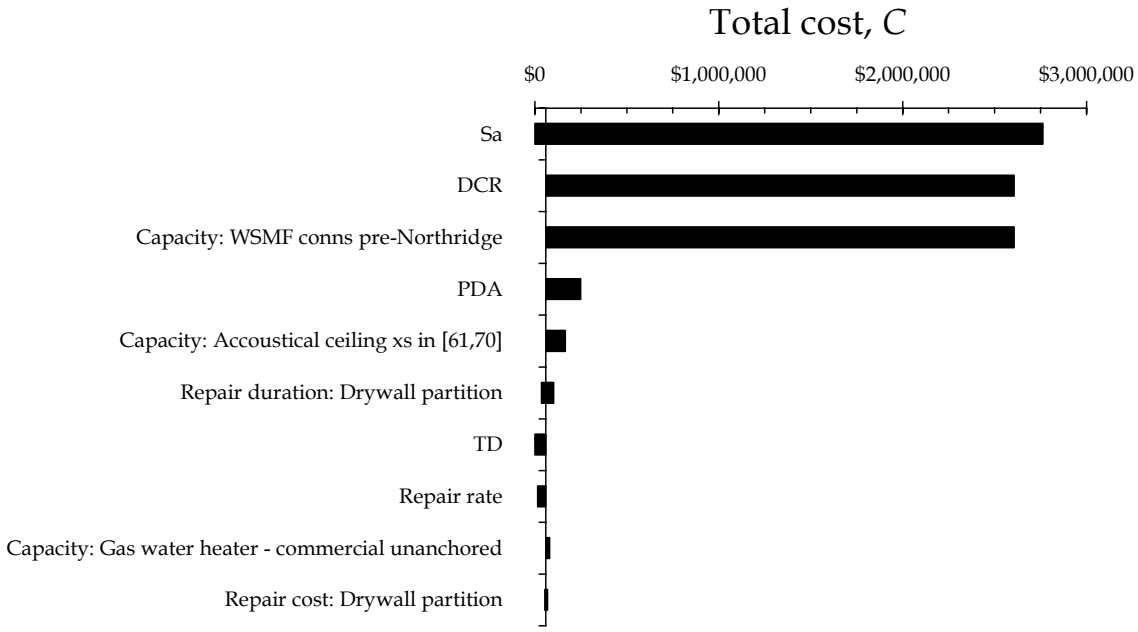

Figure 4-16. Results of deterministic sensitivity study.

Table 4-5. Structural response parameters used in deterministic sensitivity study.

Parameter	Minimum	Average	Maximum
PDA, g	0.05	0.98	2.73
IDI	0.000	0.006	0.018
DCR	0.07	0.52	1.92

Table 4-6. Assembly capacities used in deterministic sensitivity study.

Assembly type	Response parameter	Minimum	Median	Maximum
WSMF connections pre-NR	DCR	0.18	1.6	14.1
Glazing, 5x6 ft. lite, ¼ - 1 in., Al frame, elastic sealant	IDI	0.03	0.04	0.06
Drywall partition, 5/8-in., 2 sides, metal stud, screws	IDI	0	0	0
Acoustical ceiling, lightweight, Al T-bar, 2x4 frame, x_s in [11,20]	PDA	1.1	3.07	8.54
Acoustical ceiling, lightweight, Al T-bar, 2x4 frame, x_s in [21,30]	PDA	0.66	1.84	5.12
Acoustical ceiling, lightweight, Al T-bar, 2x4 frame, x_s in [51,60]	PDA	0.3	0.84	2.33
Acoustical ceiling, lightweight, Al T-bar, 2x4 frame, x_s in [61,70]	PDA	0.25	0.71	1.97
Sprinkler pipe, unbraced	PDA	2.67	16	rugged
Switchgear, low volt. unanchored	PDA	0.48	1.1	2.5
Switchgear, med. volt. unanchored	PDA	0.57	1.6	4.45
Motor installation unanchored	PDA	0.41	0.79	1.54
Generator unanchored	PDA	0.45	0.87	1.67

Table 4-7. Unit repair costs used in deterministic sensitivity study.

Assembly type	Damage state	Minimum	Median	Maximum
WSMF connections pre-NR	Fracture	11,376	23,900	50,213
Glazing, 5x6 ft. lite, ¼ - 1 in., Al frame, elastic sealant	Cracking	315	439	612
Drywall partition, 5/8-in., 2 sides, metal stud, screws	Visible damage	26	50	95
Acoustical ceiling, lightweight, Al T-bar, 2x4 frame, x_s in [11,20]	Collapse	262	497	943
Acoustical ceiling, lightweight, Al T-bar, 2x4 frame, x_s in [21,30]	Collapse	728	1,381	2,620
Acoustical ceiling, lightweight, Al T-bar, 2x4 frame, x_s in [51,60]	Collapse	3,525	6,685	12,678
Acoustical ceiling, lightweight, Al T-bar, 2x4 frame, x_s in [61,70]	Collapse	4,923	9,337	17,708
Sprinkler pipe, unbraced	Fracture	422	800	1,517
Switchgear, low volt. unanchored	Inoperative	278	1,000	3,597
Switchgear, med. volt. unanchored	Inoperative	278	1,000	3,597
Motor installation unanchored	Inoperative	278	1,000	3,597
Generator unanchored	Inoperative	1,390	5,000	17,983

Table 4-8. Unit repair durations (hours) used in deterministic sensitivity study.

Assembly type	Damage state	Minimum	Median	Maximum
WSMF connections pre-NR	Fracture	23	65	181
Glazing, 5x6 ft. lite, ¼ - 1 in., Al frame, elastic sealant	Cracking	0	0	1
Drywall partition, 5/8-in., 2 sides, metal stud, screws	Visible damage	1	1	2
Acoustical ceiling, lightweight, Al T-bar, 2x4 frame, x_s in [11,20]	Collapse	2	4	7
Acoustical ceiling, lightweight, Al T-bar, 2x4 frame, x_s in [21,30]	Collapse	5	10	19
Acoustical ceiling, lightweight, Al T-bar, 2x4 frame, x_s in [51,60]	Collapse	26	48	92
Acoustical ceiling, lightweight, Al T-bar, 2x4 frame, x_s in [61,70]	Collapse	36	68	128
Sprinkler pipe, unbraced	Fracture	1	1	2
Switchgear, low volt. unanchored	Inoperative	2	8	29
Switchgear, low volt. anchored	Inoperative	2	8	29
Switchgear, med. volt. unanchored	Inoperative	2	8	29
Motor installation unanchored	Inoperative	2	8	29
Generator unanchored	Inoperative	4	16	58

4.5. CHECKING THE REASONABLENESS OF THE RESULTS

The question of how reasonable are the results shown in Figure 4-11 is now addressed. One interesting point is that the highest simulation of (total cost/replacement cost) for S_a = 0.1g exceeds the lowest simulation at S_a = 1.5g. It is tempting to say that this defies reasoning, since the shaking of the latter case is 15 times that of the former, but such an observation is misleading. It is more meaningful to consider two similar (though not necessarily identical) buildings: Building A is shaken at S_a = 0.1g, while Building B is shaken at S_a = 1.5g. Now consider the probability that Building A would experience damage exceeding that of Building B. Both buildings fit the description of the example building, and thus have the same vulnerability function using ABV.

Let Y_A represent the total cost as a fraction of replacement cost (C/V) at S_a = 0.1, and Y_B represents this ratio at S_a = 1.5g. The two cumulative distributions $F_{YA}(y)$, $F_{YB}(y)$ can be plotted on the same axis, to help visualize the overlap at these widely disparate values of S_a. The curves for the fast-repair case are shown in Figure 4-17. There is a 78% probability that the first building would experience cost less than 10% of value, whereas there is only a 2% probability of the second building experiencing that level of cost or less. It is virtually certain that the first building would experience cost less than 30% of value, whereas the second building is more than likely (53%) to experience greater cost.

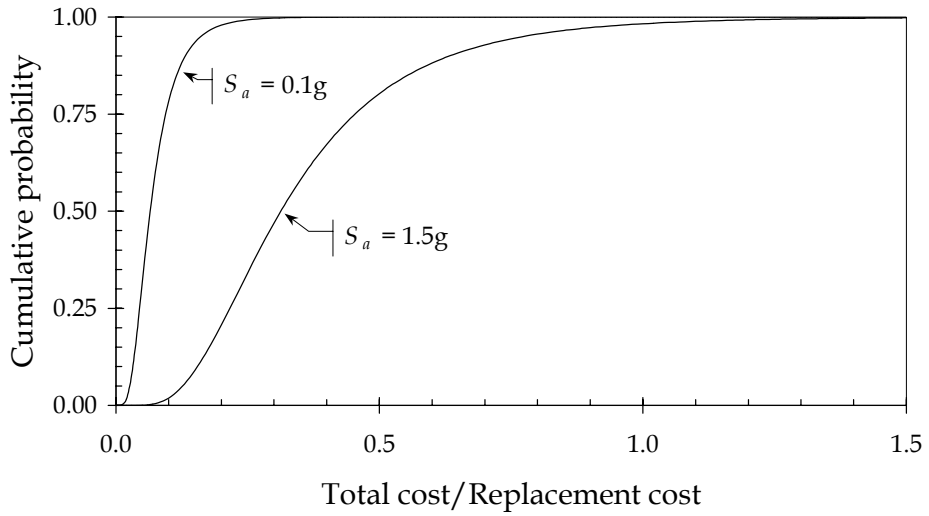

Figure 4-17. Overlap in cost as a fraction of value at extremes of S_a.

Consider now the probability that the first building experiences damage in excess of the second. The probability $P[Y_A > Y_B]$ is given by Equation 4-35. For lognormal Y_A and Y_B with mean values μ_y = 0.076 and 0.36, respectively, and logarithmic standard deviation of 0.54, Equation 4-21 evaluates to be 0.022. Considering the sample data of 108 simulations each of Y_A and Y_B, there are 11664 pairs (Y_A, Y_B). One would therefore expect 0.022*11664 = 257 pairs to satisfy the condition $Y_A > Y_B$. In fact there are 376 such pairs in the simulation, for a sample probability $P[Y_A > Y_B]$ = 3.2%, close to expectation. Thus the observed overlap is mathematically consistent.

$$P[Y_A > Y_B] = \int_{s=0}^{\infty} \int_{t=0}^{s} f_{YA}(s) f_{YB}(t) dt ds \tag{4-35}$$

$$P[Y_A > Y_B] = \int_{b=0}^{\infty} \int_{a=b}^{\infty} f_{YA}(a) f_{YB}(b) da db \tag{4-35}$$

The next question is whether this feature of the example vulnerability function is reasonable from an engineering standpoint. The question might appear to be whether there is a 3% probability that two identical buildings, one shaken with S_a = 0.1g, the other with S_a = 1.5g, would result in total cost to the first exceeding total cost to the

second. However, to state the question this way indicates an erroneous reading of the vulnerability function. This is an important point: two buildings need not be identical to be described by the same vulnerability function.

The vulnerability function estimates (as a function of S_a) the total cost for any building fitting the description of the model, that is, any building having the model's structural system, geometry, and inventory of assemblies. Within that building description and for that S_a, significant variability is allowed:

- Precise ground motion record. One S_a value can describe an infinite variety of earthquake ground motions.

- Details of assembly construction. For example, one fragility function is used to model any pre-Northridge WSMF connection, regardless of weld quality, presence of backing bar, and so on. Similarly, for a single fragility function, there is a great deal of variety allowed in the details of suspended ceiling construction, gypsum-board wall partition, glazing, and so on.

- Repair needs. For example, congestion of MEP components near a damaged WSMF connection can vary greatly, and strongly affect actual repair cost and duration. A single repair-duration distribution is used, with large enough uncertainty to account for the variability of actual conditions.

- Contractor material cost, labor costs, and productivity. These parameters also vary in practice. The owner of the first building could engage an inefficient or inexperienced contractor, while the owner of the second building hires a highly experienced and efficient contractor. Such variability is accounted for in the cost distributions.

In sum, these uncertainties are accounted for in the ABV model, and are reflected in the uncertainty of the resulting vulnerability function. The ABV method does not

uniquely and completely define a particular building, damage state, or contractor, but merely describes them in far more detail than do category-based approaches. To impute greater resolution to the model is to misunderstand its probabilistic nature.

It is problematic to check this result. Few if any engineers have the experience of examining two such similar buildings after an earthquake and little if any data are available from past earthquakes to justify the answer, and the accuracy of opinions of probability without such experience is problematic, particularly in regard to estimating uncertainty. As shown by Spetzler and Von Holstein [1972], experts tend to underestimate uncertainty in probability judgments as a result of unconscious and inappropriate assumptions, unless great care is taken to avoid heuristic biases.

However, some information is available for comparison purposes. As noted in Chapter 2, a great deal of expert opinion of seismic vulnerability is embodied in ATC-13 [ATC, 1985]. For convenience of comparison then, let the problem be restated in terms of the mean and variability of cost at various levels of ground shaking. Could the expected total cost at S_a = 1.5g be 5 times that at 0.1g, and could the logarithmic standard deviation of cost be 0.55 in both cases? Suppose that S_a = 0.1g equates with Modified Mercalli Intensity (MMI) of VI, and S_a = 1.5g equates with MMI IX or X. Using the ATC-13 [ATC, 1985] damage probability matrix for low-rise, steel perimeter moment frame (facility class 15) at MMI VI, IX, and X, mean damage is estimated to be, respectively, 0.015, 0.069, and 0.171, suggesting a ratio of damage factor at S_a = 1.5g to that of 0.1g of 4 to 11 times. Thus, the ATC [1985] damage probability matrix for low-rise steel perimeter moment frame tends to support the 5-times increase in mean damage estimated using ABV.

The coefficient of variation at these intensity levels is estimated to be 1.3, 0.7, and 0.3, respectively. Although these tend to agree with the 0.65 logarithmic standard deviation of 0.55, the comparison is somewhat apples-to-oranges, as the ATC [1985] data are intended to reflect a wider variability in detailed design and shaking than is allowed by the ABV model. The ABV uncertainty should be below all those of ATC [1985], since

the former embodies less randomness in detailed design. Assuming that the ATC [1985] experts tended to underestimate uncertainty, the values of 1.3, 0.7, and 0.3 are probably low, and the ABV-based value of 0.65 (at least for this particular building) is a more reasonable estimate of uncertainty.

CHAPTER 5
USING ASSEMBLY-BASED VULNERABILITY IN SEISMIC RISK-MANAGEMENT DECISIONS

5.1. RISK-MANAGEMENT DECISIONS

Assembly-based vulnerability (ABV) provides probabilistic estimates of financial loss on a building-specific basis without extensive reliance on expert judgment. These estimates can be used to support operational guidelines businesses use to manage seismic risk. For example, lenders and insurers routinely apply loss estimates to underwriting guidelines during decisions such as whether to insure a building owner, whether to underwrite a commercial mortgage, and how much reinsurance to buy. ABV can be used to inform the decisions.

Another important application of ABV is a building owner's decision regarding risk mitigation: whether to purchase earthquake insurance; whether to perform seismic retrofit; what kind of emergency planning should be performed; and where to add operational redundancy. Where business guidelines do not exist, decision analysis can be used with ABV to identify alternatives that optimize expected utility. This chapter presents procedures for both types of analysis.

5.2. USE OF ABV TO ESTIMATE INSURANCE AND LENDING PARAMETERS

Lenders and insurers commonly make underwriting and reinsurance decisions based on estimates of risk. Two parameters of risk that insurers and lenders use are probable maximum loss (*PML*) and pure premium, which is also known as expected annualized loss, denoted *EAL*. This study does not address the guidelines lenders and insurers use to make risk-management decisions, such as what if any *PML* is appropriate for a lender to use as a threshold for requiring the borrower to purchase insurance. However, ABV can be used to estimate the *PML* and *EAL* that appear in those guidelines, as follows.

There is no universally accepted quantitative definition for *PML* [ASTM, 1999; Rubin, 1991]. One common definition of *PML* is the loss associated with a (stated) high probability of non-exceedance during a stated period of time, considering all possible ground motions at the site of the building.

In another definition, and the one that is used for present purposes, *PML* is defined as the level of loss with non-exceedance probability $F_{C|Sa}(c|s) = p$, conditioned on the occurrence of a spectral acceleration $s = S_a(T_1)$ with return period T. Considering an insurance policy with deductible denoted d and limit of liability denoted l, ABV can be used to determine the *PML* as shown in Equation 5-1.

$$PML = q\left(F^{-1}_{C|Sa=s_f}(p)\right) \tag{5-1}$$

where

$$q(c) = \begin{cases} 0 & c < d \\ c - d & d \le c < d + l \\ l - d & d + l \le c \end{cases} \tag{5-2}$$

$q(c)$ = claim associated with insured loss of c, from Equation 5-2.

$F_{C|Sa}(c|s)$ = cumulative probability distribution of cost C conditioned on spectral acceleration S_a, from Equation 4-23.

p = non-exceedance probability associated with the *PML*

c = insured loss

d = deductible, the amount the insured must pay before the insurer will pay

l = limit of liability, the maximum loss amount for which the insurer is liable

The pure premium, or *EAL*, is the amount of premium an insurance company would have to collect from a policyholder to equal the expected value of claims against

that policy, without loadings for the insurer's expenses, premium taxes, contingencies, and profits. Equation 5-3 gives the expected annualized loss, *EAL*.

$$EAL = \int_{s=s_0}^{S_m} \int_{c=0}^{\infty} -q(c) f_{C|Sa}(c \mid s) \nu'(s) dc ds \tag{5-3}$$

where

S_m = maximum spectral acceleration considered.

$f_{C|Sa}(c \mid s) = \mathrm{d}F_{C|Sa}(c \mid s)/\mathrm{d}c$

$\nu'(s) = \mathrm{d}\nu(s)/\mathrm{d}s$

$\nu(s)$ = annual rate of events with $S_a > s$.

Equation 5-3 implies that if more than one earthquake affects the building during the period of interest, the building is restored to its pre-earthquake condition and the policy is reinstated. Since earthquake insurance policies are typically written on an annual basis, and since it is unlikely that two damaging earthquakes occur during the policy period, this assumption is reasonable. The development of the probabilistic seismic hazard data $\nu(s)$ are treated in depth elsewhere, and will not be detailed here.

5.3. PRINCIPLES OF A RISK-MANAGEMENT DECISION ANALYSIS USING ABV

In contrast with decisions based on *PML* and pure premium, risk-management decisions by a building owner or occupant are more important, because pre-established guidelines for managing seismic risk do not exist in most companies outside the insurance and banking industry. The framework for a decision-analysis approach to the risk-mitigation decision is presented here.

A decision analysis requires examining the decision from the perspective of the person who has final authority to allocate resources to risk management. This person is referred to as the decision-maker (DM). The DM may be a building owner, occupant,

insurer, or other stakeholder. As noted in Chapter 2, decision analysis requires three basic elements: alternatives, information, and preferences. As applied for seismic risk management, these elements are represented by risk-management options (alternatives); the seismic hazard at the building location and ABV loss estimates (information); and DM's utility function, planning period, and cost of capital (preferences). The framework for performing the decision analysis is described in the following subsections, which are followed by a method to implement the decision analysis, and a sample application using the example building.

5.3.1. Risk-management alternatives

The owner's risk-management alternatives include various levels of earthquake insurance and of seismic retrofit, along with a variety of emergency planning alternatives. Retrofit alternatives can range from the relatively inexpensive to the very costly. Inexpensive options can include modifications to installation conditions of equipment and content assemblies by anchoring or bracing. Moderate-cost options include modifications to distributed systems such as sprinkler systems. High-cost options include modifications to the lateral force resisting system of the building. Specific measures depend on the demands and design of the specific building in question, as discussed in Chapter 2. Effective retrofit can be expected appreciably to reduce repair costs and repair durations, and hence loss-of-use costs, in the event of an earthquake.

Emergency planning alternatives do not reduce repair costs, but can appreciably reduce loss-of-use cost in the event of an earthquake, either by hastening repairs or by enabling the building to be used sooner despite damage. Their effects on loss-of-use duration are idiosyncratic to the building and the emergency plan. These effects should be apparent to the modeler considering a specific building and emergency plan.

Let N_a represent the number of mutually exclusive risk-management alternatives available to the DM. The objective of the decision analysis is to select the "best" alternative $a \in \{1, 2, \ldots N_a\}$.

5.3.2. Seismic hazard analysis, mitigation cost, and post-earthquake cost

Distinct from the alternatives is the information that affects the value of the outcome. That is, the information comprises the deterministic and random variables that relate the alternative to the outcome. Key information to be considered includes the following. Note that several of the parameters can depend on the alternative a selected. For clarity, the notation omits reference to the selected alternative. Let:

T = the owner's planning period

i = the owner's discount rate

C_0 = the present value of the cost of the alternative, for example the construction cost of a seismic retrofit.

R = present value of the facility to the owner, including revenue expected during the planning period and the liquidation value at the end of the planning period, but omitting the cost of the risk-management alternative. This value may depend on alternative a.

$N \in \{0, 1, \ldots \infty\}$ = the number of damaging earthquakes occurring within the planning period T

$\underline{T} = \{T_{e1}, T_{e2} \ldots T_{eN}\}$, representing the times to damaging earthquakes 1, 2, … N, where $T_{e1} < T_{e2} < \ldots T_{eN} < T$

$\underline{S} = \{S_1, S_2, \ldots S_N\}$, the spectral accelerations resulting from earthquakes 1, 2, … N

$\underline{C} = \{C_1, C_2, \ldots C_N\}$, the total costs resulting from earthquakes 1, 2, … N.

$q(c)$ = the liability function, that is, a function giving the loss to the DM resulting from a known total cost c. Equation 5-2 is a special case relating to earthquake insurance.

Then the present value of facility given the mitigation measure, denoted by X, is given by Equation 5-4.

$$X = R - C_0 - \sum_{j=1}^{N} \exp\left(-iT_{ej}\right) q\left(C_j\right) \tag{5-4}$$

Observe that X, N, T_{ej}, and C_j are random variables. The variables N and T_{ej} depend on the seismic setting at the building location. Cost C_j is related to S_j and to the risk-management alternative selected, through the vulnerability function $F_{C|Sa}(c|s)$, where s = S_j. The vulnerability function is derived using ABV as described in Chapter 4. Note that the spectral acceleration S_j is also random, and depends on the seismic setting at the building location. Let:

$$F_X(x) = \mathrm{P}[X \le x|a]\text{: } a \in \{1, 2, \ldots N_a\} \tag{5-5}$$

5.3.3. Decision-maker preferences

The objective of a decision analysis approach to decision-making is the optimization of the expected utility of outcome X. In general, outcomes are measured using any values of interest to the DM, which can include financial outcomes, casualties, and a variety of intangibles such as loss of prestige. In the present methodology, only financial outcomes are considered. The DM's preferences for financial outcomes are measured using the DM's utility function [Von Neumann and Morgenstern, 1944]. Let $u(x)$ denote the DM's utility for financial outcome x. Equation 5-5 gives the probability distribution on the financial outcome. Equation 5-6 gives the expected value of utility of a risk-management alternative. In Equation 5-6, $f_X(x)$ represents the probability density function of X, that is, $f_X(x) = \mathrm{d}F_X(x)/\mathrm{d}x$.

$$E\left[u(x)\right] = \int_{x=-\infty}^{\infty} u(x) f_X(x) dx \tag{5-6}$$

5.3.4. Identifying the preferred risk-management alternative

The alternative that maximizes $E[u(x)]$ in Equation 5-6 is then the preferred alternative, that is, the alternative that produces the greatest expected utility for the DM. Equivalently, one can consider the certain equivalent, *CE*, defined as the inverse of the expected value of utility, $u^{-1}(E[u(x)])$. The *CE* is the amount of money that the DM should be indifferent between receiving for certain, versus possessing the uncertain deal with expected utility $E[u(x)]$. The utility function monotonically increases, so the preferred alternative will have both the maximum $E[u(x)]$ and the maximum *CE*.

$$CE = u^{-1}(E[u(x)]) \tag{5-7}$$

Note that the preferred alternative need not be the one that maximizes the expected value of the financial outcome. (For risk-neutral decision-making, the preferred alternative produces both the highest expected value of financial outcome and the highest expected value of utility.)

Nor is the preferred alternative necessarily the one that produces the maximum possible financial outcome or the greatest probability of achieving a large financial outcome. Similarly, the preferred alternative need not have the least probability of producing a negative financial outcome.

Rather, the alternative with the maximum $E[u(x)]$ is the best one considering all possible outcomes, their associated probabilities, and the desirability of each outcome from the DM's viewpoint. This alternative is the one that is most consistent with the DM's preferences, considering all the available information.

5.4. IMPLEMENTING THE DECISION ANALYSIS

Equation 5-5 and hence Equation 5-6 are very difficult to evaluate analytically. A simulation approach is therefore used to determine the expected utility of the risk-mitigation options. The first step in the approach is to compile the alternatives, information, and DM preferences. The information and alternatives are described in the

next section, which is followed by a method to determine DM preferences. The simulation procedure then follows.

5.4.1. Expressing the alternatives and information

A variety of alternatives are discussed in Section 5.3.1 and in Chapter 2. For each alternative, the analyst must determine the C_0, R, and I of Section 5.3.2. The liability function, denoted by $q(c)$, must also be specified.

For seismic retrofit alternatives, C_0 is estimated using standard construction cost estimation techniques. For earthquake insurance, C_0 is the present value of the insurance premiums. The parameter R is determined using standard financial tools that are not discussed here. Furthermore, the DM must select a planning period T and discount rate i. Then for each alternative, the vulnerability function $F_{C|Sa}(c|s)$ is evaluated using the methodology described in Chapter 4.

Next, the seismic hazard at the building site must be evaluated. Several means are available to characterize the site hazard. One interesting approach is presented by Lutz and Kiremidjian [1993], who use a generalized semi-Markov process to model earthquake occurrence. The method allows consideration of the spatial and temporal dependence of earthquakes. In the present approach, however, a simpler technique is used. It requires a probability distribution sometimes called a hazard curve, denoted by $G_{Sa}(s)$, which gives the annual probability that a site will experience spectral acceleration in excess of s, considering all possible earthquakes, as shown in Equation 5-8. A seismic hazard analysis (not described here) is necessary to develop $G_{Sa}(s)$.

$$G_{Sa}(s) = 1 - F_{Sa}(s) = \mathrm{P}[S_a > s] \tag{5-8}$$

5.4.2. Determining the decision-maker's preferences

The last step is to determine the DM's utility function. The utility can take an arbitrary form, as long as it is continuous and monotonically increasing with increasing wealth state. As noted in Chapter 2, however, only a linear or exponential utility

function allows the analyst to consider the decision situation without reference to the DM's wealth state and the DM's other financial activities that might affect his or her wealth state. The linear utility function is essentially a special case of the exponential utility function, where the risk tolerance ρ is far in excess of the range of financial outcomes under consideration. For that reason, an exponential utility function is employed here.

Before discussing the methodology used to elicit DM risk attitude, it is useful to illustrate in somewhat greater detail the meaning of risk tolerance, ρ, shown in Equation 2-7, and repeated for convenience in Equation 5-9. In the equation, $u(x)$ represents the utility of the monetary amount x, a and b are arbitrary constants ($b < 0$), and ρ is risk tolerance.

$$u(x) = a + b\exp(-x/\rho) \tag{5-9}$$

When decisions have financial outcomes whose absolute values are significantly below ρ, perhaps half an order of magnitude or more, the DM acts relatively risk-neutral, that is, the alternative with the greatest expected value of financial outcome is the most desirable one. When outcomes reach or exceed the order of magnitude of ρ, however, the DM acts with greater and greater caution, demanding expected values of financial outcome significantly above what a risk-neutral attitude would dictate as reasonable. Alternatively, the DM requires higher and higher probability of success before accepting deals that involve the possibility of large loss.

For example, consider a double-or-nothing bet, where the stakes are to gain or lose a value x with probability p. When the stakes are small with respect to risk tolerance ρ, one accepts the deal if the probability of winning is as low as $p = 0.5$; at this probability or higher, the expected value of the financial outcome is nonnegative. When the stakes grow higher, however, the probability of winning must be closer and closer to 1.0 to make the DM willing to take the bet. The probability at which the DM is just indifferent between taking the bet and rejecting it, called the *indifference probability*, is readily plotted as a function of x/ρ, as shown in Figure 5-1. (An event-tree depiction of

the double-or-nothing bet is shown as an inset of Figure 5-1.) The indifference probability is used in the present study to elicit a DM's risk attitude, and to infer the DM's risk tolerance ρ.

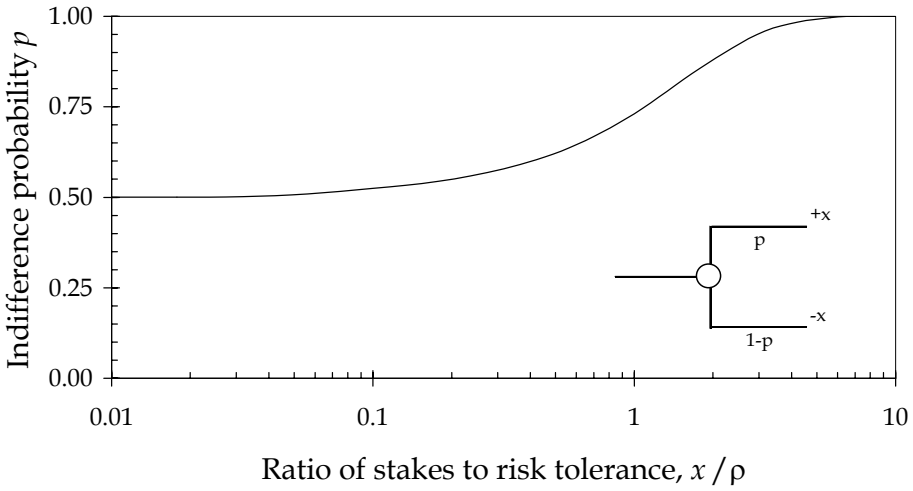

Figure 5-1. Risk tolerance ρ illustrated in terms of a double-or-nothing bet.

To determine the DM's utility function, an interview process similar to that of Spetzler [1968] is performed. This reference, though old, provides the best-documented, most-systematic procedure found. The procedure employs a series of N hypothetical deals of the form shown in the event tree of Figure 5-2. Each deal has two possible outcomes of fixed value: success, which involves a net gain of g, or failure, which involves a net loss of l. The probability of success in each deal is a variable. The interview process determines the DM's indifference probability p for each deal. When the DM is just indifferent between accepting the deal and rejecting it, the utility of the deal is identically equal to the utility of zero change in wealth state.

If the arbitrary parameters a and b of Equation 5-9 are set to 1 and –1, respectively, the utility of a zero change in wealth is zero ($u(x=0) = 0$), regardless of the value of ρ. Thus, for the deal shown in Figure 5-2, when p = the indifference probability, the utility of the deal is zero. Then, if the DM's utility function has exponential form as

in Equation 5-9, the sum of the utilities of all the hypothetical deals equals zero, and the sum of the squares of these utilities is also zero.

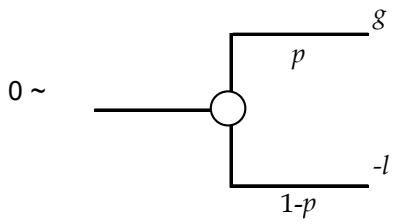

Figure 5-2. Two-outcome financial decision situation used in interview.

Consider then the series of N hypothetical deals with various values of g and l. An interview procedure elicits the DM's indifference probability p for each deal. Let g_i refer to net gain from deal i, l_i refers to net loss from deal i, and p_i refers to indifference probability from deal i, where i = 1, 2, … N. The arbitrary constants a and b of Equation 5-9 are set to 1 and –1, respectively. The expected utility of a single hypothetical deal i is given by Equation 5-10.

$$E[u_i] = p_i(1 - \exp(-g_i/\rho)) + (1 - p_i)(1 - \exp(l_i/\rho)) \tag{5-10}$$

For a DM with a perfectly exponential utility function, the expected utility shown in Equation 5-10 is zero. An exponential utility function approximating the DM's risk attitude can therefore be determined by determining ρ that minimizes the sum of the squared errors, $e(\rho)$, shown in Equation 5-11.

$$e(\rho) = \sum_{i=1}^{N} \left(E[u_i]\right)^2 \tag{5-11}$$

Appendix C provides details of an interview procedure that can be used to elicit the DM's risk tolerance, ρ. Briefly, the procedure poses a series of N = 40 hypothetical deals, with the magnitude of the deal scaled to the size of the financial decisions typically made by the DM. Appendix C also contains interview results of five DMs, ranging from a partner in a small accounting firm to the risk manager of an institution with a $2 billion annual budget. It was found that, for the range of financial outcomes

typical of the deals handled by the DM, an exponential utility function described the DM's risk attitude well. Figure 5-3 shows results for one such interview: that of the investment manager of a real estate investment company with $20 million annual revenues. Figure 5-4 shows that, based on this limited sample size of five DMs, there appears to be an exponential relationship between the size of the DM's company and the DM's risk attitude.

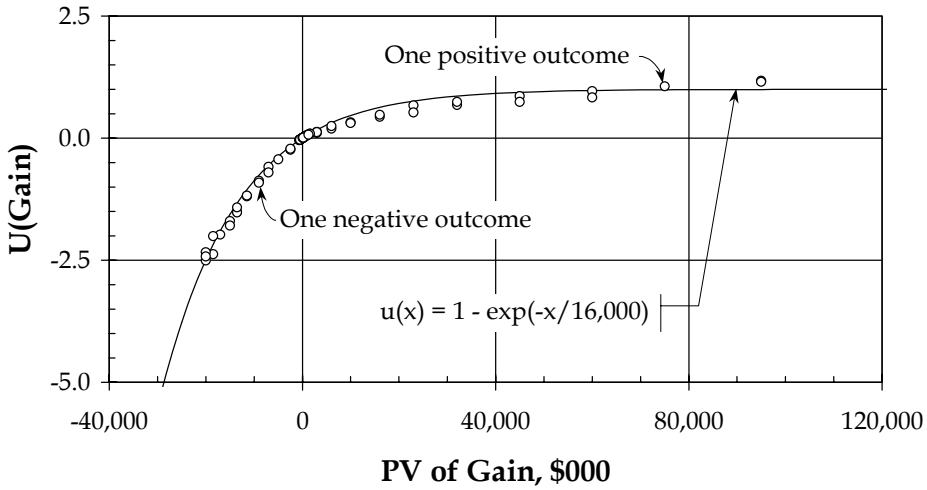

Figure 5-3. Utility function fit to interview data.

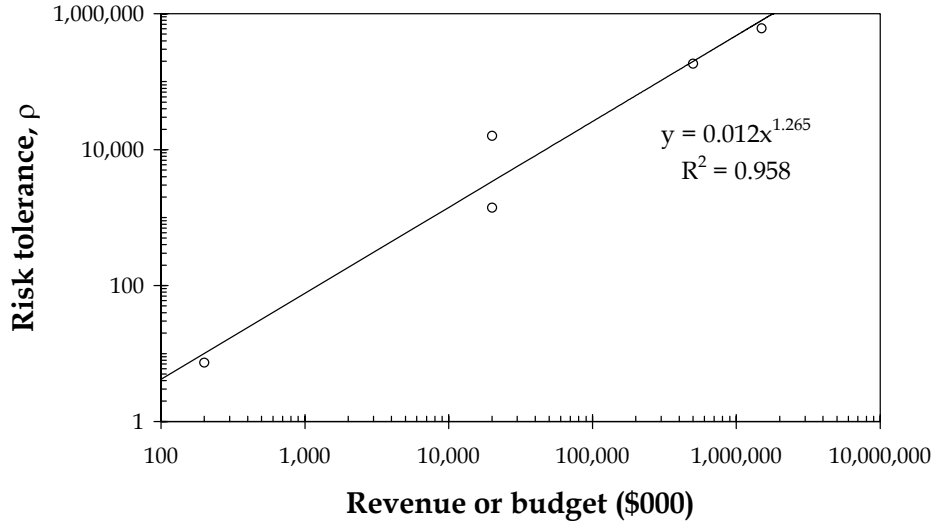

Figure 5-4. Relationship between size of firm and risk tolerance.

5.4.3. Simulation

First, it is assumed that at most one damaging earthquake occurs during a single year. Let

s_0 = a threshold value of spectral acceleration, denoted by s_0, selected in advance to represent the minimum shaking intensity that causes significant loss.

$\underline{S} = \{S_1, S_2, \ldots S_T\}$: $0 \le S_t \le S_{max}$, and $t = 1, 2, \ldots T$.

$\underline{C} = \{C_1, C_2, \ldots C_T\}$

T = the owner's planning period

i = the owner's discount rate

C_0 = the present value of the cost of the alternative.

R = present value of the facility to the owner, including revenue expected during the planning period and the liquidation value at the end of the planning

period, but omitting the cost of the risk-management alternative. This value may depend on alternative a.

where S_t refers to the maximum spectral acceleration affecting a site in year t, and C_t refers to the total cost resulting from the earthquake in year t. Given the information described in Sections 5.4.1 and 5.4.2, the simulation of the expected utility $E[u(x)]$proceeds as follows.

For each year t = 1, 2, … T, earthquake occurrence is simulated using the inverse method of Equation 5-12. In the equation, $F_{Sa}(s)$ refers to the complement of the hazard function, as shown in Equation 5-8, and is taken to be right-continuous at discontinuities. If $S_t > s_0$, a damaging earthquake has been modeled to occur. The cost from the earthquake is simulated using Equation 5-13. Otherwise, $S_t = C_t = 0$.

$$S_t = F_{Sa}^{-1}(u_1) \tag{5-12}$$

$$C_t = F_{C|Sa}^{-1}(u_2 \mid S_t) = Vy(S_t)F_{\Psi}^{-1}(u_2) \tag{5-13}$$

where u_1 and u_2 are samples from two independent streams of uniform(0,1) random variates. The value of alternative a under the simulated sequence of earthquakes is then given by Equation 5-14. Equation 5-15 gives the utility of the alternative.

$$X = R - C_0 - \sum_{t=1}^{T} \exp(-it)q(C_t) \tag{5-14}$$

$$u(X) = a + b\exp(-X/\rho) \tag{5-13}$$

Each iteration of $\underline{S}$ and $\underline{C}$ produces a sample value of $u(X)$. Numerous iterations are performed to produce a sample set of $u(X)$, and the sample mean is used as an estimate of $E[u(X)]$, as shown in Equation 5-14. Equation 5-7 gives the certain equivalent of the alternative. In Equation 5-14, N represents the number of iterations, and $u_k(X)$ represents the sample of Equation 5-13 from iteration k.

$$E[u(X)] \approx \frac{1}{N}\sum_{k=1}^{N} u_k(X) \tag{5-14}$$

The procedure is repeated for each alternative $a = 1, 2, \ldots N_a$. The alternative that maximizes $E[u(X)]$ is the preferred alternative, that is, the alternative that the DM should take to be consistent with the information available and the preferences the DM has expressed.

5.4.4. Alternative methods of earthquake simulation

One disadvantage of the approach described in Section 5.4.3 is that it is memoryless. That is, it ignores temporal or spatial correlation of earthquakes, and instead treats past earthquake occurrences as immaterial to future ones. Reasoning based on Reid's elastic rebound theory [Bullen and Bolt, 1985] argues that the annual probability of a second earthquake shortly after one has occurred on the same segment is greatly reduced from the probability before the first earthquake, and thus individual fault segments are not memoryless. Furthermore, earthquake occurrence on one fault may affect the probability of rupture on other faults.

An alternative is to model earthquake occurrence as a generalized semi-Markov process (GSMP), which allows dependence of future events on past ones. Haas [1998] summarizes the GSMP as a series of states $\{S(t): t \geq 0\}$ making stochastic state transitions when one or more events associated with the occupied state occur. Each event has an associated clock – set according to an arbitrary distribution – that reads the time until the event occurs. Events compete to trigger the next transition. At each state transition, new events can be scheduled and old events can be cancelled. Each event or set of events has its own distribution for determining the next state.

Lutz and Kiremidjian [1993] developed an application of a GSMP to earthquake occurrence. This approach models sequences of events $\{E_1, E_2, \ldots E_K\}$, each event E_i associated with magnitude M_i, location O_i, and time t_i. Magnitude, distance, and site soil conditions can then be used with a seismic attenuation relationship such as Boore,

Joyner, and Fumal [1997] to simulate spectral acceleration. This technique allows for consideration of temporally and spatially dependent earthquake occurrences.

A third alternative is to model seismicity as a combination of moderate events with (memoryless) Poisson frequencies and exponentially distributed inter-arrival time, and larger, rarer characteristic events whose inter-arrival times are modeled as lognormal, gamma, or Weibull distributed. Kiremidjian [1999] presents this approach.

Either of these alternatives can be used to model earthquake occurrences affecting the building site of interest. Both require more information regarding the seismic setting than simply the hazard curve, $G_{Sa}(s)$. The Lutz and Kiremidjian [1993] approach, in particular, requires a very detailed model of nearby fault geometry and seismicity.

The simple approach described in Section 5.4.3 is probably a reasonable approximation for ordinary business planning periods of 5 to 10 years, in which at most one damaging earthquake is likely to occur to affect a building of interest. For longer planning periods, such as those considered by large institutions or governments, a more sophisticated model of earthquake occurrence may be warranted.

5.5. SAMPLE DECISION ANALYSIS

5.5.1. Sample decision situation: the purchase of an office building

The decision-analysis process described in the preceding sections is illustrated with the following example. A real estate investment firm is considering the purchase of the example building. The building has a replacement value V = \$4.9 million and an asking price of \$8 million. If the investment firm buys the building, the purchase will be financed with \$500,000 of equity and a commercial mortgage of \$7.5 million secured by the property. The firm's planning period T is 5 years, and their discount rate i = 9%. The investment firm estimates the present value of its net income stream and resale price after 5 years to be R = \$3.1 million, after considering operating expenses, debt service,

and other non-operating costs. It is concerned about seismic risk management, and contracts to have a decision analysis performed to determine the best alternative.

5.5.2. Alternatives: insurance, modest retrofit, extensive retrofit

The range of possible risk-management alternatives is diverse. For simplicity, five alternatives are considered here. The first two alternatives are to forego the investment (do not buy), or to buy the building but not to mitigate the risk. If they buy the building, several risk-mitigation alternatives also exist, which for simplicity of illustration are limited to the following three. First, insure the building as-is, with a deductible of \$250,000 and limit $l \geq 0.25V$ to be determined. It is assumed the insurer offers a policy with premium $a = 0.04l$ (4% rate on line, or *ROL*) for a limit-to-value ratio $LTV = 0.25$, with *ROL* decreasing linearly with *LTV* to 2.5% for $LTV = 1$. The present value of insurance premiums during the five-year planning period is shown in Figure 5-5.

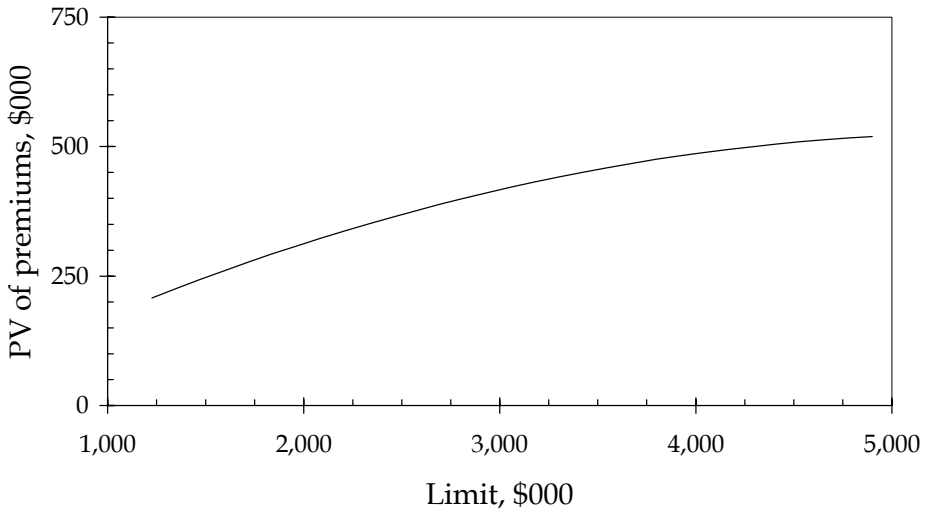

Figure 5-5. Cost of earthquake insurance.

Alternative 4 is a modest seismic retrofit of equipment anchorage. Anchorage of spring-mounted equipment such as fans and generators will be provided with seismic snubbers (typically steel angles rigidly fixed to the diaphragm but not to the equipment,

designed to prevent excessive movement of the equipment). All other mechanical and electrical equipment currently unanchored to floor slabs will be anchored. Tall electrical components will be braced. Unbraced automatic sprinkler lines will be braced.

Alternative 5 is an extensive seismic retrofit, including the equipment measures as well as strengthening of the lateral force resisting system by adding the WT device discussed in Chapter 3 to every moment connection. If the seismic retrofit were performed, the investment firm indicates that it would also perform various nonstructural upgrades to the building that would increase its net value R to \$4.1 million.

5.5.3. Information: mitigation cost, hazard, and vulnerability

The initial cost (C_0) of alternatives 1 and 2 is zero. The cost of the insurance alternative depends on LTV, as illustrated in Figure 5-5. The cost of the alternative 4, the equipment seismic retrofit, is estimated to be approximately C_0 = \$100,000, as summarized in Table 5-1. This cost has significant uncertainty associated with it, but for simplicity only the best-estimate cost is used in the present analysis. These costs are based on FEMA-74 [FEMA, 1994] and judgment. It is estimated that the construction cost to add the WT devices to the WSMF connections is \$35,000 per each of 72 devices in the building, for a total of \$2.5 million. Considering the structural retrofit, equipment retrofit, and other upgrades proposed by the investment firm, alternative 5 is estimated to cost \$3.0 million. Initial costs are summarized in Table 5-2. The seismic hazard curve for the site is shown in Figure 5-6.

The owner's liability structure for alternatives 2, 4, and 5 are $q(c) = c$. That is, the owner is liable for all costs. (The possibility of loan default is ignored here for simplicity.) For alternative 3 (buy and insure), Equation 5-16 gives the liability structure.

$$q = \begin{cases} c & c < d \\ d & d \le c < l \\ c - l + d & l \le c \end{cases} \tag{5-16}$$

Table 5-1. Cost of equipment retrofit.

Description	Retrofit	Unit	Qty	Low	Best	High	Total
Elevator equipment	Anchor to slab	ea	2	200	325	500	650
Gas water heater	Anchor to slab	ea	1	200	325	500	325
Sprinkler lines	Brace at 12' OC	12 lf	225	250	400	600	90000
Chiller	Snubbers	ea	1	350	700	1400	700
Switchgear -- low volt	Anchor to slab	ea	1	200	325	500	325
Switchgear – med volt	Anchor to slab	ea	1	200	325	500	325
Motor installation	Snubbers	ea	1	350	700	1400	700
Generator	Snubbers	ea	1	350	700	1400	700
Total							94000

Table 5-2. Summary of alternatives.

Alternative	C_0 ($000)	R ($000)
1. Do not buy	0	0
2. Buy, do not mitigate	0	0
3. Buy, insure	Varies	3,100
4. Buy, equipment retrofit	100	3,100
5. Buy, equipment and structure retrofit, other upgrades	3,000	4,100

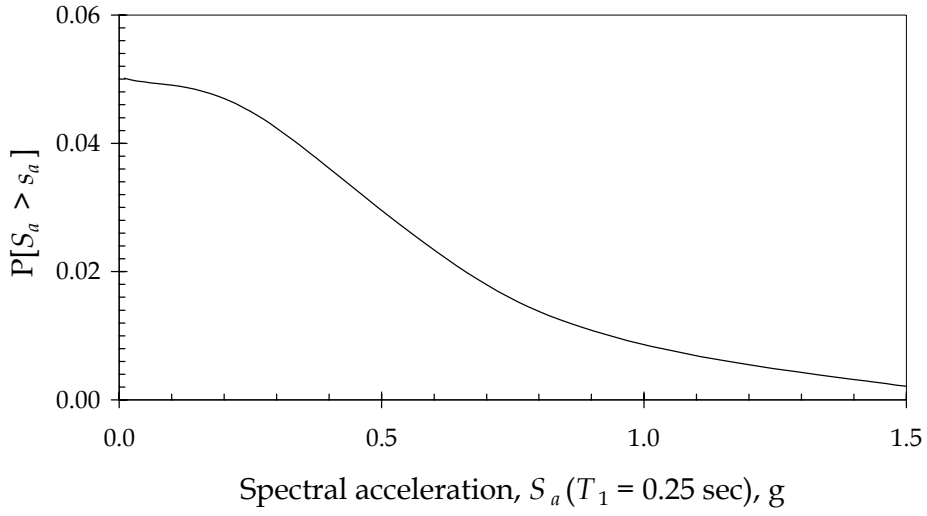

Figure 5-6. Site hazard $G_{Sa}(s)$ for the example building.

Mean normalized vulnerability under as-is conditions (fast-repair case), shown in Figure 4-10, is repeated in Equation 5-14. The procedure described in Chapter 4 is performed considering both retrofit measures. Equation 5-15 shows mean building vulnerability after the equipment retrofit; Equation 5-16 shows mean building vulnerability after structural and equipment retrofit. In Equations 5-14 through 5-16, s represents spectral acceleration S_a, in units of g.

In each case, loss C conditioned on S_a is modeled as a lognormal random, as shown in Equation 4-21, which is repeated for convenience in Equation 5-17. In the equation, V represents replacement cost ($4.9 million) and Ψ is a lognormal random variable with expected value $\mu_\Psi = 1.0$ and standard deviation $\sigma_\Psi = 0.57$.

$$y = 0.328s^{0.466} \qquad \text{As-is} \qquad (5\text{-}14)$$

$$y = 0.323s^{0.460} \qquad \text{Equipment retrofit} \qquad (5\text{-}15)$$

$$y = 0.163s^{0.704} \qquad \text{Structure and equipment} \qquad (5\text{-}16)$$

$$C = Vy\Psi \qquad (5\text{-}17)$$

5.5.4. Example decision-maker preferences

The DM's risk attitude is determined using the procedure described in Section 5.4.2. In this hypothetical example, the DM's risk tolerance ρ = \$5 million. This DM's planning period T = 5 yr, and discount rate i = 9%.

5.5.5. Probabilistic analysis

The expected value of utility of each alternative is evaluated using the procedures of Section 5.4. For each alternative, a set of earthquake histories $\underline{S} = \{S_1, S_2, \ldots S_5\}$ is simulated using Equation 5-10. The associated costs $\underline{C} = \{C_1, C_2, \ldots C_5\}$ are calculated using Equation 5-11. Financial outcome is calculated using Equation 5-12. The utility of the outcome is calculated using Equation 5-13, where a = 1, b = -1, and ρ = \$16 million. The process is repeated until convergence for each alternative. (Convergence is defined as the point at which all percentiles of utility from 5%, 10%, and so on up to 95% change less than 0.5% after 100 successive iterations.)

The analysis results are shown in Table 5-3, which shows that the preferred alternative is to buy but not mitigate, because this alternative has the highest expected utility and consequently the highest certain equivalent.

Table 5-3. Utility and certain equivalent of risk-management alternatives.

Alternative	$E[u(X)]$	σ_u	*CE*, \$000
1. Do not buy	0.095	0.000	500
2. Buy, do not mitigate	0.431	0.084	2,818
3. Buy, insure	0.425	0.051	2,769
4. Buy, equipment retrofit	0.420	0.084	2,723
5. Buy, equipment and structure retrofit, etc.	0.178	0.051	982

Alternative 1 (do not buy) has no uncertainty associated with it. Consequently, its certain equivalent equals the initial equity stake that the investment firm would keep if it did not purchase the building.

Alternative 2 (buy; do not mitigate risk) has a certain equivalent of $2.82 million. This is the highest *CE* of the five alternatives, and therefore represents the preferred alternative. Recall that neglecting the risk of earthquake loss, the purchase of the property is estimated to be worth $3.1 million, suggesting that the earthquake risk reduces the value by equivalent to a certain amount of $1.3 million.

Alternative 3 (buy; insure) is simulated for an insurance limit-to-value ratio of 0.25. For this alternative, the certain equivalent of $2.77 million is only slightly less than the buy but do not mitigate alternative. Note that the insurance option had an initial cost of $208,000 in present value. The expected value of insurance recovery, calculated during the simulation, is $135,000, with a standard deviation of $295,000. This indicates that the insurance would be profitable on average to the insurance company: $208,000 - $135,000 = $73,000 profit over 5 years. However, there is a 20% probability that the claims would exceed the premium, and the 95th percentile of claim is $820,000. The probability distribution on the claim is shown in Figure 5-7. (Note that the distribution is available only to the 95th percentile, because of the software used in the simulation.)

Alternatives 4 and 5, respectively, produce *CE* of $2.72 million and $0.98 million. Both retrofit options have lower *CE* than either alternatives 2 and 3. It appears that neither structural retrofit option is worthwhile from an economic viewpoint.

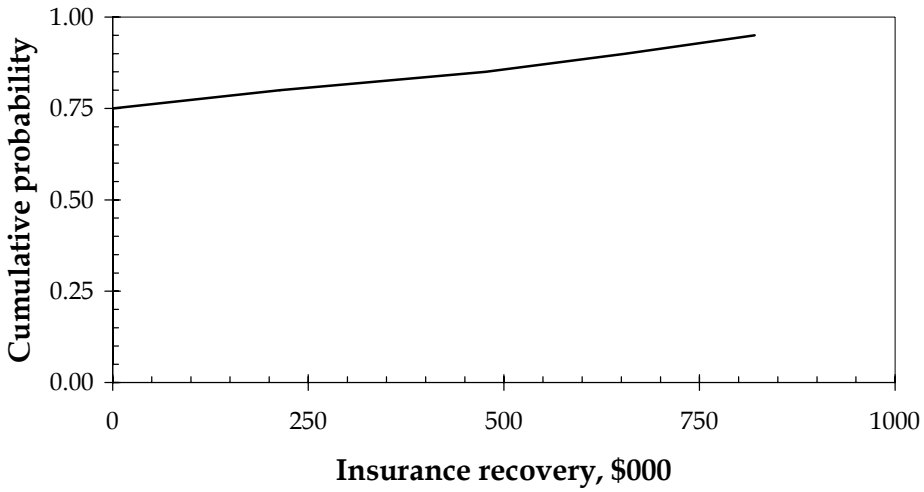

Figure 5-7. Probability of insurance claim.

5.5.6. Probabilistic sensitivity study

The sensitivity of the decision to the insurance limit can be determined by varying the limit and examining the resulting *CE*. Figure 5-8 shows that the optimal insurance limit would be approximately 0.17 of value *V*, if the insurer would provide that level of insurance. (It was given in the problem statement that the insurer would only underwrite an earthquake policy for a limit of at least 0.25*V*, or approximately $1 million.) The figure also shows that alternative 2 is nonetheless preferable to insurance and all the other alternatives.

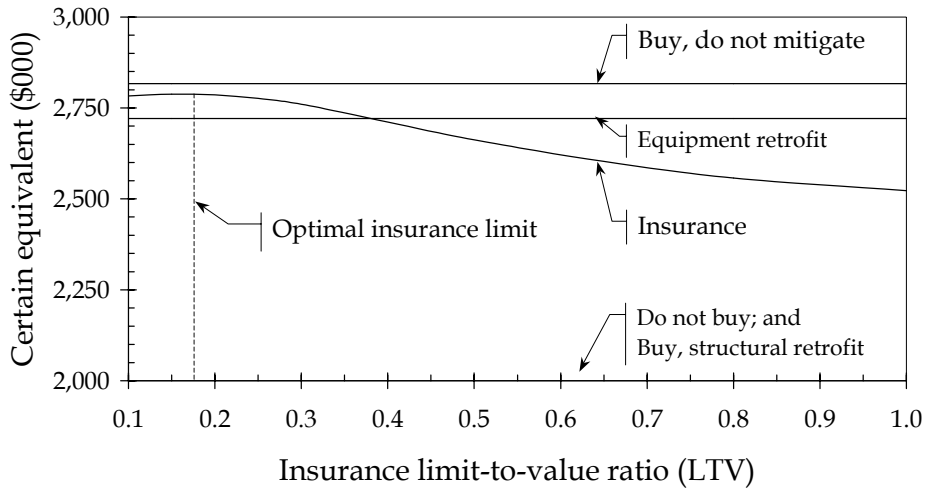

Figure 5-8. Sensitivity of decision to limit-to-value ratio.

Figure 5-9 shows that the DM's risk tolerance is material to the decision. Depending on ρ, three different options would be preferable. For ρ > $2 million, the DM is tolerant enough of the risk of earthquake loss that it is not worthwhile to purchase earthquake insurance or to perform a seismic retrofit of the building. For $200,000 < ρ ≤ $2 million, insurance is the preferable alternative. (Insurance is shown as a dashed line in Figure 5-9 solely for ease of reading.) For ρ ≤ $200,000, the best option is not to buy the building at all (alternative 1), as shown in Figure 5-10, which presents the same data on a log-log scale.

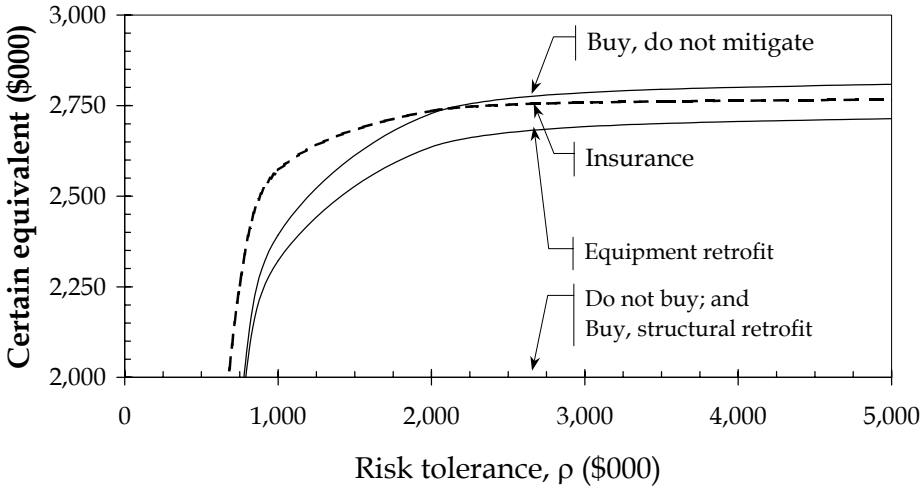

Figure 5-9. Sensitivity of decision to risk tolerance.

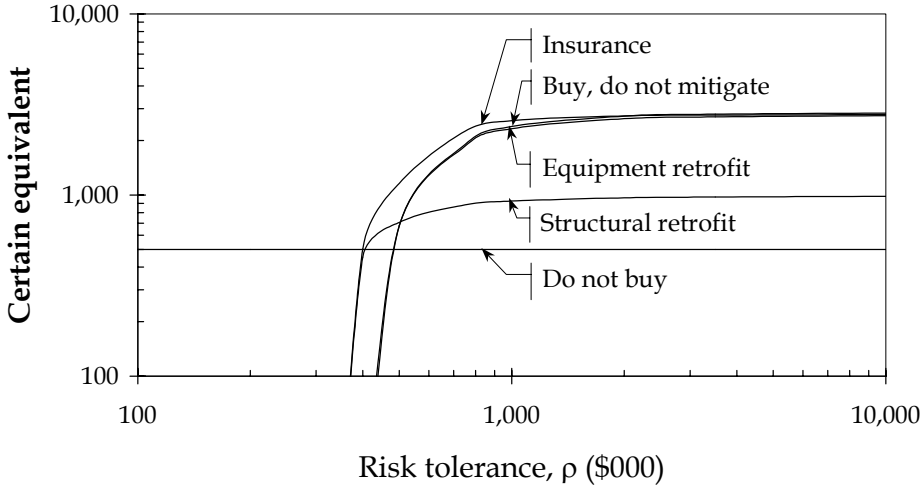

Figure 5-10. Sensitivity of decision to risk tolerance (log-log scale).

The cost of insurance is also material to the decision. If the rate on line (ROL) ≤ 0.35, alternative 3 (insurance) is preferable to alternative 2 (buy, do not mitigate). The reason is *not* that the insurance premium costs less than the expected value of claims. Figure 5-12 shows that premiums exceed the expected value of insurance claims for rates on line in excess of 0.027. That is to say that, for 0.027 < ROL ≤ 0.035, premiums exceed claims on an expected-value basis, and yet alternative 3 is still preferable to alternative 2.

Conversations with insurance professionals indicate that an earthquake *ROL* of 0.03 in the Los Angeles area is reasonable, and that the lowest prices for earthquake insurance can reach 0.01, although this low end is for very large policies [Southwell, 2000]. Therefore, negotiation with an insurer could yield a policy that is desirable to the DM and acceptable to the insurer.

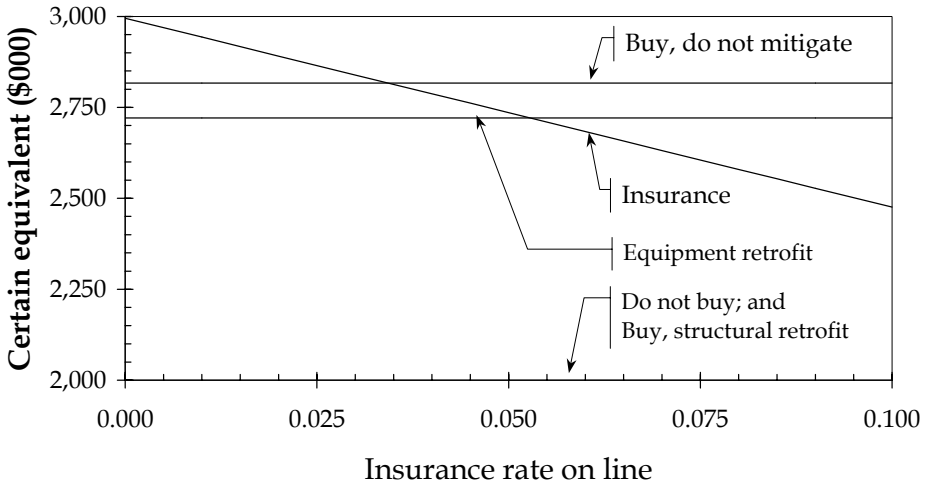

Figure 5-11. Sensitivity of decision to insurance rate on line.

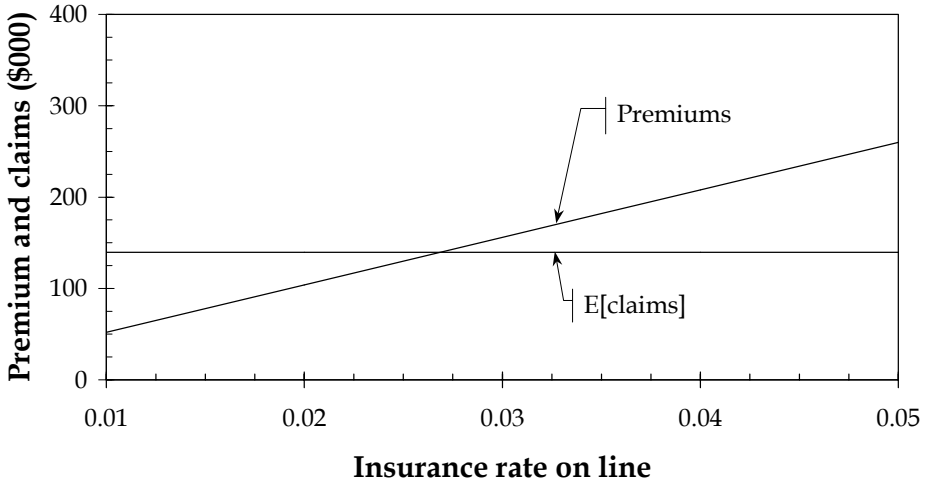

Figure 5-12. Premiums and claims versus insurance rate on line.

5.5.7. Conclusions for the sample decision analysis

For this building in this location, seismic strengthening is not economically desirable from the owner's viewpoint, despite the fact that the building is a high-risk pre-Northridge WSMF structure in a highly seismic region. The preferred alternative in some cases is to buy the building but not mitigate the risk, in others it is to buy the building and transfer the risk via earthquake insurance, and in still others the best option is not to buy the building. The preferred option depends on the DM's risk tolerance and on the insurance rate on line.

The example demonstrates that risk attitude matters. Even though a risk-management alternative is not cost effective, it can still be desirable and rational, owing to risk aversion. Insurance, if priced correctly (that is, to be profitable to the insurer), is never cost effective, but it is often desirable, depending on the insured's risk and risk attitude. Hence, risk attitude should not be omitted from analysis of a risk-management situation whenever losses are potentially significant compared with risk tolerance, ρ.

Decision procedures that do not account for the DM's risk tolerance can select an alternative that is inconsistent with the DM's preferences. Risk-neutral decision-making (equivalent to risk analysis with $\rho = \infty$) always rejects alternatives where costs exceed benefits. The example showed that risk neutrality is not necessarily a reasonable assumption, and that an alternative need not be cost-effective to be desirable. Risk-management decisions based strictly on cost-benefit analysis can erroneously reject desirable alternatives that have benefit-to-cost ratios less than 1.0.

At the opposite extreme, an analysis based on worst-case decision-making (i.e., choosing the alternative that has the highest economic value in the worst-case scenario) can also produce inappropriate recommendations. This type of analysis is equivalent to assuming a very small risk tolerance ($\rho \cong 0$). In the example, this approach to decision-making would result in a recommendation not to buy, which would be inappropriate for many DMs.

CHAPTER 6
CONCLUSIONS

6.1. MAJOR CONTRIBUTIONS

This dissertation has presented a rigorous methodology for developing building-specific seismic vulnerability functions, and for applying these vulnerability functions in a decision-analysis framework to make risk-management decisions that are consistent with the decision-maker's risk attitude and financial practices. The vulnerability functions are probabilistic, accounting for uncertainty in ground motion, structural response, assembly fragility, repair cost, repair duration, and loss due to downtime. More specifically, the major contributions of this dissertation are as follows.

The methodology subjects an idealized model of the structure to ensembles of ground motion time histories, taking into consideration nonlinear structure behavior. Probabilistic structural response is estimated on a floor-by-floor, assembly-by-assembly, basis. Because the method uses structural analysis to determine response, one can account for the detailed configuration and structural design of the building in the vulnerability function. Category-based methods do not allow for this level of building-specific analysis. Furthermore, the method can employ the state-of-the-art in structural analysis as it develops, thereby allowing for future improvement of vulnerability functions without changing other aspects of the model.

Structural response parameters are applied to probabilistic fragility functions for individual assemblies, to model the building damage state of each assembly. Because assemblies are defined at a detailed level, assembly-based vulnerability (ABV) is sensitive to common design alternatives, for example, choices between competing glazing systems of differing fragility. Prior methods that attempt to produce building-

specific vulnerability functions treat assemblies in broad categories, such as combining all mechanical equipment into one generalized component, with the broad category having a single vulnerability function. Such existing approaches do not allow for comparison of detailed design or seismic retrofit alternatives.

Because ABV treats damage estimation separately from repair cost, earthquake experience data can be more readily employed in improving the tools of the methodology. The reason is that statistical data from earthquakes need not include repair costs nor consider local contractor practices to be useful in developing vulnerability functions.

A variety of empirical and theoretical methods are presented to compute assembly fragility functions. These include binned and binary regression of earthquake experience data; direct estimation of fragility using laboratory data; mixing existing fragility functions; and development of theoretical fragility functions using reliability methods. Fragility functions are created with limit states explicitly linked to well-defined repair tasks. Fragility functions thus created can be re-used in later analyses of structure with similar assemblies.

The fragility functions developed for ABV using the empirical and theoretical methods discussed here differ from fragilities of generalized components in that the former are directly verifiable, either through new testing or new observation of earthquake experience. The fragility functions for generalized components, by contrast, cannot be directly tested, without first disaggregating the various components that make up the mixture.

The present study developed several such assembly fragility functions, including two for pre-Northridge welded steel moment frame connections. The development of these latter fragility functions demonstrated that, given presently available damage data

from the Northridge earthquake, the probability of connection damage is more strongly correlated with elastic demand-capacity ratio (*DCR*) than with beam-end inelastic beam-hinge rotation (*IBHR*) estimated by nonlinear structural analysis, and that therefore *DCR* is a better predictor of damage to these connections.

Furthermore, because the methodology is assembly-based, one can use new fragility information on one particular assembly type to improve the accuracy of an entire building vulnerability function, without changing other aspects of the model. This is in contrast to category-based approaches that require repair-cost data on many instances of an entire category of buildings, before a vulnerability function can be improved or updated.

An assembly taxonomic system is presented to facilitate the development, archiving, re-use, and improvement of assembly fragilities. Like the Linean system for categorizing organisms, the assembly taxonomy is flexible, allowing for future refinement. Such a system also facilitates learning from earthquakes, in that it offers the means to identify unambiguously and using standard categories the damage observed in earthquakes worldwide. The taxonomic system is also designed for accessibility to standard published cost manuals, for ease of estimating repair cost and repair duration.

Simplified Gantt scheduling is used to estimate loss-of-use duration and hence loss-of-use cost. Repair durations are calculated based on repair tasks that must be accomplished, as opposed to category-based approaches, which estimate a single scalar measure of building restoration based on an abstract, scalar damage state. Repair durations are estimated in the ABV approach for individual operational units within a building, such as a rental unit, allowing the analyst to account for tenant needs and lease arrangements. (The example analysis did not do so, but the methodology allows for such consideration.)

The methodology can be employed to produce vulnerability functions of an existing building under as-is and what-if conditions, where the two designs can differ only in small details of seismic retrofit that are beyond the resolution of category-based approaches. This capability facilitates analysis of choices between risk-mitigation alternatives. Furthermore, what-if analysis using ABV can be used in new design to compare life-cycle costs of competing designs.

An approach using decision analysis is presented for making normative risk-management decisions using the vulnerability functions generated by the ABV methodology. The decision-maker's risk attitude is considered, and a method to elicit that risk attitude is developed. Finally, the methodology is illustrated using an example risk-management decision situation for a hypothetical building and decision-maker. In the example, ABV and decision analysis are used to select among two realistic seismic retrofit options, an insurance alternative, and the do-nothing alternative. The example shows that risk attitude matters: that the risk tolerance of the decision-maker can make a material difference in the proper selection of a risk-management strategy.

This is in contrast with approaches that consider cost-effectiveness as the indicator of desirability. These approaches assume risk neutrality, an assumption that can erroneously reject desirable risk-management alternatives because their expected costs exceed its expected benefits. Insurance, if priced correctly, is not cost effective by this measure, but it can nonetheless be desirable.

The ABV approach results in more-detailed resolution of building damage than category-based approaches, which limit damage information to a single scalar quantity. Damage, repair costs, and repair durations can be quantified by assembly type, group of assemblies, or by room, suite, floor, or the entire building, thereby facilitating targeted seismic risk management.

Finally, unlike existing methods for creating vulnerability functions, the ABV methodology produces vulnerability functions that can be largely free of expert opinion. Where expert opinion does remain, laboratory investigation can be performed, or in some cases theoretical fragility functions can be developed, to replace judgment as needed. Thus, ABV produces vulnerability functions that are defensible on a scientific basis.

6.2. LIMITATIONS AND RESEARCH OPPORTUNITIES

6.2.1. Jurisdictional requirements and retroactive code changes

The ABV methodology does not explicitly account for possible changes in building-code requirements after earthquakes by the state or local jurisdictions. (Such changes, for example, might require a damaged building to be upgraded to a newer code, if damage exceeds a certain level.) The methodology does not, on the other hand, limit the analysis by requiring the building to be restored to its pre-earthquake condition. It merely requires the analyst to identify a unique repair task for each assembly damage state. The example building is a case in point: damaged pre-Northridge WSMF connections are assumed to be repaired to post-Northridge standards using a haunched WT steel connection.

However, no provision has been made in the methodology for changing the required repair task if more macroscopic triggers occur. An example might be the requirement of the replacement of all pre-Northridge WSMF connections, even undamaged ones, if a certain fraction of connections are fractured. Such contingencies are readily added to the methodology if they are defined in advance. The problem is that retroactive code changes enacted after future earthquakes are unpredictable and may take a variety of forms.

It is unclear however how such future legislative action could be addressed quantitatively into an ABV approach. Perhaps lessons from past retroactive code changes could provide information on the types and severity of damage conditions that can trigger such requirements.

6.2.2. Inclusion of degrading structural model

Although the example application did not use a degrading structural model, the ABV methodology does allow for its inclusion in future analyses, to model local and global collapse. A degrading structural model would allow for analysis at greater than design-basis spectral accelerations. It could thereby account for costs resulting from the most-severe 1 to 2% of earthquakes that can affect a building. Such an improvement would require consideration of indirect damage effects, that is, damage to one element affecting the survival of another. An example is the collapse of a structural element that would damage nearby nonstructural components.

6.2.3. Life-safety assessment

In addition to accounting for costs from rare, severe earthquakes, the inclusion of a degrading structural model would assist in addressing life safety. A degrading model could indicate local and global collapse, which are strongly related to occupant casualties. Probabilistic occupancy patterns would also be required, as would relationships among building materials, collapse geometry, and lethality.

Other damage besides collapse can also pose a casualty threat: for example, damage to automatic sprinklers can contribute to uncontrolled post-earthquake fire, and overturned furniture and fallen ceiling and above-ceiling systems can cause trauma injuries. These hazards could be addressed as follows. For every assembly failure mode that can threaten life safety, estimate the probability of various types of casualty,

conditioned on the failure mode and the presence within a predefined area of a building occupant or passerby. Knowledge of occupancy patterns and the application of the chain rule provide the desired result. Two benefits of this development would be the ability to estimate the probability of meeting life-safety performance objectives, and the ability to evaluate the most cost-effective means of improving life safety, either in the retrofit situation or during code development.

6.2.4. Demand-driven cost inflation (demand surge)

Anecdotal evidence suggests that repair costs in catastrophic earthquakes can increase over pre-earthquake conditions. This macroeconomic effect has not been included in the present methodology, which operates on a microeconomic, building-specific scale. However, knowledge of magnitude, location, and macroeconomic consequences of earthquakes could perhaps be used to estimate a demand-driven inflation cost factor to account for this effect, if the functional relationships were better understood.

It is reasonable to assume that prices increase after a disaster as a result of the high demand and limited supply of goods and services as asserted by GeoRisk [1998]. The exact mechanisms of these cost increases are not understood, however. Price gouging by contractors may be responsible for such cost increases, as implied by consumer-protection legislation to amend the California State Civil and Penal Codes after the Northridge Earthquake [California State Assembly, 1994], but other causes are possible.

For example, material shortages can require the contractor to use more expensive materials than would otherwise be necessary, or to transport construction materials quickly from great distances. Contractors might have to offer higher wages to attract laborers. The cost to travel great distances from the contractor's normal market area to

the affected area can be passed on to the building owner. Scarcity of local accommodations for temporary labor could result in the need to use higher-cost accommodations. The difficulty of travel within the affected area could cause lower contractor productivity, or lack of utility services that require the contractor to provide backup utilities not normally needed. Detailed empirical investigation of these possible effects could inform the development of an economic model of demand surge.

6.2.5. Simplification of analysis requirements

It would be valuable to simplify aspects of ABV analysis, such as via examination of the error produced by application of either purely linear-elastic dynamic analysis (as opposed to nonlinear) or linear-elastic spectral analysis (as opposed to dynamic analysis). A question to be answered is whether the complex and time-consuming analytical methods prescribed in the present study make a material difference in risk-management decisions. It would be valuable to define the conditions under which one arrives at the same decisions using more common, state-of-the-practice techniques.

6.2.6. Automating ABV

Data requirements for ABV analysis are intensive. For any particular building, assembly quantities must be measured from construction drawings, a walkthrough of the building, or both. Quantity takeoff is a standard procedure in construction contracting – construction bids are based on them – but the process nonetheless takes time. Depending on the age of a building, much of the data required to create an assembly inventory may be available electronically in the form of computer-aided drafting and design (CADD) files. It is likely that in-person examination of building assemblies will still be required to determine as-built details of installation that are unlikely to appear (or to appear accurately) in CADD files, such as whether building-service equipment is provided with seismic anchorage. Nonetheless, a great deal of

relevant inventory data might be extracted from CADD files to reduce the data-acquisition labor of an application of the ABV methodology.

Furthermore, the ABV methodology developed here could be implemented in a relational database with computational code, for ease and uniformity of application. Such code would be necessary to demonstrate that an ABV analysis can be performed efficiently and consistently, within practical budgetary and time constraints. (The example building described here was analyzed using a combination of DRAIN-2DX analyses, with custom pre- and post-processor computer code, a spreadsheet, a simulation add-in, and extensive data handling. Such a construction is appropriate to demonstrate that capability to perform ABV analyses, but not for regular use on real applications.)

6.2.7. Expanding the library of capacity and cost distributions

The assembly fragilities developed to illustrate the example building represent only the beginning of a potentially powerful tool. To make ABV more broadly useful will require development of a large library of fragility functions and cost and duration distributions. Key assemblies calling for new fragility and repair-cost distribution include: ductile and nonductile reinforced concrete joints; reinforced concrete shear walls; pre- and post-San Fernando tilt-up wall panel-to-panel connections; pre- and post-San Fernando tilt-up wall-to-roof connections; post-Northridge steel moment-frame connections of various types; beams and columns of ductile steel-frame buildings; various types of exterior wall cladding; glazing systems of various framing, sealing and pane-size configurations; above-ceiling systems such as air duct and cable trays; elevators and escalators; various rooftop mechanical components; various interior partition systems; other automatic sprinkler systems such as braced wet systems, braced and unbraced dry (preaction) systems, and systems using damage-resistant sprinkler heads.

6.2.8. Procedures for use with imperfect building information

Another interesting development would be to establish ABV procedures to use when design and construction knowledge is imperfect. There are various situations where this would be useful. At the simplest level are cases where the precise type of a particular assembly is hidden; this would require the application of a probabilistic mixture of possible detailed assemblies. A procedure is required for the appropriate selection of weights in this mixture. Since an ABV analysis that considers probabilistic mixtures of assemblies would result in additional uncertainty in loss, it would be valuable to establish a procedure to determine the value of reducing this uncertainty by gathering additional information: under what situations is it worthwhile to uncover the hidden assembly before making a final risk-management decision? It is likely that this problem would be readily tractable using standard decision-analysis techniques.

At the opposite end of this spectrum is the case where only summary building information is available: location, use, size, and structure type. The solution to this latter problem may be to develop category-based vulnerability functions based on a probabilistic mix of building-specific ABV analyses. This requires the compilation of a library of ABV analyses reflecting a range of building vulnerability functions within a common category. Perhaps such a library could be created by stochastic modeling of a large number of hypothetical buildings with varying dimensions, configurations, detailed assembly types and inventories. A particularly interesting outcome of such a study would be insight into the variability of a category-based vulnerability function. It seems likely that the coefficient of variation of some structure types would be greater than that used by current techniques based on expert opinion.

6.2.9. Implications for performance-based engineering

Perhaps the most interesting research opportunity offered by the ABV has to do with performance-based design (PBD) verification. Because it examines performance at the assembly level, ABV offers the ability to characterize the building component damage and system operation at the same level of detail as do PBD codes currently in development. PBD requirements currently being developed, such as those in FEMA-273 [FEMA, 1997], employ qualitative descriptions of damage, such as "few broken windows," "minor leakage," and so on, terms which do not emerge from engineering calculations. A probabilistic, quantitative performance-based code would require the development of numerical ranges corresponding to these descriptive requirements, and the establishment of minimum acceptable passing probabilities. ABV therefore offers a systematic, statistically rigorous method to estimate the probability of achieving detailed, component-specific quantitative PBD requirements. Given such numerical criteria, an approach based on ABV can readily determine passing probabilities on an assembly-by-assembly basis.

FEMA-273 [FEMA, 1997] does associate certain drift limits with actual performance objectives, but these may or may not provide the level of performance desired. First, not all assemblies are primarily sensitive to drift. Second, drift and acceleration only indirectly relate to the performance issues of interest to the building owner, such as ceiling damage, window breakage, and other aspects of damage that materially and directly affect post-earthquake safety and operability. For this reason, drift limitations prevent possible tradeoffs between structural stiffness and flexible assemblies.

If code-writing authorities were to establish quantitative PBD goals and minimum acceptable passing probabilities, ABV would enable designers to select between competing assembly configurations so as to meet the PBD requirements as

economically as possible. Thus, a designer may allow a structure greater flexibility if the building assemblies allow for that flexibility. This facilitates tradeoffs between structural and nonstructural design on the basis of cost and performance. This aspect of ABV was not examined in detail in the present study, but is the subject of a manuscript currently in review.

Aside from PBD compliance verification, ABV offers an opportunity to examine PBD objectives from a normative viewpoint, that is, in determining the degree to which a particular performance goal *should* be assured. This is a generic tolerable-risk problem similar to one the author addressed in a study of life-safety equipment reliability [Porter, Scawthorn, Taylor, et al., 1998], and may be tractable by similar techniques.

PBD aspects of ABV can be used by owners or developers of critical facilities who require their building and its critical equipment systems to remain operational after severe earthquakes with high confidence. Examples include hospitals, bank data centers, telephone central offices, and other emergency-response facilities, as well as high-technology manufacturing facilities where brief loss of function can be very costly in terms of market share. Current methodologies do not allow the analyst to quantify the probability of meeting detailed performance goals. When combined with systems analysis, however, ABV can estimate these probabilities, and indicate the major sources of risk to operational failure. Existing buildings or new designs that do not meet these requirements can be iterated to do so, either with additional strength, modified stiffness, increased component capacities, or increased redundancy.

6.2.10. Estimation of post-earthquake safety evaluation

Finally, one last interesting aspect of PBD verification is that many performance indicators are contained in post-earthquake seismic safety evaluations. A popular evaluation procedure, ATC-20 [ATC, 1990], uses visible cues on the building exterior

such as residual drift and visible damage to structural elements to indicate whether a building poses an unacceptable life-safety threat. Output of PBD aspects from ABV analyses could help to estimate building seismic fragility in terms of probability of being posted unsafe or limited entry (red-tagged or yellow-tagged) after an earthquake.

6.3. SUMMARY

ABV offers a number of potentially valuable opportunities for practical applications and theoretical research, by allowing the engineer to model building performance at a very detailed level on a building-specific basis. Many outputs of ABV can replace the expert judgment embodied in category-based vulnerability functions. Others aspects of ABV such as detailed economic assessment of seismic retrofit alternatives could not be addressed by previously existing techniques. By linking well-established methods of seismic hazard analysis, ground motion simulation, structural analysis, assembly fragility, construction cost estimation, construction scheduling, and decision analysis, ABV represents a novel, systematic, and highly flexible analytical methodology for probabilistic seismic risk management and performance-based engineering, code development and design verification.

CHAPTER 7
REFERENCES

American Institute of Steel Construction, Inc. (AISC), 1986, ***Load and Resistance Factor Design, First Edition,*** Chicago: AISC

American Society for Testing and Materials (ASTM), 1996, "E1557-96 Standard Classification for Building Elements and Related Sitework – UNIFORMAT II," in ***1997 Annual Book of ASTM Standards, Section 4, Construction, Volume 04.11 Building Constructions,*** West Conshohocken, PA: ASTM, pp. 630-639

American Society for Testing and Materials (ASTM), 1999, ***E 2026-99 Standard Guide for the Estimation of Building Damageability in Earthquakes,*** West Conshohocken, PA: ASTM, 24 pp.

ANCO Engineers, Inc., 1983, ***Seismic Hazard Assessment of Nonstructural Ceiling Components – Phase I, National Science Foundation grant CEE-8114155,*** Culver City, CA: ANCO Engineers, Inc., 125 pp.

Anderson, J.C., and X. Duan, 1998, ***Repair/Upgrade Procedures for Welded Beam to Column Connections, PEER 98-03,*** Berkeley CA: Pacific Earthquake Engineering Research Center, 202 pp.

Applied Technology Council (ATC), 1985, ***ATC-13: Earthquake Damage Evaluation Data for California***, Redwood City, CA: Applied Technology Council, 492 pp.

Applied Technology Council (ATC), 1990, ***ATC-20: Procedures for Postearthquake Safety Evaluation of Buildings,*** Redwood City, CA: Applied Technology Council, 152 pp.

Applied Technology Council (ATC), 1998, ***ATC-29-1: Proceedings of Seminar on Seismic Design, Retrofit, and Performance of Nonstructural Components, January 22-23, 1998, San Francisco, California,*** Redwood City, CA: Applied Technology Council, 518 pp.

Astaneh, A., 2000, personal communication.

Beck, J., A. Kiremidjian, S. Wilkie et al., 1999, ***Social, Economic, and Systems Aspects of Earthquake Recovery and Reconstruction, Year Two Research Report,*** Tokyo: Kajima Corporation, 105 pp.

Behr, R.A., A. Belarbi, and C.J. Culp, 1995, "Dynamic Racking Tests of Curtain Wall Glass Elements with In-Plane and Out-of-Plane Motions," in ***Earthquake Engineering and Structural Dynamics, vol. 24,*** New York: J. Wiley & Sons, Inc., pp. 1-14

Behr, R.A., and C.L. Worrell, 1998, "Limit States for Architectural Glass Under Simulated Seismic Loadings," in ***Proc., Seminar on Seismic Design, Retrofit, and Performance of Nonstructural Components, ATC-29-1 January 22-23, 1998, San Francisco,*** Redwood City, CA: Applied Technology Council, pp. 229-240

Bier, V.M., 1999, "Challenges to the Acceptance of Probabilistic Risk Analysis," ***Risk Analysis*** vol. 19 no. 4, McLean VA: Society for Risk Analysis, pp. 703-710

Bier, V.M., Y.Y. Haimes, J.H. Lambert, N.C. Matalas, and R. Zimmerman, 1999, "A Survey of Approaches for Assessing and Managing the Risk of Extremes," ***Risk Analysis*** vol. 19 no. 1, McLean VA: Society for Risk Analysis, pp. 83-94

Boore, D.M., W.B. Joyner, and T.E. Fumal, 1997, "Equations for Estimating Horizontal Response Spectra and Peak Accelerations from Western North American Earthquakes: a Summary of Recent Work," in ***Seismological Research Letters, Vol. 68, No. 1, January/February1997,*** El Cerrito, CA: Seismological Society of America, pp. 128-153

Box, G.E.P., G.M. Jenkins, and G.C. Reinsel, 1994, ***Time Series Analysis; Forecasting and Control, 3rd ed.,*** Englewood Cliffs, NJ: Prentice Hall Inc., 598 pp.

Building Seismic Safety Council, 1997, ***FEMA 302, NEHRP Recommended Provisions for Seismic Regulations for New Buildings***, Washington, DC: Federal Emergency Management Agency, 337 pp.

Bullen, K.E., and B.A. Bolt, 1985, ***An Introduction to the Theory of Seismology, 4th edition,*** Palo Alto: Cambridge University Press, 499 pp.

California State Assembly, 1994, ***A.B. No. 57 (1st Ex. Sess.), An Act to Amend Sections 1689.5, 1689.6, 1689.7, and 1689.13 of, and to Add Section 1689.14 to, the Civil Code,***

and to Add Section 396 to the Penal Code, Relating to Consumer Protection, Sacramento, CA: California State Assembly, http://www.leginfo.ca.gov/pub/93-94/bill/asm/ab_0051-0100/abx1_57_bill_940927_chaptered

Construction Specifications Institute (CSI), 1995, ***Master List of Numbers and Titles for the Construction Industry, MP-2-1,*** Construction Specifications Institute, Alexandria, Virginia

Conte, J.P., K.S. Pister, and S.A. Mahin, 1992, "Nonstationary ARMA Modeling of Seismic Motions," in ***Soil Dynamics and Earthquake Engineering, November, 1992,*** New York: Elsevier Science, pp. 411-426

Dalkey, N., B. Brown, and S. Cochrane, 1970, "Use of Self-Ratings to Improve Group Estimates," ***Technological Forecasting: An International Journal, vol. 1., no. 3.,*** New York: American Elsevier Publishing, pp. 283-291

Eidinger, J., and K. Goettel, 1998, "The Benefits and Costs of Seismic Retrofits of Nonstructural Components for Hospitals, Essential Facilities, and Schools," ***ATC-29-1, Proceedings of Seminar on Seismic Design, Retrofit, and Performance on Nonstructural Components, January 22-23, 1998, San Francisco, California,*** Redwood City, CA: Applied Technology Council, pp. 491-504

Emco Ltd., 1996, ***Wood-fibre Technical Specifications,*** London, Ontario: Emco Ltd.

Emhart Fastening Technologies, 1998, "Blind POP Rivets," ***Product Catalog,*** Irvine CA: Emhart Fastening Technologies

Engelhardt, M.D., K. Kim, T.A. Sabol, L. Ho, H.I. Kim, J. Uzarski, A. Husain, 1995, "Analysis of a Six-Story Steel Moment-Frame Building in Santa Monica," ***Technical Report: Analytical and Field Investigations of Buildings Affected by the Northridge Earthquake of January 17, 1994, Report No. SAC 95-04,*** Sacramento, CA: SAC Steel Project

Federal Emergency Management Agency (FEMA), 1989, ***FEMA-157, Tytpical Costs for Seismic Rehabilitation of Existing Buildings, vol. 2: Supporting Documentation,*** Washington DC, 100 pp.

Federal Emergency Management Agency (FEMA), 1994, ***FEMA-74, Reducing the Risks of Nonstructural Earthquake Damage, A Practical Guide.*** Washington DC, 131 pp..

Federal Emergency Management Agency (FEMA), 1997, ***FEMA-273: NEHRP Guidelines for the Seismic Rehabilitation of Buildings,*** Washington, DC: FEMA, 386 pp.

FIMS, Inc., 1987, ***Data Processing Facilities: Guidelines for Earthquake Hazard Mitigation,*** Sacramento CA: VSP Associates, 125 pp.

Flynn, G., 1998, personal communication.

Freudenthal, A.M., J.M. Garrelts, and M. Shinozuka, 1966, "The Analysis of Structural Safety," ***Journal of the Structural Division, vol. 92, no. ST1,*** Reston, VA: American Society of Civil Engineers, February 1966, pp. 267-325

GeoRisk, 1998, ***Risk Management Terminology***, Santa Clara, CA: http://www.georisk.com/terminol/termrisk.shtml

Gordon, T.J., and O. Helmer, 1964, ***Report on a Long Range Forecasting Study, RAND Paper P-2982,*** Santa Monica CA: RAND Corporation

Griffin, M.J., and W. Tong, 1992, "Performance of Suspended Ceilings in Earthquakes with Recommended Strengthening Techniques for Damage Mitigation," ***ATC-29: Proc., Seminar and Workshop on Seismic Design and Performance of Equipment and Nonstructural Elements in Buildings and Industrial Structures; Irvine, California, October 3-5, 1990*** Redwood City, CA: Applied Technology Council, pp. 75-85

Haas, P.J., 1998, "Generalized Semi-Markov Processes," ***EESOR 232, Simulation Lecture Notes #3,*** Stanford, CA: Stanford University, 7 pp.

Hart, G.C., S.C. Huang, R.F. Lobo, and J. Stewart, 1995, "Elastic and Inelastic Analysis for Weld Failure Prediction of Two Adjacent Steel Buildings," ***Technical Report: Analytical and Field Investigations of Buildings Affected by the Northridge Earthquake of January 17, 1994, Report No. SAC 95-04,*** Richmond, CA: SAC Steel Project

Holden Architectural Ltd., 1998, ***Ecophon Acoustic Suspended Ceiling Systems***, Wellington New Zealand: Holden Architectural Ltd.

Howard, R.A., 1966, "Decision Analysis: Applied Decision Theory," ***Proc., Fourth International Conference on Operations Research,*** D.B. Hertz and J. Melese, eds., New York: Wiley Interscience, pp. 55-71

Howard, R.A., 1970, "Risk Preference," ***Readings on The Principles and Applications of Decision Analysis, vol. 2: Professional Collection,*** R.A. Howard and J. E. Matheson, eds., Menlo Park, CA: Strategic Decisions Group, pp. 627-663

Howard, R.A., 1988, "Decision Analysis: Practice and Promise," ***Management Science, vol. 34, no. 6., June 1988,*** Linthicum, MD: The Institute for Operations Research and the Management Sciences (INFORMS).

Howard, R.A., 1992, "In Praise of the Old Time Religion," ***Utility Theories: Measurements and Applications,*** W. Edwards, ed., Boston: Kluwer Academic Publishers, pp. 27-55

Howard, R.A., 1997, ***Decision Analysis, Manuscript in Progress,*** Stanford CA: Stanford Bookstore Custom Publishing.

International Conference of Building Officials (ICBO), 1988, ***Uniform Building Code (UBC) Standards***, 1988 edition, Whittier, CA: ICBO, 1448 pp.

Jeffery, R.C., 1965, ***The Logic of Decision,*** San Francisco: McGraw-Hill, 201 pp.

Jin, M., and A. Astaneh, 1998, "Study of Seismc Resistance of Desktop Computers," ***ATC 29-1, Proceedings of Seminar on Seismic Design, Retrofit, and Performance of Nonstructural Components,*** Redwood City CA: Applied Technology Council, pp. 379-392

Johnson, G.S., R.E. Sheppard, M.D. Quilici, S.J. Eder, and C.R. Scawthorn, 1999, ***Seismic Reliability Assessment of Critical Facilities: A Handbook, Supporting Documentation, and Model Code Provisions, MCEER 99-0008,*** Buffalo, NY: Multidisciplinary Center for Earthquake Engineering Research.

Kao, A., T.T. Soong, and A. Vender, 1999, ***Nonstructural Damage Database, MCEER 99-0014,*** Buffalo NY: Multidisciplinary Center for Earthquake Engineering Research

Kariotis, J., and T.J. Eiamani, "Analysis of a Seventeen-Story Steel Moment-Frame Building Damaged by the Northridge Earthquake," ***Technical Report: Analytical***

and Field Investigations of Buildings Affected by the Northridge Earthquake of January 17, 1994, Report No. SAC 95-04, Richmond, CA: SAC Steel Project

Kennedy, R.P., and M.K. Ravindra, 1984, "Seismic Fragilities for Nuclear Power Plant Risk Studies," ***Nuclear Engineering and Design 79,*** Philadelphia PA: Elsevier Science Publishers pp. 47-67

Kiremidjian, A.S., 1999, "Multiple Earthquake Event Loss Estimation Methodology," ***Proc., 11th European Conference on Earthquake Engineering, Paris, France, Sept. 6-11, 1998,*** Rotterdam: A.A. Balkema, pp. 151-160

Kleindorfer, P.R., and H. Kunreuther, 1999, "The Complementary Roles of Mitigation and Insurance in Managing Catastrophic Risks," ***Risk Analysis*** 19 (4):727-738, August 1999, Society for Risk Analysis

Krauwinkler, H., A. Alali, C.C. Thiel, and J.M.Dunlea, 1995, "Analysis of a Damaged Four-Story Building and an Undamaged Two-Story Building," ***Technical Report: Analytical and Field Investigations of Buildings Affected by the Northridge Earthquake of January 17, 1994, Report No. SAC 95-04,*** Richmond, CA: SAC Steel Project

KRTA Ltd., 1992, ***Earthquake and War Damage Commission Recommendations on Minimum Requirements for the Seismic Design and Detailing of Suspended Ceiling Grid Systems,*** Project 8513, Aukland, New Zealand: KRTA Ltd., 83 pp.

Kunreuther, H., 2000, "Managing Catastrophic Risks," ***Building Standards, vol. LXIX, no. 2, April 2000,*** Irvine, CA: International Conference of Building Officials, pp. 45-47

Kustu, O., 1986, "Earthquake Damage Prediction for Buildings Using Component Test Data," ***Proc. Third U.S. National Conference on Earthquake Engineering, Aug 24-28, 1986, Charleston, SC,*** El Cerrito, CA: Earthquake Engineering Research Institute, pp. 1493-1504

Kutsu, O., D.D. Miller, and S.T. Brokken, 1982, ***Development of Damage Functions for Highrise Building Components,*** San Francisco: URS/John A Blume & Associates for the US Department of Energy

Lutz, K.A. and A.S. Kiremidjian, 1993, ***Generalized Semi-Markov Process For Modeling Spatially And Temporally Dependent Earthquakes,*** Stanford, CA: John A. Blume Earthquake Engineering Center, 88 pp.

Mahaney, J.A., T.F. Paret, B.E. Kehoe, et al., 1993, "The Capacity Spectrum Method for Earthquake Response During the Loma Prieta Earthquake," ***Proc. 1993 U.S. National Earthquake Conference, Memphis TN, May 2-5, 1993,*** Memphis, TN: Central United States Earthquake Consortium, 1993, Volume II, pp. 501-510

Melcher, R.E., 1999, ***Structural Reliability Analysis and Prediction, 2nd ed.,*** New York: John Wiley & Sons, 437 pp.

Naeim, F., R. DiJulio, K. Benuska, A.M. Reinhorn, and C. Li, 1995, "Evaluation of Seismic Performance of an 11-Story Steel Moment Frame Building During the 1994 Northridge Earthquake," ***Technical Report: Analytical and Field Investigations of Buildings Affected by the Northridge Earthquake of January 17, 1994, Report No. SAC 95-04,*** Richmond, CA: SAC Steel Project

Nakata, S., H. Itoh, A. Baba, and S. Okamoto, 1984, "US-Japan Cooperative Research on R/C Full-Scale Building Test," ***Proceedings of the Eighth World Conference on Earthquake Engineering, July 21-28, 1984, San Francisco CA,*** Englewood Cliffs NJ: Prentice-Hall, Inc., vol. VI, pp. 611-618

National Fire Protection Association (NFPA), 1991, ***Fire Protection Handbook, 17th Edition,*** A.E. Cote and J. L. Linville, eds., Quincy, MA: NFPA, ~2000 pp.

National Institute of Building Sciences (NIBS), 1995, ***Development of a Standardized Earthquake Loss Estimation Methodology,*** Washington, DC: Federal Emergency Management Agency, 500 pp.

Oliva, M.G., 1990, ***Racking Behavior of Wood-framed Gypsum Panels Under Dynamic Load, Report No. UBC/EERC-85/06,*** Berkeley CA: Earthquake Engineering Research Center, 49 pp.

Owens, L., 2000, personal communication

Pantelides, C.P., and R.A. Behr, 1994, "Dynamic In-Plane Racking Tests of Curtain Wall Glass Elements," in ***Earthquake Engineering and Structural Dynamics, vol. 23,*** New York: J. Wiley & Sons, Inc., pp. 211-228

Park, Y-J., A.H-S. Ang, and Y.K. Wen, 1984, "Seismic Damage Analysis and Damage-Limiting Design of RC Buildings," ***Structural Research Series, Report no. UILU-ENGINEER-84-2007,*** Urbana IL., University of Illinois at Urbana-Champaign

Peurifoy, R.L., 1975, ***Estimating Construction Costs, 3rd edition,*** San Francisco: McGraw-Hill, 456 pp.

Polhemus, N.W., and A.S. Cakmak, 1981, "Simulation of Earthquake Ground Motions Using Autoregressive Moving Average Models," in ***Earthquake Engineering and Structural Dynamics, vol. 9,*** New York: John Wiley & Sons, Inc., pp. 343-354

Porter, K.A., C. Scawthorn, C. Taylor, N. Blais, 1998, ***Appropriate Seismic Reliability for Critical Equipment Systems: Recommendations Based on Regional Analysis of Financial and Life Loss,*** MCEER-98-0016, Buffalo, NY: Multidisciplinary Center for Earthquake Engineering Research, State University of New York, Buffalo, 104 pp.

Porter, K.A., C. Scawthorn, D.G. Honegger, T.D. O'Rourke, and F. Blackburn, 1992, "Performance of Water Supply Pipelines in Liquefied Soil," in Eguchi, R.T., ed., ***Proceedings of the 4th US-Japan Workshop on Earthquake Disaster Prevention for Lifeline Systems; Los Angeles, August 19-21, 1991*** Gaithersburg MD: National Institute of Standards and Technology, pages 3-17.

Porter, K.A., G.S. Johnson, M.M. Zadeh, C.R. Scawthorn, and S.J. Eder, 1993, ***Seismic Vulnerability of Equipment in Critical Facilities: Life-Safety and Operational Consequences, Technical Report NCEER-93-0022,*** Buffalo NY: National Center for Earthquake Engineering Research, 365 pp.

Rihal, S.S., 1982, "Behavior of Nonstructural Building Partitions During Earthquakes," in ***Proceedings of the Seventh Symposium on Earthquake Engineering, Department of Earthquake Engineering, University of Roorke, India, November 10-12, 1982,*** Dehli: Sarita Prakashan, pp. 267-277

Rihal, S.S., 2000, personal communication.

Rihal, S.S., and G. Granneman, 1984, "Experimental Investigation of the Dynamic Behavior of Building partitions and Suspended Ceilings During Earthquakes," in ***Proceedings of the Eighth World Conference on Earthquake Engineering, July 21-28, 1984,*** San Francisco, Englewood Cliffs, NJ: Prentice-Hall, pp.1135-1142

RS Means Corp., 1997a, ***Means Construction Cost Data***, Kingston, MA: RS Means Co.

RS Means Corp., 1997b, ***Means Assemblies Cost Data,*** Kingston, MA: RS Means Co.

Rubin, H.W., 1991, ***Dictionary of Insurance Terms,*** New York: Barron's Educational Services Inc., 465 pp.

SAC Steel Project, 1995a, ***Steel Moment Frame Connection Advisory No. 3, Report No. SAC 95-01,*** Richmond, CA: SAC Steel Project, ~350 pp.

SAC Steel Project, 1995b, ***Interim Guidelines: Evaluation, Repair, Modification and Design of Steel Moment Frames, Report No. SAC 95-02,*** Richmond, CA: SAC Steel Project

SAC Steel Project, 1995c, ***Technical Report: Analytical and Field Investigations of Buildings Affected by the Northridge Earthquake of January 17, 1994, Report No. SAC 95-04,*** Richmond, CA: SAC Steel Project, 379 pp.

SAC Steel Project, 1999, ***Interim Guidelines and Advisory Number 2, Report No. SAC 99-01,*** Richmond, CA: SAC Steel Project

Saeki, T., H. Tsubokawa, and S. Midorikawa, 2000, "Seismic Damage Evaluation of Household Property by Using Geographic Information Systems (GIS)," ***Proceedings, 12th World Conference on Earthquake Engineering, , January 30 – February 5, Aukland New Zealand***, International Association for Earthquake Engineering, paper 1968, 8 pp.

Scholl, R.E., 1981, ***Seismic Damage Assessment for Highrise Buildings, Annual Technical Report, Open-file Report 81-381,*** Menlo Park, CA: US Geological Survey, 143 pp.

Scholl, R.E., and O. Kustu, 1984, "Procedures and Data Bases for Earthquake Damage Preduction and Risk Assessment," ***Primer on Improving the State of Earthquake Hazards Mitigation and Preparedness, Open File Report 84-0772,*** Gori, P., ed., Reston VA: US Geological Survey, pp. 162-213

Singhal, A., and Kiremidjian, A.S., 1997, ***A Method for Earthquake Motion-Damage Relationships with Application to Reinforced Concrete Frames, Technical Report NCEER 97-0008,*** Buffalo, NY: National Center for Earthquake Engineering Research, 218 pp.

Somerville, P., R. Graves, and C. Siakia, 1995, ***SAC-95-03: Characterization of Ground Motions During the Northridge Earthquake of January 17, 1994,*** Richmond, CA: SAC Steel Project

Southwell, C., 2000, personal communication.

Spetzler, C.S., 1968, "The Development of a Corporate Risk Policy for Capital Investment Decisions," ***IEEE Transactions on Systems Science and Cybernetics, vol. SSC-4, no. 3.,*** September 1968, Institute of Electronics and Electrical Engineers, pp. 279-300, reprinted in 1989 ***Readings on The Principles and Applications of Decision Analysis, vol. 2: Professional Collection,*** R.A. Howard and J. E. Matheson, eds., Menlo Park, CA: Strategic Decisions Group, pp. 667-688

Spetzler, C.S., and C.S.S. Von Holstein, 1972, "Probability Encoding in Decision Analysis," ***Proc., ORSA-TIMS-AIEE 1972 Joint National Meeting, Atlantic City NJ, 8-10 November 1972***, pp. 603-625

Sprinkler Fitters U.A. Local 483, 1989, untitled, San Carlos, CA

Steinbrugge, K.V., 1982, ***Earthquakes, Volcanoes, and Tsunamis, An Anatomy of Hazards,*** New York NY: Skandia America Group, 392 pp.

Swan, S.W., and R. Kassawara, 1998, "The Use of Earthquake Experience Data for Estimates of the Seismic Fragility of Standard Industrial Equipment," ***ATC-29-1, Proc., Seminar on Seismic Design, Retrofit, and Performance of Nonstructural Components,*** Redwood City CA: Applied Technology Council, pp. 313-322

Tversky, A., and D. Kahneman, 1974, "Judgment under Uncertainty: Heuristics and Biases," ***Science***, September 27, 1974, vol. 185, pp. 1124-1131

Uang, C.M., Q.S. Yu, A. Sadre, D. Bonmowitz, and N. Youssef, 1995, "Performance of a 13-Story Steel Moment-Resisting Frame Danaged by the 1994 Northridge

Earthquake," ***Technical Report: Analytical and Field Investigations of Buildings Affected by the Northridge Earthquake of January 17, 1994, Report No. SAC 95-04,*** Richmond, CA: SAC Steel Project

URS/John A Blume & Associates, Engineers, 1989, ***Techniques for Seismically Rehabilitating Existing Buildings (Preliminary)***, San Francisco CA: URS/John A Blume & Associates, 200 pp.

Von Neumann, J., and O. Morgenstern, 1944, ***Theory of Games and Economic Behavior,*** Princeton: Princeton University Press, 625 pp.

Weir, P., 2000, personal communication.

Wetherill, E.B., 1989, ***Means Repair and Remodeling Estimating,*** Kingston, MA: R.S. Means Corp., 452 pp.

Winstone Wallboards Ltd., 1998, ***Winstone Wallboards Gibtone Suspended Ceiling Tiles***, Aukland New Zealand: Winstone Wallboards Ltd.

APPENDIX A.
ASSEMBLY TAXONOMY

Each assembly type is assumed to be primarily susceptible to one of the response parameters listed in Table A-1. Assemblies are defined according to the preliminary taxonomy shown in Table A-2, as discussed in Chapter 2. Table A-2 is intended as a starting point for the creation of fragility and cost distributions, not as the conclusion of exhaustive examination of all the listed assemblies. The assemblies shown in italics – most of the assemblies listed – are tentative types, assigned response parameters based on judgment. It is anticipated that these will undergo extensive revision as they are examined in detail, both in terms of taxonomic quantization and response parameter.

Table A-1. Hazard parameters considered for building assemblies.

Parameter	Explanation
A_f	Floor spectral acceleration. Useful for flexible acceleration-sensitive components, e.g., suspended ceilings, but not used here because of coding and computational demands, and for lack of empirical fragility data. (Some exceptions to this latter point exist, e.g., Wilcoski's [1998] study of power transfer bushings.)
DCR	Demand-capacity ratio. Ratio of maximum beam- or column-end moment demand to its yield moment as estimated under 3-dimensional linear elastic modeling. Used for WSMF beam-column connections
GD	Ground displacement. Liquefaction, landslide, differential compaction.
PADI	Park-Ang damage index. Maximum ductility demand plus a measure of energy absorbed during cyclic loading; useful for reinforced concrete connections. See Park et al. [1984] for detail.
PDA	Peak diaphragm acceleration. Peak acceleration of the diaphragm to which the assembly is attached. Used for acceleration-sensitive components as a substitute for A_f. Assemblies sensitive to *PDA* include assemblies that do not span between diaphragms, such as furniture, suspended ceilings, mechanical equipment, etc.
PGA	Peak ground acceleration. Though the most common hazard parameter, used exclusively in Kennedy et al. [1980], *pga* was rejected here in favor of *PDA*, because of the desire to capture the effect on assembly damage of structural response. Using *pga* would prevent accounting for unique structural characteristics of individual buildings, and thereby increase true uncertainty of damage and cost.
RD	Residual interstory drift ratio. Used primarily for doors, which must be used after the earthquake
Rgd	Rugged. Some assemblies are not susceptible to failure in reasonable levels of shaking. Although "rugged" is not a hazard, it is included in the list for completeness.
TD	Peak transient interstory drift ratio. Used for drift-sensitive components that span between diaphragms, e.g., partitions, cladding

Table A-2. Assembly taxonomy.

Building assembly					
Div.	**Class**	**Line**	**Cond.**	**Description**	**Hazard**
1. Foundations					
1.1	*120*	*0000*	*00*	*Spread footing*	***GF***
1.1	*140*	*0000*	*00*	*Strip footing*	***GF***
1.1	*210*	*0000*	*00*	*Walls cast in place*	***PDA***
1.1	*292*	*0000*	*00*	*Foundation dampproofing*	***rgd***
1.9	*100*	*0000*	*00*	*Excavation & backfill*	***GF***
2. Substructure					
2.1	*200*	*0000*	*00*	*Slab on grade*	***GF***
3. Superstructure					
3.1	*114*	*0000*	*00*	*Cast-in-place columns nonductile*	***PADI***
3.1	*114*	*0000*	*01*	*Cast-in-place columns ductile*	***PADI***
3.1	*120*	*0000*	*00*	*Precast concrete columns nonductile*	***PADI***
3.1	*120*	*0000*	*01*	*Precast concrete columns ductile*	***PADI***
3.1	*130*	*0000*	*00*	*Steel gravity columns*	***DCR***
3.1	*130*	*0000*	*00*	*Steel gravity beams*	***DCR***
3.1	*130*	*0000*	*00*	*Steel gravity (simple) connections*	***DCR***
3.1	*130*	*0001*	*00*	*WSMF columns*	***DCR***
3.1	**130**	**0002**	**01**	**WSMF connections pre-Northridge**	**DCR**
3.1	*130*	*0002*	*02*	*WSMF connections post-Northridge*	***DCR***
3.1	*130*	*0003*	*00*	*WSMF beams*	***DCR***
3.1	*140*	*0000*	*00*	*Wood columns*	***TD***
3.1	*190*	*0000*	*00*	*Steel columns fireproofing*	***TD***
3.1	*200*	*0000*	*00*	*Precast concrete beams nonductile*	***PDA***
3.1	*200*	*0000*	*01*	*Precast concrete beams ductile*	***PDA***
3.4	*300*	*0000*	*00*	*Metal siding support*	***PDA***
3.5	*100*	*0000*	*00*	*Cast-in-place diaphragm*	***PDA***
3.5	*200*	*0000*	*00*	*Precast concrete plank diaphragm*	***PDA***
3.5	*310*	*0000*	*00*	*Wood frame beams & girders*	***PDA***
3.5	*360*	*0000*	*00*	*Light-gage steel floor system*	***PDA***
3.5	*420*	*0000*	*00*	*Deck & joist on bearing wall*	***PDA***
3.5	*440*	*0000*	*00*	*Deck & joist on beam and wall*	***PDA***
3.5	*460*	*0000*	*00*	*Steel joists, beam & slab on columns*	***PDA***
3.5	*500*	*0000*	*00*	*Composite beam & slab*	***PDA***

Table A-2. Assembly taxonomy (cont.)

Building assembly					
Div.	**Class**	**Line**	**Cond.**	**Description**	**Hazard**
3.5	*700*	*0000*	*00*	*Wood diaphragm*	***PDA***
3.7	*400*	*0000*	*00*	*Metal roof diaphragm*	***PDA***
3.7	*500*	*0000*	*00*	*Wood roof diaphragm*	***PDA***
3.9	*100*	*0000*	*00*	*Stairs*	***PDA***
4. Exterior closure					
4.1	*110*	*0000*	*00*	*Cast in place wall*	***PDA***
4.1	*140*	*0000*	*00*	*Precast concrete panel weak conn.*	***PDA***
4.1	*140*	*0000*	*01*	*Precast concrete panel strong conn.*	***PDA***
4.1	*160*	*0000*	*00*	*Tiltup concrete panel weak conn.*	***PDA***
4.1	*160*	*0000*	*01*	*Tiltup concrete panel strong conn.*	***PDA***
4.1	*210*	*1000*	*00*	*CMU unreinforced wall*	***PDA***
4.1	*210*	*5000*	*00*	*CMU reinforced wall*	***PDA***
4.1	*230*	*0000*	*00*	*Brick wall*	***PDA***
4.1	*240*	*0000*	*00*	*Stone veneer on stud*	***PDA***
4.1	*250*	*0000*	*00*	*Brick veneer on stud*	***PDA***
4.1	*270*	*0000*	*00*	*CMU unreinforced wall, brick veneer*	***PDA***
4.1	*280*	*0000*	*00*	*Glass block*	***PDA***
4.1	*384*	*0000*	*00*	*Metal siding panel*	***TD***
4.1	*412*	*0000*	*00*	*Wood and other siding*	***TD***
4.5	*100*	*0000*	*00*	*Stucco wall finish*	***TD***
4.6	*100*	*0000*	*00*	*Exterior door*	***rgd***
4.7	*100*	*0000*	*00*	*Exterior glazing all others*	*TD*
4.7	**100**	**0001**	**00**	**Exterior glazing 5x6 pane Al frame**	**TD**
4.7	*582*	*0000*	*00*	*Tubular Al framing*	*TD*
4.7	*584*	*0000*	*00*	*Curtain wall panel*	*TD*
5. Roofing					
5.1	*000*	*0000*	*00*	*Roof cover*	*rgd*
5.7	*000*	*0000*	*00*	*Roof deck rigid insulation*	*rgd*
5.8	*000*	*0000*	*00*	*Roof openings & finishes*	*rgd*
6. Interior construction					
6.1	*210*	*0000*	*00*	*CMU unreinforced partition*	*TD*
6.1	*270*	*0000*	*00*	*Hollow clay tile partition*	*TD*
6.1	*500*	*0000*	*00*	*Drywall partition, metal stud, screws, all others*	*TD*
6.1	**500**	**0000**	**01**	**Drywall partition 5/8", 2 side, mtl stud, screws**	**TD**
6.1	*500*	*0100*	*00*	*Drywall partition, wood stud, nails*	*TD*
6.1	*600*	*0000*	*00*	*Plaster partition*	*TD*
6.1	*820*	*0000*	*00*	*Folding partition*	*rgd*

Table A-2. Assembly taxonomy (cont.)

Building assembly					
Div.	**Class**	**Line**	**Cond.**	**Description**	**Hazard**
6.1	*870*	*0000*	*00*	*Toilet partition*	*rgd*
6.4	*000*	*0000*	*00*	*Interior doors*	*RD*
6.5	*000*	*0000*	*00*	*Wall finishes*	*TD*
6.6	*000*	*0000*	*00*	*Floor finishes*	*PDA*
6.7	*100*	*2400*	*00*	*Plaster ceiling*	*PDA*
6.7	*100*	*4800*	*00*	*Drywall ceiling*	*PDA*
6.7	*100*	*5800*	*00*	*Acoustical ceiling all others*	*PDA*
6.7	**100**	**5800**	**02**	**Acoustical ceiling 2′x4′ light Al grid attached x_s in [11, 20 ft]**	**PDA**
6.7	**100**	**5800**	**03**	**Acoustical ceiling 2′x4′ light Al grid attached x_s in [21, 30 ft]**	**PDA**
6.7	**100**	**5800**	**06**	**Acoustical ceiling 2′x4′ light Al grid attached x_s in [51, 60 ft]**	**PDA**
6.7	**100**	**5800**	**07**	**Acoustical ceiling 2′x4′ light Al grid attached x_s in [61, 70 ft]**	**PDA**
6.9	*000*	*0000*	*00*	*Int fin/ext wall*	*TD*
7. Conveying					
7.1	*100*	*0000*	*00*	*Hydraulic elevator*	*TD*
7.1	*200*	*0000*	*00*	*Traction geared elevator*	*TD*
7.1	*300*	*0000*	*00*	*Traction gearless elevator*	*TD*
8. Mechanical					
8.1	*040*	*0000*	*00*	*Piping*	*PDA*
8.1	*120*	*0000*	*00*	*Gas water heater – residential*	*PDA*
8.1	*130*	*0000*	*00*	*Oil water heater – residential*	*PDA*
8.1	*160*	*0000*	*00*	*Electric water heater – commercial*	*PDA*
8.1	*170*	*0000*	*01*	*Gas water heater – commercial unanchored*	*PDA*
8.1	*180*	*0000*	*00*	*Oil water heater – commercial*	*PDA*
8.1	*310*	*0000*	*00*	*Roof drain system*	*rgd*
8.1	*410*	*0000*	*00*	*Bathtub system*	*rgd*
8.1	*420*	*0000*	*00*	*Drinking fountain system*	*rgd*
8.1	*430*	*0000*	*00*	*Sink system*	*rgd*
8.1	*440*	*0000*	*00*	*Shower system*	*rgd*
8.1	*450*	*0000*	*00*	*Urinal system*	*rgd*
8.1	*460*	*0000*	*00*	*Water cooler*	*PDA*
8.1	*470*	*0000*	*00*	*Water closet system*	*rgd*
8.1	*510*	*0000*	*00*	*Water closet group*	*rgd*
8.1	*560*	*0000*	*00*	*Group wash fountain*	*rgd*
8.1	*600*	*0000*	*00*	*Complete residential bathroom fixtures*	*rgd*

Table A-2. Assembly taxonomy (cont.)

Building assembly					
Div.	**Class**	**Line**	**Cond.**	**Description**	**Hazard**
8.2	**110**	**0000**	**01**	**Wet-pipe sprinkler system unbraced**	**PDA**
8.2	**110**	**0000**	**02**	**Wet-pipe sprinkler system braced**	**PDA**
8.2	*120*	*0000*	*00*	*Dry-pipe sprinkler system unbraced*	*PDA*
8.2	*120*	*0000*	*01*	*Dry-pipe sprinkler system braced*	*PDA*
8.2	*130*	*0000*	*00*	*Preaction sprinkler system unbraced*	*PDA*
8.2	*130*	*0000*	*01*	*Preaction sprinkler system braced*	*PDA*
8.2	*140*	*0000*	*00*	*Deluge sprinkler system unbraced*	*PDA*
8.2	*140*	*0000*	*01*	*Deluge sprinkler system braced*	*PDA*
8.2	*150*	*0000*	*00*	*Firecycle sprinkler system unbraced*	*PDA*
8.2	*150*	*0000*	*01*	*Firecycle sprinkler system braced*	*PDA*
8.2	*310*	*0000*	*00*	*Wet standpipe riser*	*PDA*
8.2	*320*	*0000*	*00*	*Dry standpipe riser*	*PDA*
8.2	*390*	*0000*	*00*	*Standpipe equipment*	*rgd*
8.2	*810*	*0000*	*00*	*FM200 (chemical) fire suppression*	*PDA*
8.3	*110*	*0000*	*00*	*Heating electric boiler unanchored*	*PDA*
8.3	*110*	*0000*	*01*	*Heating electric boiler anchored*	*PDA*
8.3	*140*	*0000*	*00*	*Heating fossil-fuel unanchored*	*PDA*
8.3	*140*	*0000*	*01*	*Heating fossil-fuel anchored*	*PDA*
8.3	*161*	*0000*	*00*	*Commercial building heating fin-tube*	*rgd*
8.3	*162*	*0000*	*00*	*Commercial building heating terminal unit*	*PDA*
8.4	*110*	*0000*	*00*	*Chilled water air cooled condenser*	*PDA*
8.4	*120*	*0000*	*01*	*Chilled water cooling tower unanchored*	*PDA*
8.4	*120*	*0000*	*02*	*Chilled water cooling tower anchored*	*PDA*
8.4	*210*	*0000*	*00*	*Rooftop single-zone unit unanchored*	*PDA*
8.4	*210*	*0000*	*01*	*Rooftop single-zone unit anchored*	*PDA*
8.4	*220*	*0000*	*00*	*Rooftop multi-zone unit unanchored*	*PDA*
8.4	*220*	*0000*	*01*	*Rooftop multi-zone unit anchored*	*PDA*
8.4	*230*	*0000*	*00*	*Self-contained water-cooled unit system*	*PDA*
8.4	*240*	*0000*	*00*	*Self-contained air-cooled unit system*	*PDA*
8.4	*250*	*0000*	*00*	*Split system (dry interior)*	*PDA*
8.5	*110*	*0000*	*00*	*Garage exhaust system*	*rgd*
9. Electrical					
9.1	*210*	*0000*	*00*	*Electric service*	*rgd*

Table A-2. Assembly taxonomy (cont.)

Building assembly					
Div.	**Class**	**Line**	**Cond.**	**Description**	**Hazard**
9.1	*310*	*0000*		*00 Feeder installation*	*rgd*
9.1	**410**	**1000**		**01 Switchgear low voltage unanchored**	**PDA**
9.1	**410**	**1000**		**02 Switchgear low voltage anchored**	**PDA**
9.1	**410**	**2000**		**01 Switchgear med. voltage unanchored**	**PDA**
9.1	**410**	**2000**		**02 Switchgear med. voltage anchored**	**PDA**
9.2	*210*	*0000*		*00 Fluorescent fixture*	*PDA*
9.2	*220*	*0000*		*00 Incandescent fixture*	*rgd*
9.2	*230*	*0000*		*00 HID fixture high-bay (hanging)*	*rgd*
9.2	*240*	*0000*		*00 HID fixture low-bay (fixed)*	*rgd*
9.2	*252*	*0000*		*00 Light pole*	*PDA*
9.2	*500*	*0000*		*00 Receptacles and switches*	*rgd*
9.2	**700**	**0000**		**01 Motor installation unanchored**	**PDA**
9.2	**700**	**0000**		**02 Motor installation anchored**	**PDA**
9.4	*100*	*0000*		*00 Communication & alarm system*	*rgd*
9.4	**310**	**0000**		**01 Generator diesel unanchored**	**PDA**
9.4	**310**	**0000**		**02 Generator diesel anchored**	**PDA**

APPENDIX B
ASSEMBLY CAPACITY, REPAIR COST, AND REPAIR DURATIONS

B.1. PRE-NORTHRIDGE WSMF CONNECTIONS

B.1.1. Pre-Northridge WSMF connection fragility

The surprisingly brittle nature of welded steel moment frames (WSMF) affected by the 1994 Northridge earthquake has proven to be one of the most significant and costly lessons of that event. The connection exhibits a variety of failure modes, which SAC-95-04 [SAC Steel Project, 1995c] categorizes into 24 types: four categories of beam damage (denoted by G1 through G4), five of column damage (C1 through C5), four of flange weld (W1, etc.), five of shear connection (S1 etc.), four of panel zone (P1 etc.), and two of column web (P5 and P6). Most involve visible damage; the two exceptions (C1 and W1) refer to incipient cracks detected by ultrasonic testing. Failure modes are depicted in Figure B-1. A longer list from SAC-99-01 [SAC Steel Project, 1999] is shown in Table B-1.

All 24 failure modes are recommended for repair by SAC Steel Project workshop participants in SAC-95-01 [1995a]. By contrast, FEMA-273 [1997] does not appear to consider incipient fracture (equivalent to W1 and C1) in its draft performance-based design (PBD) objectives. Two limit states are therefore defined: occurrence of any SAC failure mode, and the occurrence of any SAC failure except W1 and C1.

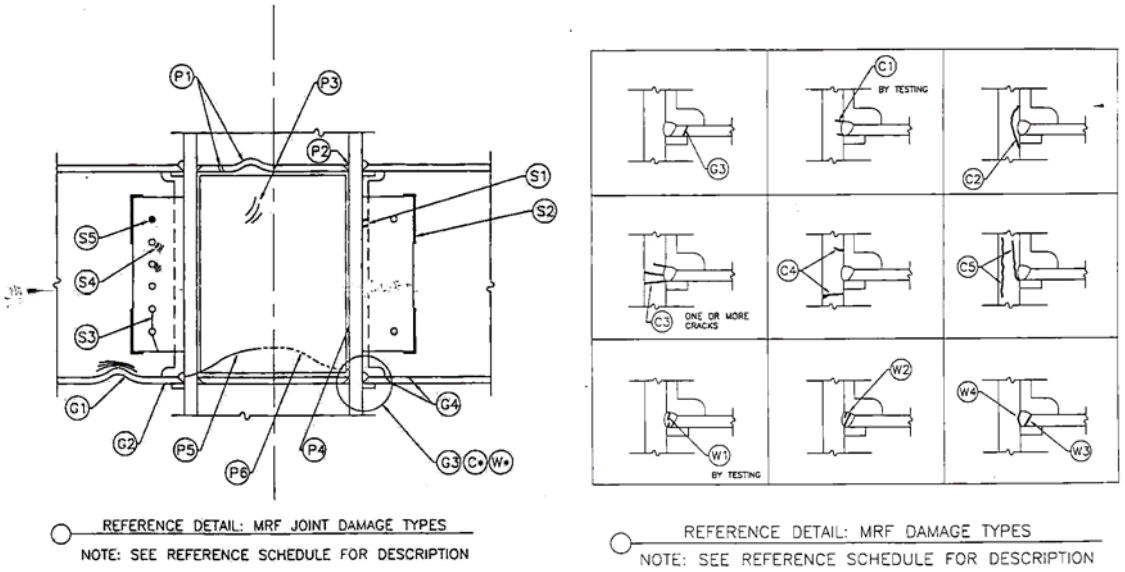

Figure B-1. Failure modes [SAC Steel Project, 1995c].

Table B-1. SAC Steel Project connection damage types.

Type	Location	Description
G1	Girder	Buckled flange
G2	Girder	Yielded flange
G3	Girder	Top or bottom flange fracture in HAZ
G4	Girder	Top or bottom flange fracture outside HAZ
G5	Girder	Top and bottom flange fracture
G6	Girder	Yielding or buckling of web
G7	Girder	Fracture of web
G8	Girder	Lateral-torsional buckling
C1	Column	Incipient flange crack (detectable by P.I.)
C2	Column	Flange tear-out or divot
C3	Column	Full or partial flange crack outside HAZ
C4	Column	Full or partial flange crack in HAZ
C5	Column	Lamellar flange tearing
C6	Column	Buckled flange
C7	Column	Fractured column splice
W1a	CJP weld	Minor root indication - thickness <3/16" or $t_f/4$; width < $b_f/4$
W1b	CJP weld	Root indication - thickness > 3/16" or $t_f/4$ or width > $b_f/4$
W2	CJP weld	Crack through weld metal thickness
W3	CJP weld	Fracture at girder interface
W4	CJP weld	Fracture at column interface
W5	CJP weld	Root indication—non-rejectable
S1a	Shear tab	Partial crack at weld to column (beam flanges sound)
S1b	Shear tab	Partial crack at weld to column (beam flange cracked)
S2a	Shear tab	Crack in supplemental weld (beam flanges sound)
S2b	Shear tab	Crack in supplemental weld (beam flange cracked)
S3	Shear tab	Fracture through tab at bolt holes
S4	Shear tab	Yielding or buckling of tab
S5	Shear tab	Damaged, or missing bolts
S6	Shear tab	Full length fracture of weld to column
P1	Panel zone	Fracture, buckle, or yield of continuity plate
P2	Panel zone	Fracture of continuity plate welds
P3	Panel zone	Yielding or ductile deformation of web
P4	Panel zone	Fracture of doubler plate welds
P5	Panel zone	Partial depth fracture in doubler plate
P6	Panel zone	Partial depth fracture in web
P7	Panel zone	Full (or near full) depth fracture in web or doubler plate
P8	Panel zone	Web buckling
P9	Panel zone	Fully severed column

SAC Steel Project investigators present results of a series of dynamic structural analyses performed on the study buildings [Engelhardt, Kim, Sabol, et al., 1995; Hart, Huang, Lobo, et al., 1995; Kariotis and Eiamani, 1995; Krauwinkler, Alali, Thiel, et al., 1995; Naeim, DiJulio, Benuska, et al., 1995; and Uang, Yu, Sadre, et al., 1995]. It can be argued that the quality of the analyses and of the assumptions varies between these studies, but given the apparent endorsement of the SAC Steel Project in publishing them, they are taken at face value here.

Each analysis uses either ground motions experienced by the building during the Northridge earthquake, or nearby ground-motion records, which are used as proxies for site ground motion. Using these records, the investigators perform three-dimensional linear elastic dynamic analyses, and report the ratio of maximum applied moment to yield moment of the beam end. This ratio is referred to as elastic demand-to-capacity ratio (elastic *DCR*), or simply *DCR*. As a result of these analyses, connection damage and *DCR* is available for 2,236 connections.

These damage data are analyzed using the binning method described in Section 3.1.2. Bin sizes (Equation 3-6) are set to N_i = 100 data points each (except the last, N_{23}, which contains the 36 remaining connections), resulting in unequal bin ranges (Equation 3-3). The analysis indicates that a relationship between *DCR* and damage does exist, as shown in Figure B-2. Two trends are shown: one for the occurrence at a connection of any SAC failure mode, and one considering as failed only connections that experienced damage except W1 or C1. Both trends are strong enough to reject the null hyporeport (that no such trend exists) at the 1% significance level. Again, each data point in the figure represents 100 connections.

While W1 and C1 account for 40% of all observed failures (Figure B-3), they predominate at lower values of structural response (Figure B-4); this feature is perhaps inadequately reflected in the trendlines shown in Figure B-2. However, the simplicity of the lognormal distribution of capacity argues against selection of a more complicated distribution that might more closely match the binned data.

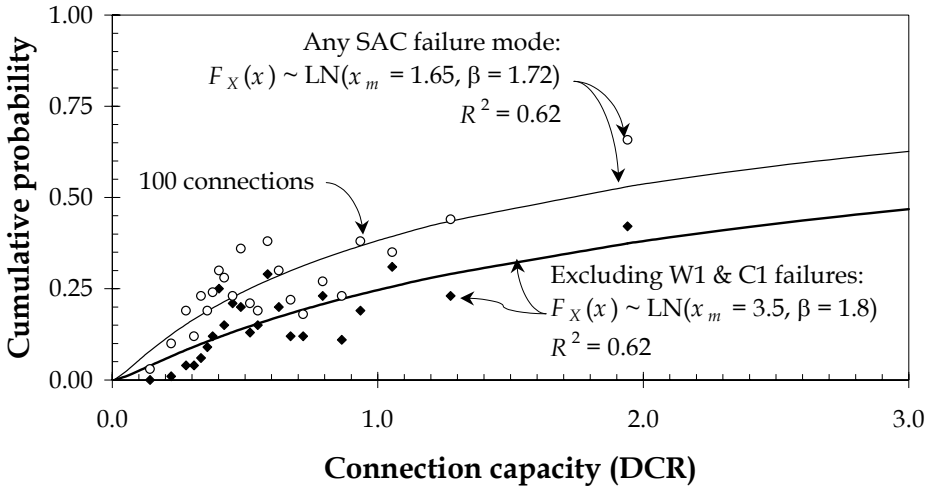

Figure B-2. Pre-Northridge WSMF connection capacity in terms of *DCR*.

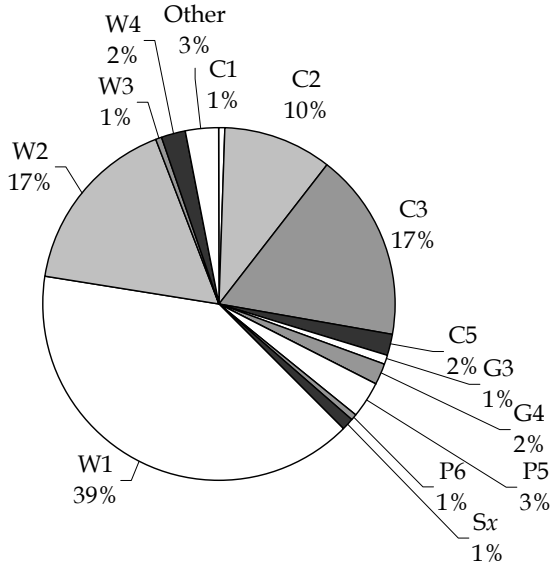

Figure B-3. Failure modes of 663 WSMF connection failures.

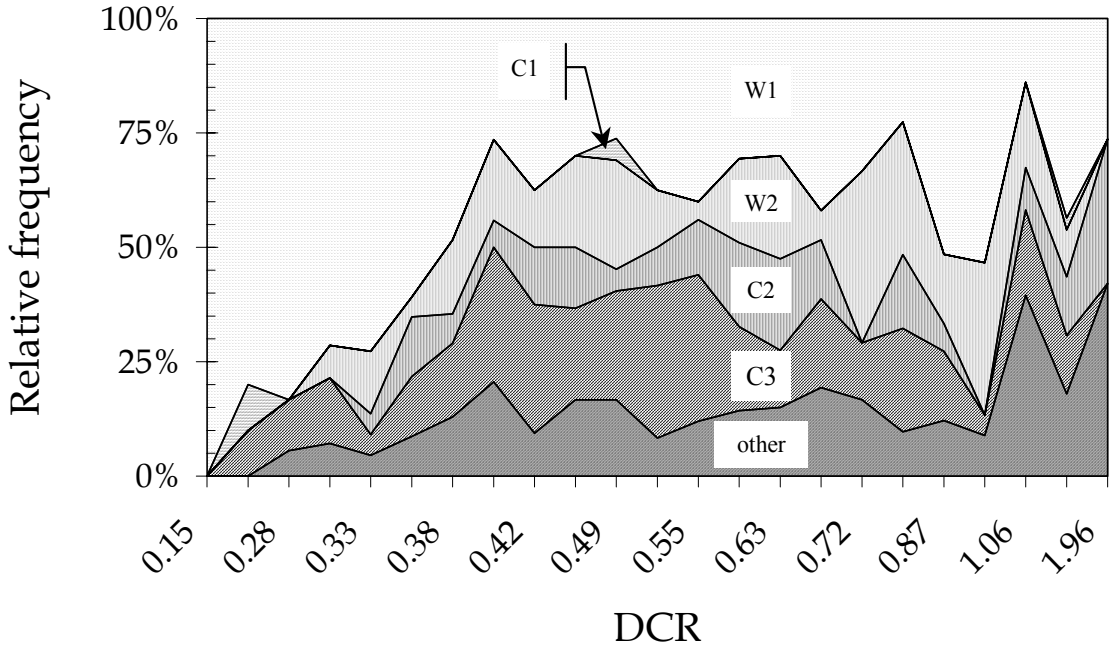

Figure B-4. Trend in WSMF connection failure mode with structural response. (Note x-axis not linear scale)

Two studies also examined individual plane frames subjected to dynamic two-dimensional inelastic structural analysis [Engelhardt, Kim, Sabol, et al., 1995; and Krauwinkler, Alali, Thiel, et al., 1995]. Investigators tabulated maximum inelastic beam hinge rotation (*IBHR*) for each connection. These analyses were more limited than the linear elastic ones: six frames in two buildings, 152 connections, of which 83 were damaged, 41 of them with zero *IBHR*. A linear regression of failure probability versus *IBHR* indicates that no trend exists ($\rho << 0.01$, from 11 observations), as shown in Figure B-5. In the figure, data are binned by *IBHR*, which were reported to three decimal places. Each data point represent approximately 5 to 10 connections, except for 93 connections with *IBHR* = 0.000.

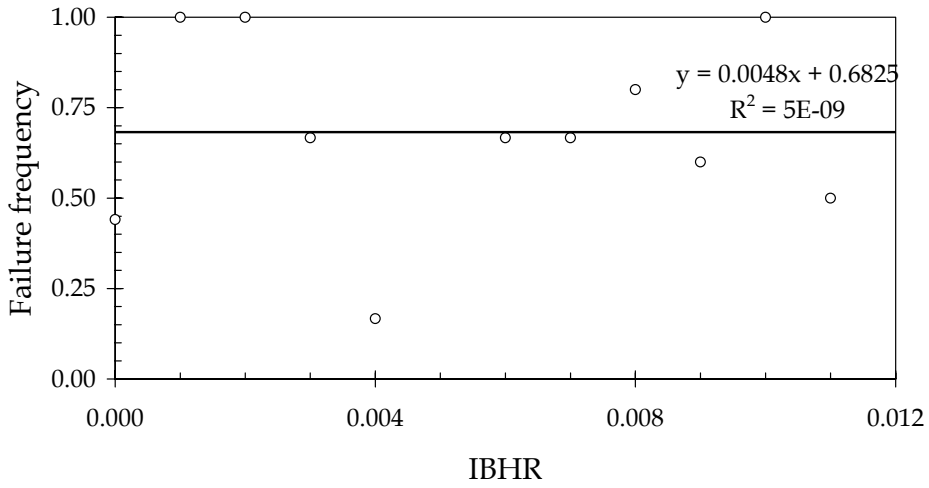

Figure B-5. WSMF connection damage versus IBHR.

The data point for the 93 connections with zero *IBHR* tends to rule out using *IBHR* as a predictor of failure probability, as it implies that 45% of connections fail without being subjected to measurable structural response. Because of this, the practically zero correlation coefficient between *IBHR* and failure probability, and the satisfactory correlation between *DCR* and failure probability, *DCR* is used in the present study as the structural response parameter relevant to pre-Northridge WSMF connection failure. Based on the foregoing analysis, WSMF connection capacities are given by Equations B-1 and B-2.

$$F_{X1}(x) = \Phi\left(\frac{\ln(x/1.65)}{1.72}\right) \tag{B-1}$$

$$F_{X2}(x) = \Phi\left(\frac{\ln(x/3.5)}{1.8}\right) \tag{B-2}$$

where X_1 refers to the connection *DCR* capacity for any SAC failure mode, and X_2 refers to the connection *DCR* capacity for any SAC failure mode except W1 or C1.

B.1.2. Connection repair cost and duration

Repair measures for pre-Northridge WSMF connections have been proposed by a number of authors. For example, Anderson and Duan [1998] tested several measures: two weld enhancements (gouging and replacement; overlay of the existing weld by new weld material); the addition of rectangular cover plates to top and bottom flanges with welded connections; the addition of vertical triangular fins to top and bottom flanges; and beam section reduction with drilled holes that approximate the cross-section of the dogbone fix. Of these tested measures, weld overlays and horizontal cover plates achieved plastic rotations in excess of 3%. Estimated construction costs however are not provided.

The SAC Steel Project [1995b] recommends a welded haunch connection, that is, a WT steel shape with its web cut into a triangular shape, and welded to top and bottom flanges, thus forming the haunch shown in Figure B-6. The SAC authors do not provide a cost estimate for this connection, but an unpublished, detailed cost estimate was provided to the present author, dealing with a pre-Northridge southern California hospital that experienced extensive damage to WSMF connections in 1994. The estimate was provided on the condition of anonymity; hence a reference cannot be provided. However, the key parameters are corroborated by the experience of the Parsons Corporation in dealing with the seismic retrofit of two WSMF buildings on the campus of the California State University at Northridge [Owens, 2000].

The estimator of the hospital contract determined costs to replace 80 connections with WT steel fixtures. The estimator presents costs on a task-by-task basis for each joint to be repaired. (A joint is a point at which one or more beams frames into a column. It may therefore comprise one or more connections.) The statistics for these connections therefore represent samples of mean repair cost estimated by a single expert; see Figure B-7.

Owens [2000] recalls that repairs to the CSU Northridge buildings by the Parsons Corporation cost $20,000 to $50,000 per connection, with an average on the order of

$35,000, for a retrofit measure similar to that shown in Figure B-6. This range of costs tends to support the distribution shown in Figure B-7. Pre-heat and post-heat represented a substantial portion of the retrofit task. Concrete deck and finishes near the connection tended to absorb heat too quickly for the contractor to maintain the desired temperature on the connection; these elements had to be removed and replaced in order to satisfy heating requirements, a fact tending to support the pre-heat portion of Figure B-7. Furthermore, fire-safety concerns were substantial: while the connection was hot, several workers stood by with fire extinguishers and hoses, a fact tending to support the relatively large fraction of cost attributable to fire protection in the figure.

The variability expressed in these samples reflects variability in conditions of installation, as opposed to uncertainty of the modeler. Installation conditions are not reflected in the ABV model, so this source of variability is properly ascribed to randomness, or aleatory uncertainty, which is denoted for the lognormal distribution by β_r.

It is problematic to impute modeling uncertainty (epistemic uncertainty, denoted by β_u), as no data on actual costs observed after installation are available. An amount selected by judgment is applied, and β_u is taken as 0.10, resulting in total uncertainty on the cost of WSMF connection repair using the WT taken as 0.58, per Equation B-3.

$$\beta = \sqrt{\beta_r^2 + \beta_u^2} \tag{B-3}$$

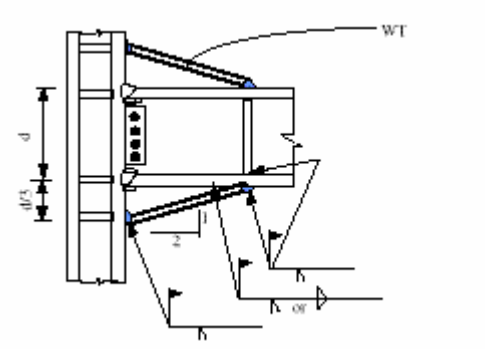

Figure B-6. SAC Steel Project [1995b] haunched WT retrofit scheme.

To what degree might this cost be generalized to other installation conditions, buildings with other uses, etc.? Considering again Figure B-8, several aspects of this figure are interesting. First, asbestos abatement is not an issue. If it were, the cost would be greater. None of the costs in the figure are unique to a hospital, thus unit cost is relatively insensitive to building use. Finally, installation of WTs represents less than 20% of the per-connection or per-joint total, suggesting that the total unit cost is relatively insensitive to the precise detail of the retrofit. The fact of welding is more relevant: among all item costs, pre-heat and post-heat, fire safety, and exhaust and cooling represent 64% of the total.

Duration of repairs is not available from the cost estimate. Labor-intensive aspects of Figure B-8 suggest that between 50% and 80% of total cost is labor. It is assumed that labor costs the owner \$50 to \$100 per man-hour, and that the crew size is between two and six. Taking the stated bounds as 10th and 90th percentiles of lognormal distributions, repair duration is lognormally distributed with median x_m = 65 hours and logarithmic standard deviation β = 0.80. (Owens [2000] recalls connections taking as little as 5 and as many as 11 days each to repair, which tends to support this range.)

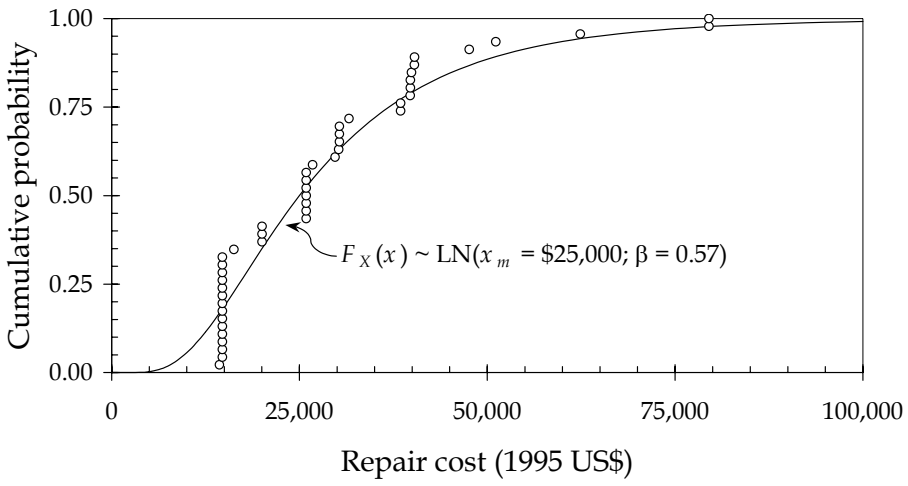

Figure B-7. Per-connection repair cost.

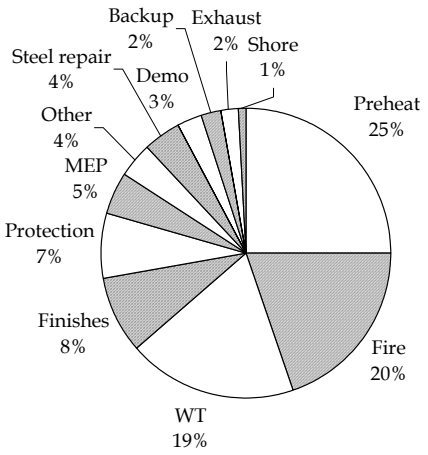

Figure B-8. Contributors to connection repair cost.

B.2. WALLBOARD PARTITIONS

B.2.1. Gypsum wallboard partition on metal studs, drywall screws

Rihal's [1982] experimental investigations of 8'-0 x 8'-0 building partitions are used to create fragility functions for 5/8" wallboard partitions on 3-5/8" metal stud with screw fasteners. Two limit states are identified: onset of noticeable damage (limit state 1) and onset of failure and significant damage (limit state 2). Rihal [2000] believes it is reasonable to associate limit state 1 with the onset of a situation where a contractor or architect would recommend repair via tape, mud, and paint; and to associate limit state 2 with a contractor or architect recommending demolition and replacement of the wall segment. At this limit state, "Most of the damage was around the perimeter. Facing panels had crumbled pretty badly, and taped joints sheared. Bottom hold-downs were heavily damaged. Some people might want to cut out the damaged portion and reuse the undamaged part," but Rihal [2000] questioned whether this would be adequate in terms of strength. Rihal [1982] reports the drift at which each sample reached each limit state; hence the logarithmic mean and logarithmic standard deviation of each capacity distribution are calculated directly. The resulting lognormal capacity distributions are

shown in Figure B-9; they pass Kolmogorov-Smirnov goodness-of-fit tests at 5% significance levels.

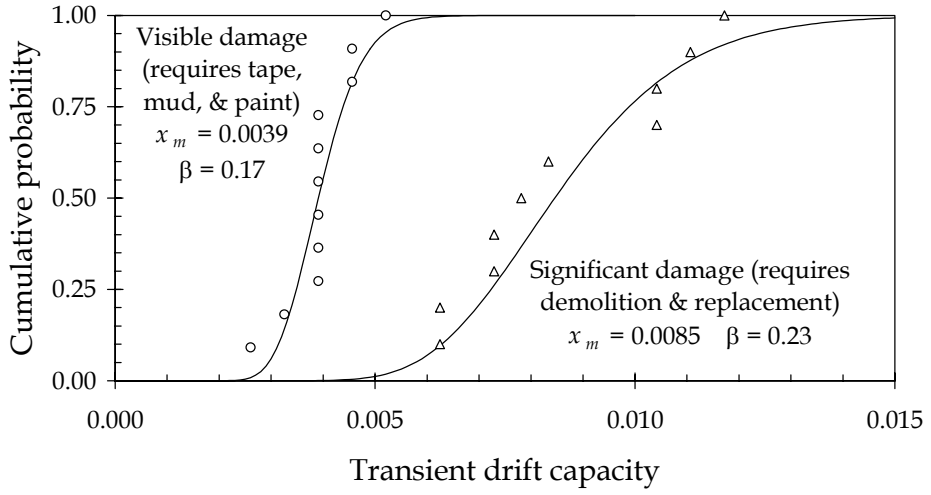

Figure B-9. Fragility of 5/8" wallboard partitions on 3-5/8" metal-stud framing.

B.2.2. Wallboard partition repair cost and duration

RS Means Corp. [1997a and 1997b] is used as a basis for estimating the repair cost and duration. The costs reflect two-sided fire-resistant drywall without a base layer such as sound-dampening drywall, with either regular, water-resistant, or fire resistant wallboard. Repairs for limit state 1 are taken to be tape, mud, and paint, for which RS Means Corp. [1997a] indicates an average cost of $32 per 8 lf to tape, mud, and finish, and approximately $16 more to paint. The total median cost is taken to be $50 per 8-lf unit, with median duration of 1.2 hr.

Limit state 2 is repaired by demolishing the existing wall and installing a new wall. The cost for the latter repair is estimated by adding 10% to the new-installation cost, to account for demolition of the damaged wall. The median total cost for limit state 2 is estimated to be $230, with median repair duration of 2.3 hr per 8-lf unit [RS Means Corp., 1997b]. The logarithmic standard deviation on cost for both repairs is taken to be β = 0.50, to account both for the variability of labor and material costs (epistemic

uncertainty) and for the variety of detailed construction alternatives possible within these categories of repair (aleatory uncertainty).

B.3. GLAZING

B.3.1. Laboratory test data for a glazing system

As noted in Chapter 2, laboratory data are available for a particular brand of glazing system. Behr and Worrell's [1998] data for in-plane racking capacity of Horizon Wall glazing systems are duplicated in Figure B-10. Each ID in the figure reflects results for a set of five to 12 similar tests, with six being the typical regimen; error bars show one standard deviation in the observed capacity. The tests reflect 14 combinations of framing system, glass type, and sealant, as detailed in Table B-2. Two limit states are of interest: visible cracking and glass fallout. Only the cracking limit state is material for economic loss, but fallout will be useful for later consideration of life safety.

The fragility data can be used directly if a building is known to have glazing with framing system, glass type, pane size, and sealant matching one of the combinations shown in Table B-2. Fragility parameters x_m and β for a lognormal capacity distribution are shown in Table B-3. These parameters are calculated based on the mean and standard deviation of capacity shown in Figure B-10. The last row of Table B-3 considers an alternative case: a probabilistic mixture of types.

The fragility of the mixture is created using the procedure outlined in Section 3.1.2, using Equations 3-13 and 3-14 to create a sample set of capacity data for the mixture, to which a lognormal distribution is fit. In the present case, N = 14. The moments in Equation 3-14 are taken from Figure B-10. The results of the simulation are shown in Figure B-11, along with lognormal distributions fit to the data. Both curves pass Kolmogorov-Smirnov goodness-of-fit tests at the 5% significance level.

B.3.2. Comparison of glazing fragility with other data

Note that these fragility functions are appropriate only for in-plane racking of glazing systems similar to those tested by Behr and Worrell [1998]: 5-ft by 6-ft lites with framing systems, glazing type, and sealant similar to the Horizon Wall system. They are not intended to reflect fragility of all glazing systems, in which glass type, pane thickness, pane dimensions, the gap between frame and glass, and other parameters could significantly affect racking fragility.

The relatively high capacity of the Horizon Wall systems is illustrated by comparison with the glazing tested by Nakata, Itoh, Baba, et al. [1984], who report that "cracks were found in fixed windows with elastic sealant when the story drift was around 1/125-1/73", or 0.008 to 0.014. The latter tests include six fixed panes of 5-mm glass with elastic sealant. (Pane length and width are not reported; diagrams suggest dimensions of 2 to 3 ft. by 5 to 6 ft.) These data are inadequate to construct a fragility function, and the description of framing system, glass type, and sealant are inadequate to define the assembly type. However, some comparison is possible. Assuming that "cracks were found" indicates that one or two panes out of six were cracked (P_f = 0.17 to 0.33) at peak transient drift of x = 0.008 to 0.014, that capacity is distributed lognormally, and that logarithmic standard deviation of capacity is β = 0.25 to 0.75, then median capacity x_m is in [0.01, 0.03], in terms of peak transient interstory drift ratio. This range is less than the median capacity of 4% peak transient drift shown in Figure B-11, but within the same order of magnitude. This tends to support the credibility of Figure B-11.

B.3.3. Glazing repair costs

RS Means Corp. [1997a and 1997b] provides mean labor and material costs for installation of new glazing. The labor costs are corroborated by the U.S. Bureau of Labor Statistics [Pilot, 1998] and Dillon [1999], which also provides a measure of uncertainty on cost. The median unit cost and repair duration for the Los Angeles area are taken to be $439 and 0.4 hours, respectively. The uncertainty on unit cost is reflected by a

logarithmic standard deviation of $\beta = 0.26$. Absent better information, uncertainty on duration is conservatively assumed: $\beta = 0.5$.

Table B-2. Behr and Worrell [1998] in-plane racking tests.

ID	System	Glazing Type	Sealant
1	MR	6mm annealed monolithic	Dry
2	MR	6mm heat-strengthened monolithic	Dry
3	MR	6mm fully tempered monolithic	Dry
4	MR	25mm annealed insulating glass unit (IGU)	Dry
5	MR	25mm heat-strengthened IGU	Dry
6	MR	6mm annealed monolithic w/0.1mm plastic film (PET)	Dry
7	MR	6mm annealed laminated	Dry
8	MR	10mm heat-strengthened laminated	Dry
9	SF	6mm annealed monolithic	Dry
10	SF	6mm fully tempered monolithic	Dry
11	SF	6mm annealed laminated	Dry
12	SF	25mm annealed insulating glass unit (IGU)	Dry
13	MR	6mm heat-strengthened monolithic	SSG
14	MR	25mm annealed insulating glass unit (IGU)	SSG

MR = Dry glazed, midrise curtain-wall system
SF = Storefront wall system
Dry = Polymeric (rubber) gaskets wedged between glass edges and frame
SSG = Bead of structural silicone sealant was used on the vertical glass edges and dry glazing gaskets were used on the horizontal edges.

Table B-3. Cracking and fallout fragility parameters for Horizon Wall glazing.

ID	*Cracking*		*Fallout*	
	x_m	β	x_m	β
1	0.028	0.097	0.031	0.12
2	0.034	0.14	0.035	0.15
3	0.040	0.16	0.040	0.16
4	0.036	0.18	0.044	0.16
5	0.038	0.16	0.038	0.16
6	0.027	0.18	0.058	
7	0.025	0.16	0.080	
8	0.032	0.12	0.074	
9	0.044	0.13	0.059	0.14
10	0.055	0.10	0.055	0.10
11	0.066	0.14	0.084	
12	0.067	0.084	0.077	0.036
13	0.046	0.16	0.049	0.16
14	0.051	0.15	0.058	
Mix	0.040	0.36	0.046	0.33

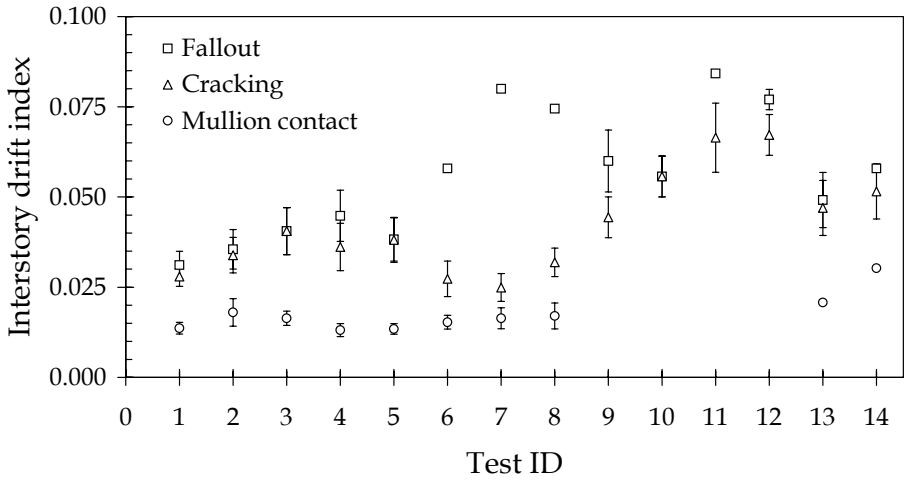

Figure B-10. Behr and Worrell [1998] in-plane racking tests of architectural glass.

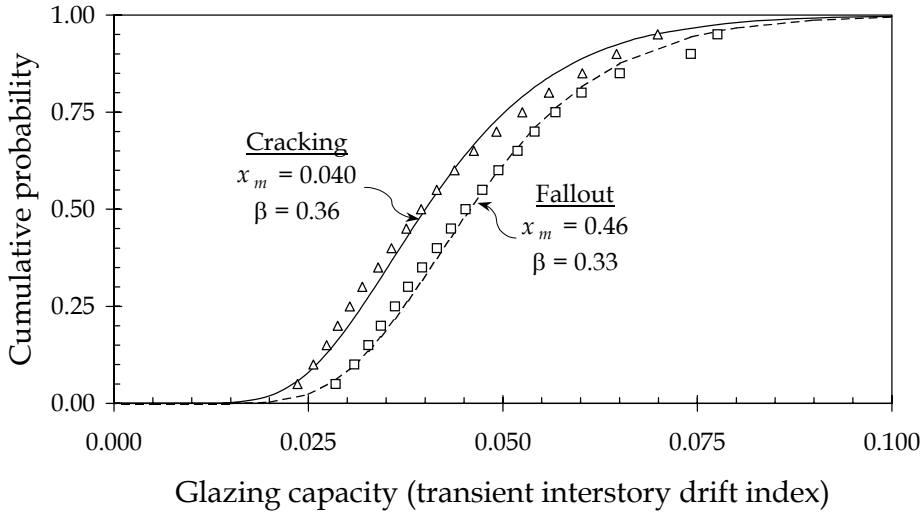

Figure B-11. Glass fragility functions.

B.4. CEILINGS

B.4.1. Creating a theoretical fragility function

As noted in Chapter 2, inadequate empirical data are available to create an empirical fragility function for suspended ceilings. However, the member material properties and assembly geometry are readily modeled, so the theoretical approach described in Section 3.1.3 is used. Before developing the fragility, it is necessary to understand the construction of suspended ceilings.

B.4.2. Description of suspended ceiling systems

A suspended ceiling represents a minor structure all by itself, and requires a description of its construction before a theoretical seismic fragility function can be developed. Two main categories of suspended ceilings are gypsum-board ceilings, which resemble gypsum board partitions in the lack of seams or joints, and manufactured ceiling systems, which are tiles resting in a gridded frame.

Gypsum-board ceilings are constructed similar to gypsum-board walls: the board is screwed to parallel furring elements, for example, metal studs, just as in a gypsum-board wall. The seams are taped, mudded, and sanded, and the entire arrangement painted. The difference between a gypsum-board ceiling and a gypsum-board wall is that in the former, furring elements hang from the diaphragm above from wires, rather than being positively fixed to structural elements. This is a clean but heavy system, weighing between 5 and 7 psf depending on drywall thickness [Peurifoy, 1975]. Its weight and monolithic nature make its seismic vulnerability significantly different from that of manufactured systems.

The broad category of manufactured ceilings include a wide variety of modular structures of extruded metal or plastic linear T-shaped elements connected into a rectangular grid at distances between nine and 48-inch centers, hung from the diaphragm above by wires. The grid of main runners is connected by cross tees and supports lightweight panels. Panel varieties include acoustical tile and acoustical board (rectangular panels typically ¾-in. thick, made of fiberglass, mineral fiber, or wood fiber) and linear panels or rectangular pans of light-gage steel or aluminum. Acoustical tile and linear metal ceilings rest in a concealed grid; acoustical board and rectangular metal pans rest in an exposed grid.

All the manufactured systems are suspended by metal wires attached to the floor or roof diaphragm above at 2′-0″ to 4′-0″ centers. The connection to the diaphragm above is made with eyepins, rawl plugs, expansion anchors, drive-in inserts, etc. Failure of some types of these connections is not uncommon in earthquakes. In theory, the lateral-force resistance is provided by splay wires and vertical compression struts at maximum 12-ft. centers each way, starting within 6 feet of the wall, and located at vertical hanger locations [ICBO, 1988]. In practice, the lateral resistance is provided by the edge restraint of the walls.

All the manufactured systems employ channels or angles at wall moldings. The ceiling system is often positively connected to these perimeter supports at two adjacent

edges to facilitate installation alignment. Although proprietary systems differ, a typical connection is a 1/8-in. rivet. This connection, being stiffer than the splay-wire system, tends to act as the de facto lateral force resisting system for the ceiling.

The ceiling frame is typically used to support lights and duct vents. Because of their mass, lights tends to have a significant effect on the seismic vulnerability of ceilings. Although rectangular fluorescent fixtures have two (slack) safety wires at opposite corners of the fixture that are connected to the floor diaphragm above, these only become active if the ceiling system collapses. A typical 2-ft by 4-ft fixture may weigh up to 30 lb. (3.75 lb per square foot of ceiling), compared with 1 psf for fiberboard or 5 to 6 psf for gypsum board.

With this variety of ceiling systems in mind, a smaller category suspended ceiling system is modeled for the present study. It is a light, tile ceiling of acoustical-board with 4-ft. cross tees and 2-ft. main runners. In the system to be modeled, these 2-ft. and 4-ft. grid elements are composed of sheet steel with the cross-section shown in Figure B-12, with dimensions: t = 0.013 in.; b = 0.5625 in.; and h = 1.5 in. In rectangular rooms, two adjacent perpendicular ceiling edges are fixed to the wall with 1/8-in. galvanized-steel pop rivets such as those shown in Figure B-12.

Further strength details of the rivet are left uncertain; they are assumed to be any of those sold by Emhart Fastening Technologies [1997], with equal probability. An equal mix of those rivets would have median ultimate shear strength of 160 lb and logarithmic standard deviation of 0.67. Likewise, to reflect a variety of possible systems, ceiling tiles are defined only in terms of fixed dimension (2-ft. by 4-ft. grid) and a Gaussian probability distribution on unit mass with 2.5 psf mean and 1.1 psf standard deviation. This can represent a wide variety of lightweight ceiling systems of acoustical board, acoustical tile, or metal. Armstrong World Industries manufactures a variety of ceiling systems that might be described by these dimensions. With this information, it is possible to create a theoretical fragility model using reliability methods.

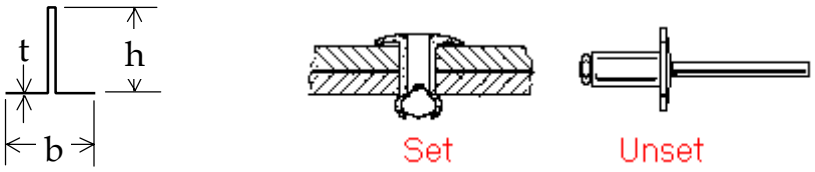

Figure B-12. Sample tee-bar cross-section (left); proprietary POP rivets (right).

B.4.3. Modeling suspended ceiling system fragility

Suspended ceiling collapse is modeled as follows. Collapse begins when grid elements buckle in compression, allowing tiles to fall out. Buckling can be facilitated by the prior shearing of rivets, which connect the grid to the wall. (A main runner or cross tee that is not connected to the wall can experience pounding, which increases the axial force and therefore the likelihood of buckling.) A grid element buckles in compression and allows a tile to fall, which causes the loss of lateral support to other runners and facilitates their buckling; progressive ceiling collapse follows.

Other failure modes are possible. Tensile connection between runner segments in the interior of the grid can fail, allowing grid deformation. Alternatively, vertical (out-of-plane) deformation of the ceiling has been observed, which can also allow tile fallout and hence progressive collapse. For the present model, it will be assumed that the grid-element design is such that tensile failure between grid elements is unlikely compared with rivet shear or compression buckling. Furthermore, it is assumed that compression struts are present. Ceiling systems that lack these features would have to be modeled to account for additional failure modes.

Considering a rectangular ceiling with main runners along the length of the room and cross tees along the width, six events associated with ceiling collapse are identified.

1. Buckling of cross tees without rivet shear
2. Buckling of main runners without river shear
3. Shearing of rivet at cross tee

4. Shearing of rivet at main runner
5. Buckling of cross tees after rivet shear
6. Buckling of main runners after rivet shear

Denoting these events by E_1 through E_6, respectively, collapse can be modeled as occurring when event E_c occurs, per Equation B-4. Each event E_i ($i \in \{1, 2, \ldots 6\}$) is modeled with a performance function $g_i(\underline{X})$, which quantifies the difference between capacity $C(\underline{X})$ and demand $D(\underline{X})$ in some aspect of performance (Equation B-5). The vector $\underline{X}$ represents the basic variables of the problem. The event E_i occurs when $g_i(\underline{X})$ demand exceeds supply (Equation B-6).

$$E_c = E_1 \cup E_2 \cup [E_3 \cap E_5] \cup [E_4 \cap E_6] \tag{B-4}$$

$$g_i(\underline{X}) = C(\underline{X}) - D(\underline{X}) \tag{B-5}$$

$$E_i = \text{TRUE iff } (g_i(\underline{X}) < 0) \tag{B-6}$$

To evaluate the probability of E_c, let

$\underline{X} = \{X_1, X_2, \ldots X_9\}^T$

X_1 = peak diaphragm acceleration

X_2 = ceiling unit mass

X_3 = buckling capacity of cross tee

X_4 = buckling capacity of main runner

X_5 = shear capacity of rivet

X_6 = room width

X_7 = room length

X_8 = Amplification ratio: (ceiling acceleration)/(diaphragm acceleration)

X_9 = Amplification of ceiling acceleration due to impact with wall

C_1 = spacing of main runners

C_2 = spacing of cross tees

The performance functions $g_1(\underline{X})$, $g_2(\underline{X})$, … $g_6(\underline{X})$ are shown in Equations B-7 through B-12. Note that these equations involve a simplifying assumption: that in the case of runner buckling after pop-rivet shearing, an acceleration equal to X_1 occurs twice, once to shear the rivet and again to cause the runner to buckle.

$$g_1(X) = X_3 - X_1X_2C_1X_6X_8 \tag{B-7}$$

$$g_2(X) = X_4 - X_1X_2C_2X_7X_9 \tag{B-8}$$

$$g_3(X) = X_5 - X_1X_2C_1X_6X_8 \tag{B-9}$$

$$g_4(X) = X_5 - X_1X_2C_2X_7X_8 \tag{B-10}$$

$$g_5(X) = X_3 - X_1X_2C_1X_6X_8X_9 \tag{B-11}$$

$$g_6(X) = X_4 - X_1X_2C_2X_7X_8X_9 \tag{B-12}$$

The parameters X_1, X_6, and X_7 are controlled; C_1 and C_2 are taken as 2 ft. and 4 ft., respectively, based on grid geometry. The unit mass X_2 is taken as normally distributed with mean 2.5 psf (0.089 slug/sf) and standard deviation 1.1 psf (0.034 slug/sf), based on AISC [1986], Winstone Wallboard Ltd. [1998], Emco Ltd. [1996], KRTA Ltd. [1992], and Holden Architectural Ltd. [1998]. The buckling capacities X_3 and X_4 are simulated based on member dimensions and theoretical Euler buckling (K = 1), using reasonable tolerances on section and material properties. The rivet shear capacity X_5 is based on the distribution of capacities quoted for 1/8-in. rivets in Emhart Fastening Technologies [1998]. The amplification X_8 is calculated based on a regression analysis of ANCO Engineers, Inc. [1983] test data, shown in Figure B-13. Note that an empirical relationship is used for the amplification factor rather than theoretical because floor spectra are not captured in the analysis, and the assumptions of an unconstrained SDOF oscillator that would be required are inappropriate for this situation.

Data are unavailable to estimate the effect of pounding; X_9 is therefore taken as 3.0, based on judgment. This is the only parameter of $\underline{X}$ for which judgment alone was used as a basis for estimating the distribution. All others are supported as noted above.

If further data become available and necessitate changing the distribution of X_9, the analysis can be readily performed to reflect better information on the theoretical fragility function.

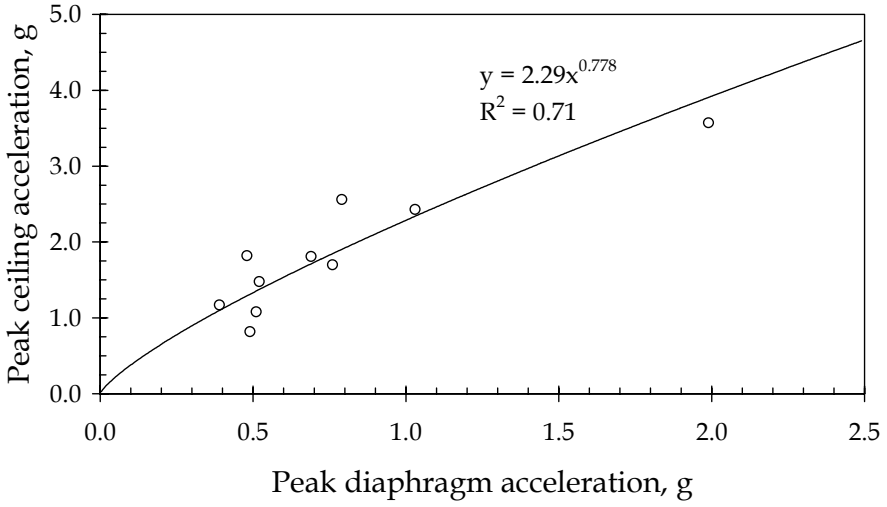

Figure B-13. Ceiling amplification factor.

With the problem thus set up, the vector $\underline{X}$ is simulated, controlling peak diaphragm acceleration X_1 and ceiling dimensions X_6 and X_7. Sample vectors $\underline{X}$ are used to evaluate Equations B-7 through B-12, which are then applied to Equations B-4, B-5, and B-6 to evaluate the probability of ceiling failure as a function of X_1, X_6 and X_7.

Considering a wide variety of ceiling dimensions between 5 ft and 60 ft., and peak diaphragm acceleration as high as 3g, it is found that ceiling capacity is very well described by a lognormal distribution. Furthermore, the logarithmic standard deviation of the capacity, denoted by β, is remarkably uniform, with a mean value of $\mu_\beta = 0.81$, and a coefficient of variation $\delta_\beta = 0.04$. Capacity for this type of ceiling construction is described as lognormally distributed with logarithmic standard deviation $\beta = 0.81$ and median capacity x_m a function of geometry $\{X_6, X_7\}$. By trial and error, it is found that median capacity x_m is related to ceiling dimensions length (l) and width (w), measured in ft., as shown in Equation B-13, illustrated in Figure B-14. In Equation B-13, the length

and width are measured in ft., and the median capacity x_m is measured in terms of peak diaphragm acceleration, in units of g.

$$x_m = 92/(l + w) \tag{B-13}$$

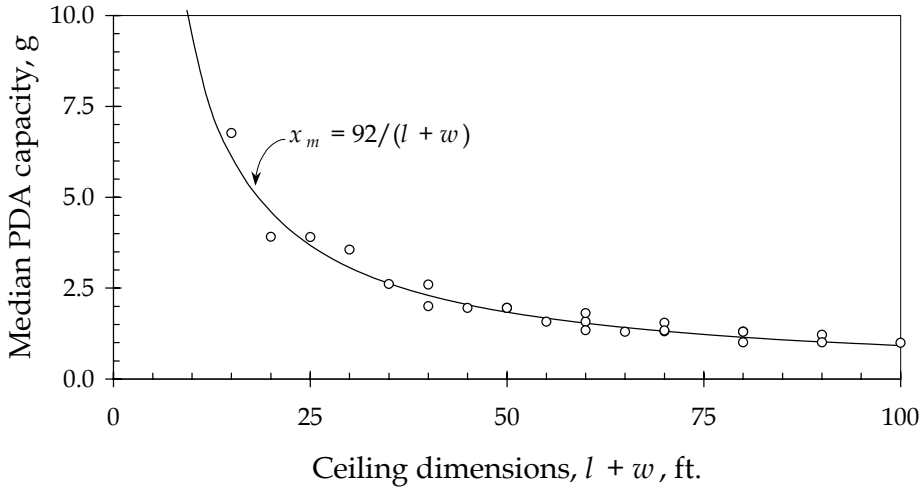

Figure B-14. Simplified median ceiling capacity.

B.4.4. Comparison of theoretical ceiling fragility with experiment

ANCO Engineers, Inc. [1983] reports test results for 16 shake-table experiments in which two tests were driven to incipient collapse, one to collapse. These are shown in Figure B-15, along with the theoretical fragility curve appropriate to the dimensions of the ceiling tested (12 ft. x 28 ft.). Rivet failure and compression buckling of runners were key causes of the two near-collapses and the one collapsed ceiling.

Eidinger and Goettel [1998] present median capacity and uncertainty values for suspended ceilings, ranging from x_m = 0.5g to 1.3g, with x measuring peak ground acceleration, as opposed to peak diaphragm acceleration. Assuming diaphragm acceleration of 1.0 to 3.0 times *PGA*, x_m in terms of peak diaphragm acceleration might be 0.5g to 3.9g. The logarithmic standard deviation suggested by Eidinger and Goettel [1998] is β = 0.4 to 0.5, somewhat smaller than the theoretical value of 0.80 derived here.

One would expect a larger β value rather than smaller to reflect a broader category of component.

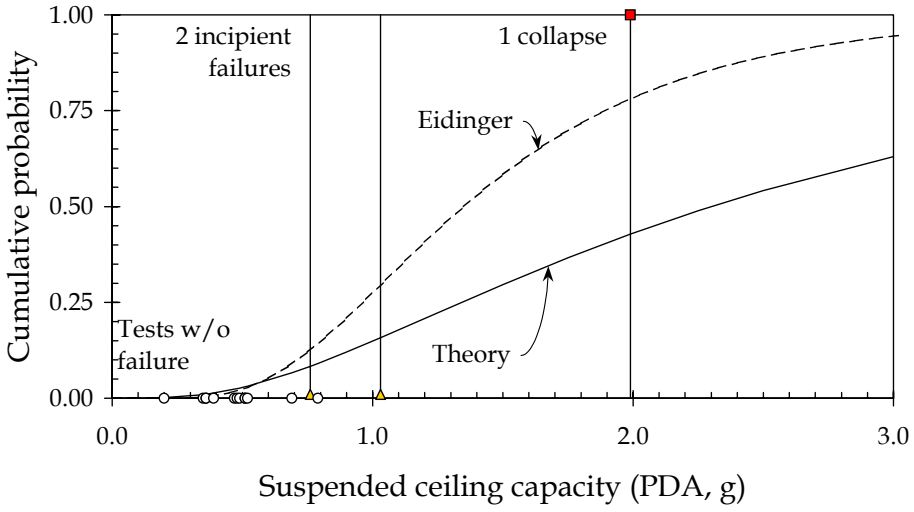

Figure B-15. Comparison of theoretical ceiling fragility with test data.

B.4.5. Ceiling repair cost and duration

The repair of a collapsed ceiling is performed by demolishing the existing ceiling and replacing it. RS Means Corp. [1997a and 1997b] is used to estimate new installation cost and duration, which are increased by 10% to account for demolition. The median total cost in 1997 for Los Angeles is estimated to be $2.21 per square foot, with a repair duration of 56 sf per hour for a crew of one carpenter. As empirical uncertainty data are not readily available, the logarithmic standard deviation of cost and of duration are assumed, conservatively, to be $\beta = 0.50$.

B.5. AUTOMATIC SPRINKLERS

B.5.1. Fragility of sprinkler systems

Several categories of building fire suppression systems exist. Most common are the systems that use water spray. Other systems use carbon dioxide, halogenated

agents, dry chemical agents, and foam. Only water-based sprinkler systems are discussed here. These are typically categorized in six classifications, the most common of which are wet-pipe and dry-pipe systems [NFPA, 1991]. In a wet-pipe system, sprinkler lines contain water under pressure at all times. When a fire occurs, heat from the fire causes individual sprinkler heads to actuate and discharge water. In dry-pipe systems, the lines are charged with pressurized gas. Heat from a fire opens the sprinkler head. The gas escapes and the pressure drops on the sprinkler-side of a valve. This allows the valve to open, filling the sprinkler line with water, which is then discharged through the open sprinkler head.

Sprinkler lines are typically long, flexible runs of pipe suspended by wires that are shot into the floor diaphragm above. In seismic areas, sprinkler lines should be braced against sidesway, but bracing is frequently missing from older buildings. In earthquakes, sprinklers can be damaged either by flexure during sway, impact with other above-ceiling components, or shearing of sprinkler heads by the suspended ceiling. This damage must be repaired, but there is a second damage issue associated with earthquake sprinkler damage. With either wet-pipe or dry-pipe systems, damage to pipes can cause unintentional discharge of water, resulting in water damage to ceilings, furnishings, and wall and floor finishes.

Damage reports from Sprinkler Fitters U.A. Local 483 [1989] provide data to regress break rate as a function of structural response x (in this case, peak diaphragm acceleration). The data are summarized in Figure B-16, which shows failure rate, denoted by ν, as a function of x. Failure probability for a single 12-ft. segment of pipe is determined by evaluating the exponential distribution with parameter $\lambda = \nu(x)*l$, where l = 12 ft. The failure probability is equivalent to the cumulative distribution of capacity evaluated at x. Assuming once again a lognormal distribution on capacity X, this approach leads to a median capacity of 16g with a logarithmic standard deviation of 1.4.

The median capacity for unbraced sprinklers may appear to be questionable. If the x_m = 16g, why consider the fragility of sprinklers at all? Does that not amount to a

rugged assembly? The answer is no, because of the high logarithmic standard deviation (β = 1.4). For a single individual 12-lf pipe segment subjected to peak diaphragm accelerations of 0.1g, 0.5g, 1g, or 3g, Equation 2-2 results in failure probabilities of 0.01%, 0.7%, 2.4%, or 12%, respectively. Considering that a fully sprinklered building of 36,000 sf has 250 such 12-ft. segments, the probability that at least one will fracture (assuming independence) is 3% for 0.1-g PDA, 80% for 0.5-g PDA, and virtual certainty for 1-g and 3-g PDA. This tends to agree with intuition that a strongly shaken building will experience some sprinkler damage with high probability. Thus, the median capacity of 16g is reasonable.

The data are sparse and the correlation between peak diaphragm acceleration and break rate is weak, with the fitted curve accounting for only 55% of the marginal variance of ν. More research is required to improve the fragility curve. Inadequate data exist to indicate the capacity of braced sprinkler lines; it is therefore assumed that braced lines have capacity twice that of unbraced lines.

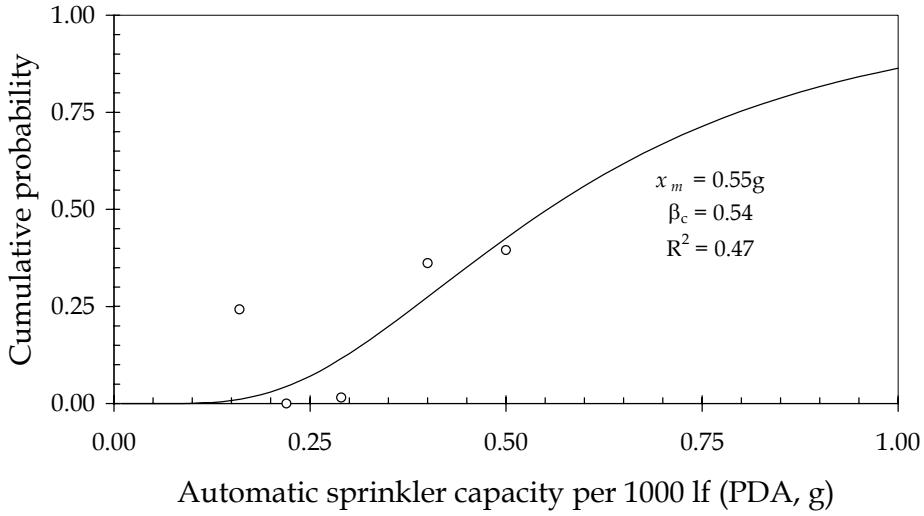

Figure B-16. Automatic sprinkler pipe capacity.

B.5.2. Sprinkler repair cost, repair duration, and retrofit

The repair cost is estimated based on RS Means Corp. [1997b], which indicates that the new installation of automatic sprinklers in the Los Angeles area costs approximately $3.50/sf. It is assumed that each break is repaired by replacing a 12-ft. segment of pipe in which the break occurred. Each segment covers 144 sf of floor area, so $3.50/sf equates with $500 per 12-lf segment. Adding 10% to account for demolition and 50% for the additional effort to repair above an existing suspended ceiling, the total median unit cost per break is estimated to be $800. It is assumed that this cost is lognormally distributed with a logarithmic standard deviation of $\beta = 0.50$. Repair duration for a crew of two plumbers is estimated to be 1 hr.

In addition to the direct repair costs, fractured sprinkler pipe leads to wetting of building finishes and contents near the break. If the pipe is pressurized, water can spray and affect an area on the order of the coverage area of a sprinkler head, approximately 150 sf, damaging ceiling tiles, wall and floor finishes, furnishings, electronic equipment, and documents. Not all wetted items are rendered worthless, but little data exist to determine what fraction of wetted value is lost. For the present, it is assumed that all wetted ceiling tiles must be replaced, all wetted computer equipment must be replaced, and that repair cost to carpets and wall finishes amounts to 25% of their replacement cost. The value of wetted documents is ignored. An approximate value of damageable finishes is $10 per square foot, so the repair of wetted finishes from a single pipe fracture could cost on the order of 0.25*$10/sf*144 sf = $360 per fracture. The total cost of a single fracture is therefore estimated to be $1160.

FEMA-74 [FEMA, 1994] provides a detail for the addition of rigid bracing. Bracing is typically installed at 16 ft. centers, at a cost of approximately $500 per brace, for a total cost of $375 per 12-ft segment of pipe, or $2.60/sf of floor area.

B.6. DESKTOP COMPUTERS

A desktop computer as defined here comprises a horizontal system unit resting on the desk and a CRT display resting on the system unit, such as those tested by Jin and Astaneh [1998]. Keyboards, printers, and other peripheral components, as well as other desktop computer configurations such as laptop computers in docking stations, upright system units on the desk or floor, and liquid crystal displays are excluded from present consideration. Two limit states are defined: limit state 1 comprises CRT monitor falloff alone. Limit state 2 comprises CRT monitor and system-unit falloff. These are progressive limit states, in that a desktop computer must proceed through limit state 1 to before it can reach limit state 2. That is, a desktop computer must be in one of three damage states: undamaged, state 1, or state 2.

Jin and Astaneh's [1998] test data are analyzed using the binary regression technique described in Section 3.1.2. The data and fitted capacity distributions are shown in Figure B-17. Following Jin and Astaneh's [1998] observations that computers strapped to the desk suffered no failures during 20 tests, it is assumed that computers installed with straps are rugged. A brief survey of replacement costs for computers suggests that cost associated with damage state 1 (monitor falloff) may be assumed to be lognormally distributed with median x_m = \$300 and logarithmic standard deviation β = 0.90. Cost associated with damage state 2 (falloff of system unit and monitor) are assumed to be lognormally distributed with median x_m = \$1800 and logarithmic standard deviation of β = 0.40.

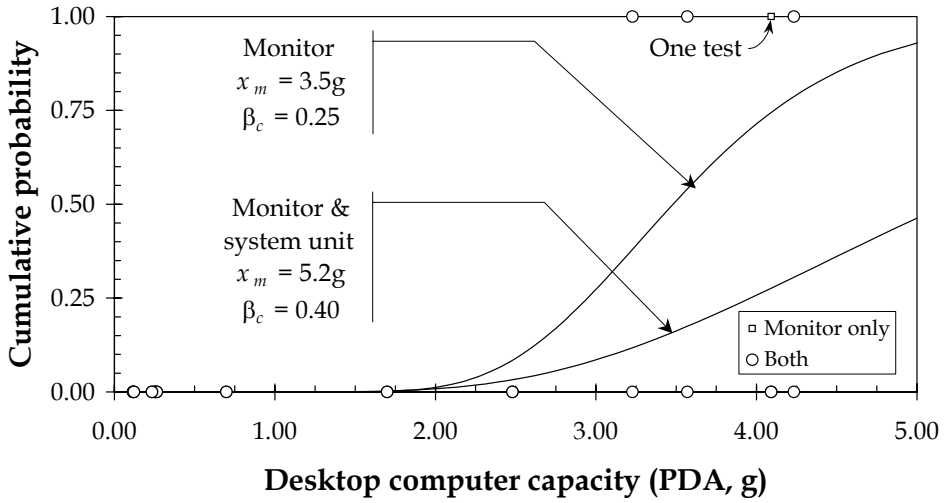

Figure B-17. Unattached desktop computer capacity.

B.7. SUMMARY OF CAPACITY, COST AND DURATION DISTRIBUTIONS

B.7.1. Assembly fragility functions

Table B-4 summarizes the assembly fragility functions developed in the present study. Most are created using empirical damage data, with the exception of suspended ceilings, whose fragility is derived theoretically. In addition to the fragility functions developed for this report, fragilities for switchgear, motor installations, and generators, developed by Swan and Kassawara [1998], are presented. Note that the fragility functions for desktop computers are presented for information purposes only, and are not used in the example analysis.

The table lists assemblies examined for the present study, the units in which these assemblies are counted, the limit states considered, and the assembly capacity relative to the limit state. All assemblies listed are modeled using a lognormal capacity distribution. The capacity parameters shown in the table are median capacity (x_m) and logarithmic standard deviation of capacity (β). The units of capacity x, as detailed in Chapter 3, are beam-end demand-capacity ratio (*DCR*), peak transient drift ratio (*TD*), and peak diaphragm acceleration (*PDA*).

Table B-4. Assembly fragility.

Assembly	Unit	Limit state	Capacity Unit	x_m	β
WSMF connections pre-Northridge	Bm-col. conn.	SAC damage (1)	DCR	1.6	1.7
WSMF connections pre-Northridge	Bm-col. conn.	SAC fracture (2)	DCR	3.5	1.8
WSMF connections with haunched T	Bm-col. conn.	SAC damage (1)	DCR	rugged	
Glazing, 5x6 ft. lite, ¼ - 1 in., Al frame, elastic sealant	pane	Cracking	TD	0.040	0.36
Glazing, 5x6 ft. lite, ¼ - 1 in., Al frame, elastic sealant	pane	Fallout	TD	0.046	0.33
Drywall partition, 5/8-in., 2 sides, metal stud, screws	8'x8'	Visible damage	TD	0.0039	0.17
Drywall partition, 5/8-in., 2 sides, metal stud, screws	8'x8'	Signif. damage	TD	0.0085	0.23
Acoustical ceiling, lightweight, Al T-bar, 2x4 frame	Room	Collapse	PDA	92/s (3)	0.81
Sprinkler pipe, unbraced	12 lf	Fracture	PDA	16g	1.4
Sprinkler pipe, braced	12 lf	Fracture	PDA	32g	1.4
Switchgear, low volt. unanchored	Set	Inoperative	PDA	1.1g	0.64
Switchgear, low volt. anchored	Set	Inoperative	PDA	rugged	
Switchgear, med. volt. unanchored	Set	Inoperative	PDA	1.6g	0.80
Switchgear, med. volt. anchored	Set	Inoperative	PDA	rugged	
Motor installation unanchored	Set	Inoperative	PDA	0.79g	0.52
Motor installation anchored	Set	Inoperative	PDA	rugged	
Generator unanchored	Set	Inoperative	PDA	0.87g	0.51
Generator anchored	Set	Inoperative	PDA	rugged	
Desktop PC system unit, unanchored	Each	Fall from desk; destroyed	PDA	3.5g	0.25
Desktop PC system unit, anchored	Each	Fall from desk; destroyed	PDA	rugged	
Desktop PC monitor, unanchored	Each	Fall from desk; destroyed	PDA	5.2g	0.74
Desktop PC monitor, anchored	Each	Fall from desk; destroyed	PDA	rugged	

1 SAC Steel Project [1995a], pg. 7-33, including G, C, W, S, and C, excluding P (panel-zone damage)
2 SAC Steel Project [1995a], pg. 7-33, including G, C, W, S, and C, excluding P, W1 and C1
3 s = ceiling length + width, ft.

B.7.2. Assembly repair-cost distributions

Table B-5 summarizes the unit repair costs and repair durations developed here. In the table, the local construction cost factor (L of Equation 4-4) is appropriate to Los Angeles. The temporal macroeconomic factor (I of Equation 4-4) is set to unity. Note that figures for which empirical cost data are unavailable are assumed based on judgment; these are shown in italics. All costs and durations are assumed to be lognormally distributed with the parameters shown.

The values shown in the table are based on available data and are not intended to represent definitive values for all future analyses. This is an important point, and highlights one of the advantages of the ABV methodology: it allows for improvement of any aspect of capacity and repair distributions as more detailed investigations or better data become available.

Table B-5. Assembly repair cost and repair duration.

			Cost/unit ($)		Time/unit (hr)	
Assembly	**Repair**	**Unit**	x_m	β	x_m	β
WSMF connections	WT(1)	Conn.	23,900	0.58	65	0.80
Glazing	Replace	30-sf pane	439	0.26	0.4	*0.5*
Drywall partition	Patch	8′x8′	50	*0.5*	1.2	*0.5*
Drywall partition	Replace	8′x8′	230	*0.5*	2.3	*0.5*
Acoustical ceiling	Replace	Room	2.21A(2)	*0.5*	0.016A(2)	*0.5*
Unbraced sprinklers	Replace	12 lf	1160	*0.5*	1	*0.5*
Braced sprinklers	Replace	12 lf	1160	*0.5*	1	*0.5*
Low volt. switchgear	Service(3)	Set	*1000*	*1.0*	*8*	*1*
Med volt. switchgear	Service(3)	Set	*1000*	*1.0*	*8*	*1*
Motor installation	Service(3)	Set	*1000*	*1.0*	*8*	*1*
Generator	Service(3)	Set	*5000*	*1.0*	*16*	*1*
Desktop PC monitor	Replace	Each	*300*	*0.9*	*0.5*	*1*
Desktop system unit	Replace	Each	*1800*	*0.4*	*1*	*1*

(1) Replace moment connection with SAC Steel Project [1995b] haunched WT
(2) A = square footage of room
(3) Service existing equipment, restore to its original position, and install seismic anchorage

APPENDIX C
ELICITING DECISION-MAKER RISK ATTITUDE

C.1. IMPLEMENTATION OF THE RISK-TOLERANCE INTERVIEW

The Spetzler [1968] procedure is used to gather the data employed in Equations 5-8 and 5-9, with some modifications. Before detailing the interview process, these differences and the reasons for them are summarized. Some of these changes are based on the Howard methodology, most notably in that the utility function is assumed to be exponential (Equation 5-7) rather than logarithmic, which permits the application of the delta property. (As noted in Chapter 2, the delta property allows one to consider costs and savings without reference to the DM's total wealth state. Use of a logarithmic utility function, which does not satisfy the delta property, requires that all decisions be made with reference to total wealth state under the various outcomes.)

A second difference is in the introduction to the interview. In the introduction, the interviewee is informed of the basic nature of a utility curve, illustrating the notion of risk aversion with example of a coin toss for ever-larger sums of money. Further, the nature of the upcoming financial questions is summarized. This introduction appears useful in preparing the DM to answer the questions more consistently than if he or she must learn the pattern during the first few deals.

A third difference is that the magnitude of financial decisions commonly made by the DM is considered as an explicit parameter of the interview process. This addition to the Spetzler [1968] procedure makes the new procedure more generally applicable to other DMs. Finally, whereas Spetzler [1968] assumes a planning period, denoted by T, and discount rate, denoted by i, and applies these to the questions, in the present study the DM's own T and i are applied to the hypothetical deals.

The interview therefore proceeds as follows. First, the introduction is given as noted above. The DM is then asked for his or her planning period T; discount rate i; a

typical investment amount (denoted by x_S) for a small deal in which he or she might engage; and that of a large deal (denoted by x_L). The DM is free to define *small* and *large* in this context. The DM is also asked for the annual revenue, or in the case of a nonprofit institution the annual budget, denoted by R, of his or her company or institution. Annual revenue appears to be relevant to risk attitude.

Individual deal outcomes g_i and l_i are scaled by x_S and x_L as shown in Equations C-1 and C-2.

$$g_i = d_i * x_i \tag{C-1}$$

$$l_i = c_i * x_i \tag{C-2}$$

In these equations, c_i and d_i are predefined constants tabulated in advance (see Table C-1), and x_i is either x_S or x_L, depending on deal i. As shown in the table, loss outcomes l range from -0.33x to -6.33x whereas gains g range from 0.6x to 19.0x.

For each deal i, the DM is posed the hypothetical deal, and asked if he or she would accept it if the probability of success were 95%. If the answer is yes, the question is posed for a probability of success of 90%. The process repeats until the DM is either indifferent between accepting and rejecting the deal, or until the DM switches from a yes answer to no. In the former case, p_i is the last probability stated. In the latter, p_i is the mean of the last two probabilities stated.

The indifference probability is recorded for each deal. The interview is concluded when all the probabilities are recorded. The analyst can then determine ρ by minimizing the objective function of Equation 5-9. Care must be taken when minimizing $e(\rho)$, as $\rho = \infty$ represents a minimal but trivial solution.

Table C-1. Hypothetical deals.

Question	Investment x	Loss multiple c	Gain multiple d
1	x_S	-1.00	0.67
2	x_L	-2.70	6.40
3	x_L	-4.00	12.00
4	x_S	-1.00	3.00
5	x_L	-1.80	1.20
6	x_S	-3.00	8.33
7	x_S	-3.67	3.00
8	x_S	-5.00	3.67
9	x_L	-2.70	3.20
10	x_L	-0.50	1.20
11	x_L	-3.40	9.00
12	x_S	-4.33	4.67
13	x_S	-0.33	1.67
14	x_L	-1.40	0.60
15	x_L	-2.30	2.00
16	x_L	-3.00	12.00
17	x_L	-3.70	9.00
18	x_L	-1.80	2.00
19	x_S	-3.00	1.67
20	x_S	-5.67	8.33
21	x_L	-3.70	19.00
22	x_S	-5.67	16.00
23	x_S	-1.67	1.67
24	x_L	-1.00	0.60
25	x_L	-4.00	19.00
26	x_S	-6.33	4.67
27	x_S	-0.33	0.67
28	x_S	-3.67	10.00
29	x_L	-0.50	0.60
30	x_S	-5.67	12.67
31	x_S	-5.00	16.00
32	x_L	-2.70	4.60
33	x_S	-2.33	3.00
34	x_L	-4.00	15.00
35	x_S	-2.33	6.33
36	x_L	-1.40	3.20
37	x_L	-2.30	6.40
38	x_S	-1.67	1.67
39	x_S	-5.00	12.67
40	x_L	-3.00	4.60

C.2. FINDINGS FROM FIVE RISK-TOLERANCE INTERVIEWS

Interviews were performed of five DMs whose companies range from very small ($200,000 per year annual revenue) to very large ($2B annual budget). The DMs interviewed for the present study were promised anonymity because their risk attitude represents sensitive business information. However, their identities are not important for present purposes. Their risk attitudes are useful primarily to illustrate the methodology and to suggest a possible relationship between risk tolerance and the magnitude of decision outcomes in which the DM is involved.

Figure C-1 illustrates a utility function developed from one such interview: that of an investment director of a commercial real estate investment company with annual revenues of $20 million. The DM has a 5-year planning period and 9% cost of capital, which is estimated to be 4% effective interest after tax and inflation. As shown in the figure, an exponential utility curve with risk tolerance coefficient ρ = $16 million fits the data well.

It is interesting to note that a trend appears to exist relating risk tolerance and size of firm. Results of the interviews are shown in Figure C-2. Limited confidence is held in the precise equation for the relationship, owing to the small sample size. However, the existence of a positive correlation supports expectation: the larger the sums a DM typically deals with, the greater the DM's risk tolerance.

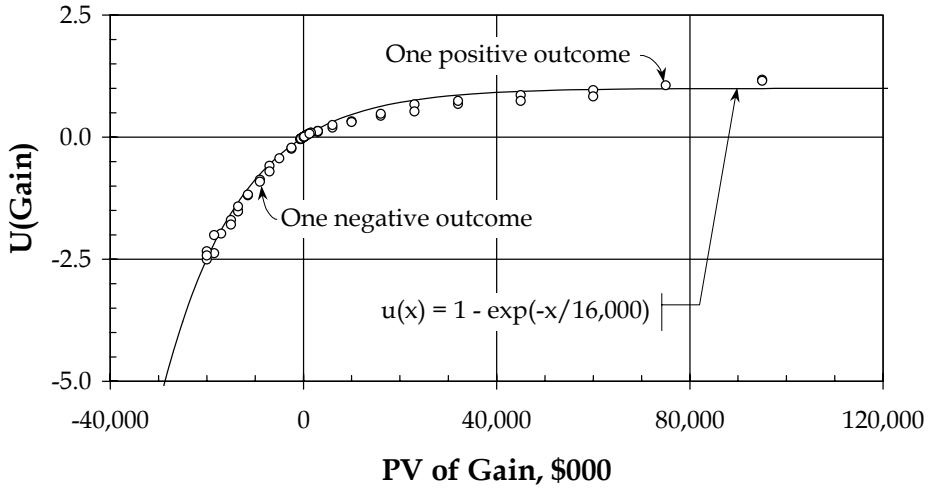

Figure C-1. Utility function fit to interview data.

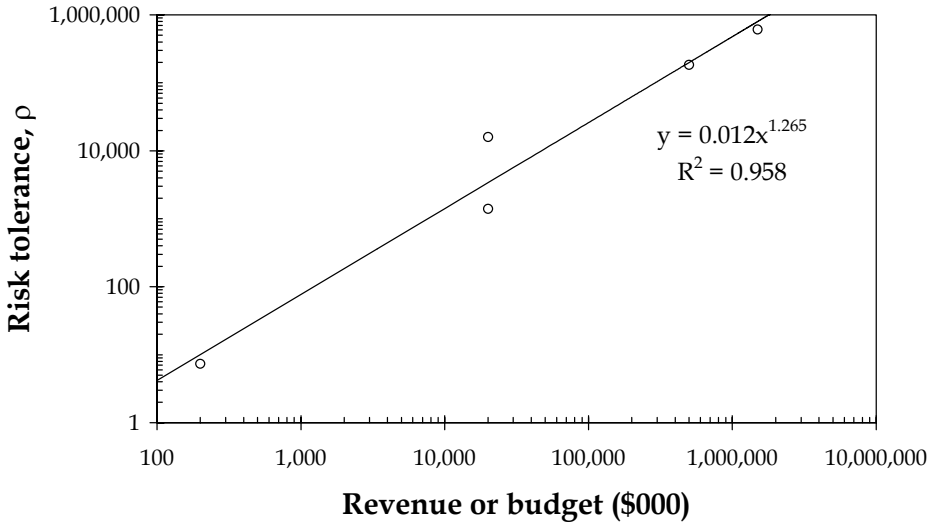

Figure C-2. Relationship between size of firm and risk tolerance.

APPENDIX D
TERMS AND ABBREVIATIONS

ABV	Assembly-based vulnerability
ARMA	Autoregressive moving-average
CADD	Computer-aided drafting and design
CE	Certain equivalent
CRT	Cathode ray tube
DCR	Demand-capacity ratio
DM	Decision-maker
EAL	Expected annualized loss
g	Acceleration due to gravity
GD	Permanent ground displacement
IBHR	Inelastic beam-end hinge rotation
JMA	Japan Meteorological Agency
LTV	Insurance limit to value ratio
MEP	Mechanical, electrical, and plumbing
MMI	Modified Mercalli intensity
PBD	Performance-based design
PDA	Peak diaphragm acceleration
PGA	Peak ground acceleration
PML	Probable maximum loss
psf	Pounds per square foot
RD	residual interstory drift ratio
ROL	Insurance rate on line (annual premium as a fraction of limit)
TD	Peak transient interstory drift ratio
UPS	Uninterruptible power supply
WSMF	Welded steel moment frame